Investigations and Design Solutions of a High Repetition Rate Satellite Laser Ranging (SLR) System

Farhat Iqbal

A dissertation submitted to the Faculty of Electrical Engineering

and Information Technology

Graz University of Technology, Austria

in partial fulfillment of the requirement for the degree of

Doctor of Philosophy at the

Institute for Broadband Communication

in co-operation with

Observatory, Lustbuhel

Supervisor: Dr.Georg Kirchner

Reviewer: Prof. Dr.Erich Leitgeb

Graz, February 2011

Deutsche Fassung:
Beschluss der Curricula-Kommission für Bachelor-, Master- und Diplomstudien vom 10.11.2008
Genehmigung des Senates am 1.12.2008

EIDESSTATTLICHE ERKLÄRUNG

Ich erkläre an Eides statt, dass ich die vorliegende Arbeit selbstständig verfasst, andere als die angegebenen Quellen/Hilfsmittel nicht benutzt, und die den benutzten Quellen wörtlich und inhaltlich entnommene Stellen als solche kenntlich gemacht habe.

Graz, am ……. ……..
(Unterschrift)

Englische Fassung:

STATUTORY DECLARATION

I declare that I have authored this thesis independently, that I have not used other than the declared sources / resources, and that I have explicitly marked all material which has been quoted either literally or by content from the used sources.

……. ……..
date (signature)

Acknowledgment

I would like to express my debt of gratitude to my Supervisor, Dr. Georg Kirchner for his guidance, technical-scientific support and encouragement throughout the period of my doctorate study; without his knowledge and support this study would not have been successful.

I acknowledge extra-ordinary support from my professor Dr. Erich Leitgeb, OeAD and higher education commission (HEC) of Pakistan in availing the scholarship at first and later for the continuation of funding for last four academic years.

I express many thanks to Dipl. Ing. F. Koidl for his scientific support and profound discussions on different modules of research. I owe a warm gratitude to all team of satellite laser ranging observatory Graz for providing me throughout a friendly and understanding environment. Thanks to my friend Mrs. Huelsman for her selfless help to manage my life in Graz. I would like to thank my husband and my daughter for their patience, cooperation and encouraging me to pursue this degree.

Abstract

Satellite Laser Ranging measures distances to satellites, orbiting at several thousand kilometers, with a few mm accuracy. The increased data rate and improved accuracy resulting from the Graz 2 kHz SLR system – as compared to traditional 10 Hz repetition rate SLR – suggests that further improvements should be possible with even higher repetition rates (up to several kHz – 10 kHz).

To design such a multi-kHz SLR system, this feasibility study for higher repetition rate SLR systems was done. One significant result was a natural limit for higher repetition rates, due to overlaps between transmitted and received laser pulses: Each transmitted laser pulse produces backscatter, when traveling through atmosphere; these backscattered photons would thus block any satellite reflected photon arriving in the same time slot, thus disabling the detector and event timers. This overlap would be more or less continuous above repetition rates of about 18 kHz. At repetition rates of about 10 kHz, it is possible to avoid overlaps by proper interleaving of transmitted and received photons.

Two new timing devices were implemented inside the Graz SLR FPGA: A fast (20 ns) medium resolution (250 ps) event timer for range gating purposes, and a fully digital, 500 ps resolution range gate generator, which replaces the presently used 100 ns FPGA counter PLUS analog delay chip. Both circuits now allow significantly higher speed, improved linearity, and better stability.

The photon link budget was analyzed for 10-100 kHz repetition rates, assuming constant power of the used laser system (lower energy per pulse for higher repetition rates, and higher energy per pulse for lower repetition rates). This analysis shows that higher repetition rates would be a big benefit for LEO (Low Earth Orbiting, up to a few 1000 km altitude) satellites, but not for HEO (High Earth Orbiting) satellites: Due to increasing noise and decreasing signal, the resulting signal to noise ratio makes it more and more difficult to detect the sparse signals. Although a simulation program demonstrated that it is possible to identify very weak signals (20 – 30 returns) out of 100000 noise points, this can be done only during post processing, but not in real time.

A real time demo program was written to monitor calibration and ranging of the Graz SLR system; it gets basic commands from the RT system of Graz SLR. It reads event times from the Riga Event Timer (which time tags the same Start/Stop pulses as Graz SLR), filters and combines them, stores all results, calculates and displays residuals. This demo program can work up to at least 10 kHz; after upgrade of the Graz 2 kHz laser system, this program will monitor the 10 kHz SLR. pulses, while the present Graz Event Timer – limited to 2.5 kHz maximum repetition rate – will “see” and measure still with the present 2 kHz.

Kurzfassung

"Satellite Laser Ranging (SLR)" misst die Entfernung zu Satelliten in Entfernungen von einigen 100 bis mehr als 20000 km mit einer Genauigkeit von wenigen Millimetern. Die erhöhte Datenrate sowie die verbesserte Genauigkeit und Stabilität des Grazer 2 kHz SLR Systems weisen darauf hin, dass eine weitere Steigerung der Messfrequenz (auf bis zu 10 kHz) den Beitrag zu fast allen SLR Anwendungen erhöhen würde.

Diese Arbeit legt die technischen Parameter eines solchen „Multi-kHz SLR Systems" fest. Ein wichtiges Resultat war eine natürliche Begrenzung für höhere Messfrequenzen durch zeitliche „Überlappung" von gesendeten und empfangenen Photonen:Jeder ausgesendete Laserimpuls produziert eine Rückstreuung (Backscatter) in der Atmosphäre. Diese Backscatter-Photonen blockieren die Detektion des zeitgleich vom Satelliten eintreffenden Photons. Diese Blockierung würde bei Messfrequenzen über ca. 18 kHz kontinuierlich sein. Bis Frequenzen von ungefähr 10 kHz ist es aber möglich, diese Überschneidungen durch entsprechende Wahl des Sendezeitpunktes der Laserimpulse in Grenzen zu halten.

Zwei neue Module wurden in der in Graz verwendeten FPGA-ISA-Karte implementiert: Ein schneller (20 ns) „Event Timer" mit einer Auflösung von 250 ps, und ein digitaler Pulsgenerator mit einer Auflösung von 500 ps. Beide Module erlauben nun eine erheblich höhere Messfrequenz und bieten zudem eine verbesserte Linearität und Stabilität.

Ausgehend von einer konstanten Ausgangsleistung eines neuen Laser-Systems wurde das Photon-Link-Budget für Messfrequenzen von 10 Hz bis 100 kHz analysiert. Dabei zeigt sich, dass höhere Messfrequenzen für LEO's (Low Earth Orbiters - Satelliten in niedrigen Orbits bis 1000 km) vorteilhaft sind, nicht aber für HEO's (High Earth Orbiters - Satelliten in hohen Umlaufbahnen). Auf Grund des sehr rasch schlechter werdenden Signal-Rausch-Verhältnisses – wenig Signal von HEOs, aber zunehmendes Rauschen bei höheren Messfrequenzen - ist es schwierig, die wenigen „echten" Returns in Echtzeit heraus zu filtern. Ein Simulationsprogramm zeigt, dass es bei Signalquoten von 20 bis 30 „echten" Punkten in 100000 Messungen nur mehr durch Analyse nach Abschluss der Messungen möglich ist, echte Returns zu identifizieren, nicht aber in Echtzeit während der Messung.

Auf einem WINDOWS-Betriebssystem wurde ein Programm zur Visualisierung und Speicherung der Messungen in Echtzeit geschrieben. Es wird über Befehle, die vom „MS-DOS" basierten Steuerprogramm des Grazer SLR-Systems gesendet werden, gesteuert. Es liest die Start- und Stopp-Event-Zeiten des „Riga-Event-Timers", filtert und kombiniert diese zu Laufzeiten, speichert diese und stellt sie auf einem grafischen Bildschirm dar. Nach Erweiterung des Grazer SLR Systems auf 10 kHz wird es die Daten mit 10 kHz verarbeiten und darstellen, während das MS-DOS System weiterhin mit 2 kHz laufen wird.

Contents

List of Figures

List of Tables

1. Introduction

Satellite Laser Ranging measures distances to satellites, orbiting at several thousand kilometers, with a few mm accuracy. The increased data rate and improved accuracy resulting from the Graz 2 kHz SLR system – as compared to traditional 10 Hz repetition rate SLR – suggests that further improvements should be possible with even higher repetition rates (up to several kHz), which would enhance the contribution to almost all SLR applications: ITRF (International Terrestrial Reference Frame), plate tectonics, POD (Precise Orbit Determination), satellite spin determination, time transfer experiment etc.

1.1 Research Objectives and Thesis outline

The number of kHz SLR systems is now increasing, due to many advantages: Higher accuracy and stability, high return rates, and significantly more additional results and applications as demonstrated at Graz kHz SLR: LIDAR applications (using atmospheric back-scatter) parallel to kHz SLR [1] & [2]; accurate spin determination [3]; data transmission using laser pulse position modulation; time transfer experiments (cf. Chapter 1, Satellite Laser Ranging).

Design and implementation of an SLR system with significantly higher repetition rates (i.e. 10 - 100 kHz) is the ongoing challenge of the present study. This upgrade needs a number of modifications in the existing instruments and techniques working at 2 kHz. To increase the laser repetition rate up to several tens of kHz will certainly improve the measurement resolution. The thesis will highlight the issues that come across during the course of feasibility study and design of higher repetition rate (10 - 100 kHz) SLR system and suggest solutions to the problem and envisage the possible advantages/disadvantages in implementation of such a system.

The key issue for the realization of the whole thesis is the availability of high repetition rate lasers with higher power, a pulse length of 10 ps, and high pulse stability. While such lasers at present time are limited to about 1 Watt power at 532 nm, it can be assumed that at least 5-Watt lasers with suitable specifications will be available within the next few years. In addition, for all such laser systems a single-photon sensitive receiver is necessary – and already used in Graz – anyway.

There is usually a trade off between repetition rate and energy per pulse of the laser system i.e. increasing the repetition rate would decrease the pulse energy at specific laser power. The present Graz laser system delivers 400 μJ per pulse at 2 kHz. If such a system is used for higher repetition rate like 100 kHz, the energy per pulse will decrease to 8 μJ. Although tests with such low energies per shot were already successfully performed in Graz to LEO satellites; the analysis shows that the resulting signal / noise ratio would be a problem or even prohibitive for HEO satellites.

Multi-kHz SLR requires essential upgrades for almost every SLR module: laser, event timer, range gate generator, detector, PC / CPU power, software, data storage etc. While the Time-Of-Flight (TOF) measurement device is commercially available (Riga event timer), it was necessary to write special assembly language routines to read the single event times with sufficient speed for 10 kHz repetition rate (which already requires a 20 kHz event timing system…).

The presently used FPGA card can handle up to 512 range gate event times in FIFO registers; however, for a 100 kHz system and a HEO satellite like GALILEO with a maximum TOF of 180 ms, at least 18000 FIFO registers will be needed, which exceeds the FPGA capacity. For the demonstrated 10 kHz system, the necessary 1800 FIFO RG registers are possible.

Another way to solve this problem for up to 100 kHz systems is to use the FPGA internal 500 ps-resolution event timers – developed within this work – and to calculate the RG event times within the FPGA, instead of calculating it in the PC downloading from outside. Several possible implementations were tested successfully (cf. chapter 2, Event Timer). For a 10 kHz system, a third solution is to keep the 500 register FPGA FIFO, to store the excess RG values in PC soft buffers, and to download them to the FPGA only for the next 20 ms maximum. (cf. chapter 3, The FPGA Based Range Gate Generator).

A crucial point is the laser backscatter - overlap of just fired pulses, and return pulses. At present, backscatter is avoided at Graz 2 kHz by shifting the laser fire pulse by 50 µs in case of a detected overlap situation (done automatically and completely within the FPGA); but at repetition rates above about 18 kHz there will be constant and therefore unavoidable backscatter. However, the backscatter intensity will decrease with higher repetition rates due to lower energy per shot, at least reducing the amount of backscatter. (cf. Chapter 4, Laser Backscatter).

The high repetition rates – combined with lower pulse energy – are creating additional noise, and decrease signal/noise ratios; detailed analysis shows the limitations imposed here (cf. Chapter 5, Signal to Noise Ratio), and requires extensive detection algorithms to detect week signals out of heavy noise. (cf. Chapter 6, simulation Program).

After solving the above mentioned challenges, a real time application was written, which gets only basic information from the main Laser PC (which still “sees” only 2 kHz due to unavailability if 10 KHz laser), but can set/store Range Gates and measure time of flight of a system running with up to 10 kHz(cf. Chapter 7, Demo program).

The advantages of such a 10 kHz – at least for LEO satellites - are enormous: At typical return quotes of about 70% for LEO satellites, the amount of data will increase up to a factor of 5. This not only accelerates acquisition during tracking, but also improves the accuracy of Normal Points accordingly. Satellite spin parameter determination also will be improved by a factor of 5: The surface and retro reflectors of the satellite are scanned each 100 µs, instead of 500 µs.

This should improve the spin phase prediction e.g. for the satellite AJISAI, and enable picosecond time scale comparisons via AJISAI mirrors via laser pulses for the first time.

1.2 Motivation

An optimized future Satellite Laser Ranging System could use a 5 watt constant power laser, emitting 10 ps pulses at 532 nm with variable repetition rates and variable energy per pulse: For LEO satellites, it should run at high repetition rates (10 kHz or more) with low energy per pulse (500 μJ or less) to maximize return numbers; for HEO satellites, it should operate at lower repetition rate (e.g. 100 Hz) with high energy per pulse (e.g. 50 mJ) to maximize signal/noise ratio. In addition, the system size should allow direct mounting on the main SLR telescope, to avoid the usual problems with Coudé path alignments, and to enable fully automatic and autonomous operation of Graz SLR station.

This thesis is focused on extensive and very sophisticated SLR techniques aiming on the success of higher repetition rate SLR. It involves many modifications in the existing system to measure time of flight along with the development of new devices and control software. The new timing system is capable of handling high repetition rate SLR data successfully. The thesis investigates the practical limitations in increasing the repetition rate. It discusses also the signal to noise ratio problems and suggest successful solutions. The present work concludes towards a successful implementation of high repetition rate SLR system.

2. Satellite Laser Ranging

Satellite Laser Ranging (SLR) is a technique to measure the distance from an Earth based Laser station to orbiting satellites. Laser pulses with ultra short pulse width (10 ps in Graz) are transmitted repeatedly (repetition rate e.g. 2 kHz for Graz) towards the satellite, knowing in advance its coarse position and orbit. The satellite reflects these laser pulses back to the earth station by means of its onboard retro reflectors. The few or single returning photons are then received at the SLR station. Start and stop events are time tagged with picosecond resolution and accuracy, resulting in round-trip time of flight determination. Applying the necessary corrections for atmospheric refraction and calibration values, defines the distance with few mm precision. Accumulation of this precise data yields an accurate satellite orbit, giving the input for many scientific applications e.g. measurements of International Terrestrial Reference Frame (ITRF), global tectonic plate motions, regional crustal deformation in near plate boundaries, the Earth's gravity field, the orientation of its polar axis and its rate of spin; ocean, ice and land topography etc. The orbits of retro reflectors-equipped satellites (called commonly as Laser Satellites) vary in altitudes from 250 km (GOCE) to more than 20,000 km [1] (GALILEO, GPS, and GLONASS).

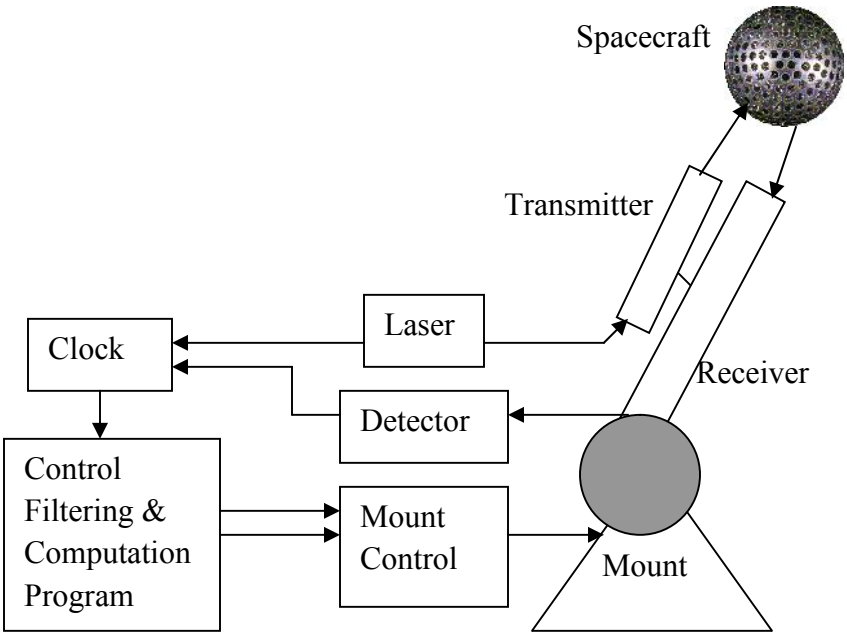

SLR Ground Station

Fig. 2.1: Basic Building Blocks of an SLR station

2.1 Brief History of SLR

Satellite Laser ranging originated when Thomas Maiman invented first solid state ruby laser in Hughes Aircraft Laboratories in early 1960. First orbit tracking was performed using microwave radar with an accuracy of 50 m. 2.5 years after the invention of Ruby laser the satellite Explorer 22 / Beacon B was launched, and few weeks later - on 31st October 1964 Goddard Space Flight Centre (GSFC) recorded few week returns on oscilloscope, determining the orbit with accuracy of 2 -3 m, which was 15-25 times more accurate than microwave tracking at that time; hence the new technology "Satellite Laser Ranging" started to develop. A first international measurement campaign started in 1967 with 6 laser satellites; 4 being launched by NASA (Explorer series) and 2 by France: Diadem 1 and 2. The data collected from this campaign resulted in the formulation of a Gravity model. Lunar laser ranging (LLR) started in 1969 after the success of Apollo mission. In 1972 a successful SLR station was established by Czech Technical University. They further sponsored SLR stations in Poland, Latvia, Cuba and India, while USA deployed SLR stations at Peru, Brazil and South Africa. SLR now became in true sense a global technology.

Geodetic and terrestrial gravity field research started with the launch of the passive satellites Starlette and Lageos-1 in 1975-1976. Stella and Lageos-2 were launched later in 1990. Data from these satellites contributes to geodetic science. In 1980's MOBLAS 4 station achieved a major success of single shot precision of 1.5 cm using mode locked solid state lasers, and micro-channel plate detectors. Later sub centimeter accuracy was regularly achieved [2].

With the advent of portable SLR systems started the study of tectonic plate motion in highly instable areas. Portable systems in 80's were used by Texas, Netherlands and Germany. First GPS satellite was launched in 1989. 1990's was a decade of considerable improvement in SLR system, like the use of high gain semiconductor Single Photon Avalanche Detector (C-SPAD) and dual color SLR systems involving the study of atmosphere and time transfer experiments [3].

21st century SLR entered into an era of pulsed conditioning electronics, fire and return epoch measurement using two different techniques: time interval counters and event timers. Continuous improvements in SLR technique during 40 years of dedicated skilled work now allow measurements with a few mm precision.

2.2 Present and Future Trends

29 stations over the world are providing SLR tracking data in 2010. The most productive stations are Yarragadee, Zimmerwald, Mt. Stromlo, Greenbelt, Changchun, Wettzell, San Juan, Graz, San Fernando, and Herstmonceux [4]. International Laser Ranging Service (ILRS) network is shown in fig.2.1.

Development of constituent technologies of SLR in recent years is quite significant. Many new devices are being developed. For example GaAsP micro channel plate photomultiplier built by Hamamatsu, high efficiency Liquid crystal optical shutter to protect backscatter, other design features, such as the Laser Pulse Repetition Frequency control (to prevent "collisions" between incoming and outgoing pulses) and the dual Risley prism unit for transmitter point ahead, development of new timing devices with features desirable by kHz SLR and many more, covering these developments is out of the scope of this thesis.

Laser Ranging with 2 kHz has been started for the first time in 2003 at Graz SLR station; several stations are following now – replacing the standard 10 Hz rates with 100 Hz, 1 kHz or 2 kHz as in Graz. The 2 kHz data of Graz greatly enhances SLR results, and delivers also new products, like spin parameters of spherical satellites, like Lageos1, Lageos2, Blits, Ajisai, GP-B, Etalon etc.

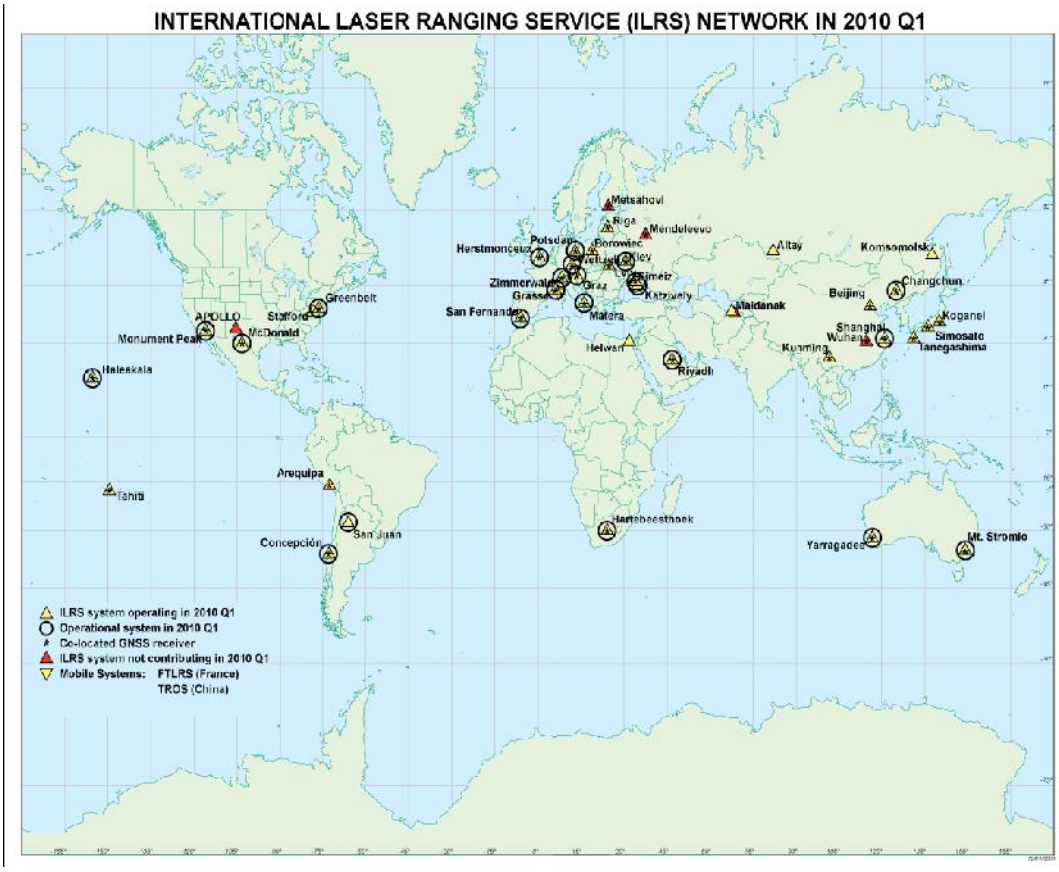

Fig. 2.2: SLR stations over the world work together with ILRS

The scientific arguments for upgrading SLR stations to higher repetition included the increase of single shot precision due shorter laser pulse width (10 ps instead of the conventional 35 – 50 ps), an increase in normal point precision due to compression of a larger number of raw data points, faster acquisition during tracking, and a growing number of add-on experiments possible only with kHz SLR (most of them running in parallel with SLR). Herstmonceux SLR station has also upgraded the SLR system to 2 kHz.

Zimmerwald has recently installed a 100 Hz system, providing a good compromise between traditional 10 Hz SLR systems and higher repetition rate system (2 kHz).The Altay SLR station has been upgraded with a new 300 Hz (instead of 5 Hz) laser, delivering also a higher average output power (0.75 W instead of 0.25 W). All MOBLAS systems (except Tahiti) and MLRS operate at 10Hz on low satellites. In Canberra, Russia unveiled a planned 15 station network of very compact SLR stations with a 25 cm telescope aperture to be completed by 2010. They have also designed a mobile sister station having a larger 60cm aperture. The new Russian stations, equipped with a higher energy (2.5 mJ) but lower rep rate (300 Hz) transmitter, bridge the gap between the older 5-10 Hz systems and the new kHz systems. Performance of different stations in 2009-10 is displayed in fig 2.3.

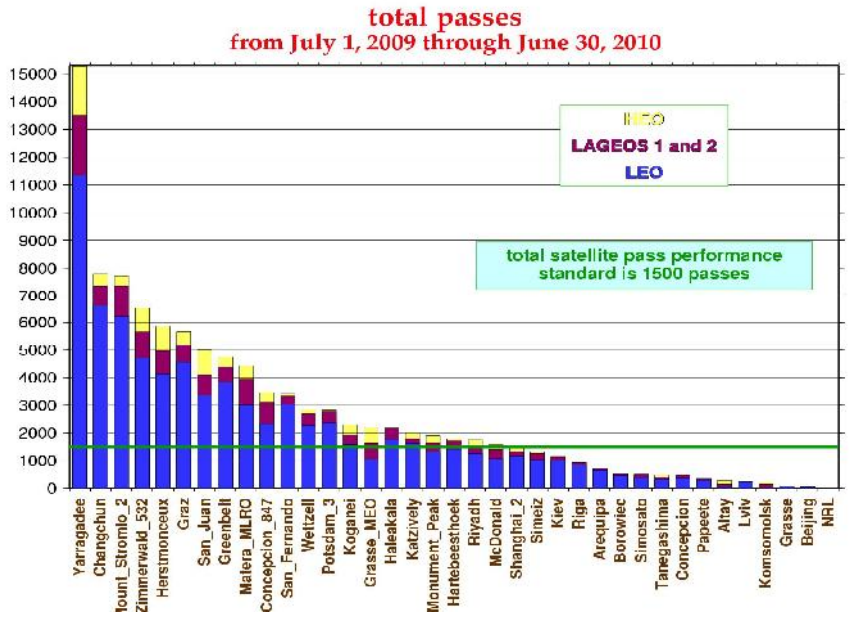

Fig. 2.3: Performance of SLR stations during the previous year

SLR station all over the world vary in their basic operational features but they have some common future tendencies like (1) Increased automation of SLR stations to produce cost effective data throughput; unmanned fully automatic operation and data upload is the ultimate goal of all SLR stations.

Mount Stromlo and SLR 2000 of NASA are two operational examples of autonomous systems. (2) Two color ranging provides more promising modeling of atmospheric refractions. Several stations (e.g. Goddard, Wettzell, Graz and Matera) have demonstrated dual -wavelength capability; however the goal of getting data for better modeling of atmospheric parameters has not yet been reached. (3) The third obvious aim is to develop more powerful stations with large aperture telescopes and efficient optical/mechanical parts to improve the data to achieve single -shot range precision of a few millimeters. The Matera station in southern Italy and the remotely controlled station Tanegashima in Japan both use powerful lasers and large optics.

(4) With the availability of better communications and web access, many stations now submit their data on an hourly basis (5) kHz lasers: With higher repetition rate lasers, faster event timers, and better control software, SLR systems are now able to significantly improve the ranging results. The new Graz SLR station was the first to successfully operate a 2 kHz laser system, increasing the data volume by up to two orders of magnitude. The SLR 2000 prototype is also being developed with this capability, as are upgrades at several other stations mentioned already above." We think that kHz systems will be the future SLR standard; we assume that SLR stations switch to kHz within the next years; this is not a very easy task, but it can be done! …" was well envisaged by "G. Kirchner "[5].

2.3 Components of Satellite Laser Ranging System

Any SLR system is characterized by a number of system parameters, which are optimized to track satellites with sufficient accuracy. Accuracy is characterized by the minimum possible range resolution explained by (Eq.2.1)

$$R = -\frac{c}{2} T_p \tag{2.1}$$

A laser pulse of 10 ps pulse width allows a range resolution of 1.5 mm, if single photon detection is used (which HAS to be used for kHz SLR due to low single pulse energy). Other limitations in accuracy are caused by detectors, electronics and event timers. The basic components of satellite laser ranging unit include transmitter, receiver, timing unit and the process control computer. Transmitter consists of a Laser system and transmit telescope to transmit laser pulses at a certain repetition rate. Receiver includes receive telescope and detector system. Timing unit is consisting of devices which can measure time of flight of laser pulses and determine the epoch timing i.e. Event Timer and Range gate generator. The process control computer executes the SLR operation software.

2.3.1 Transmitter

The transmitter includes laser system transmit telescope and the software control routines. A laser system (LASER; Light Amplification by Stimulated Emission of Radiation) usually consists of an optical resonator (laser resonator, laser cavity) in which light can circulate (e.g. between two mirrors) and within this a resonator gain medium (e.g. a laser crystal), which serves to amplify the light.

The pumping energy excites the laser material to a higher energy state (fig 2.4). If pumping energy is permanently provided to the system, the state of emission becomes stationary and the reflection of the light by the mirrors at both sides is brought to an oscillation at the characteristic wavelength determined by the laser material. The SLR community is currently using two types of lasers. Ruby Laser (1st and 2nd generation SLR), Nd: YAG (3rd generation SLR) and derivates (e.g. Nd: Vanadate).

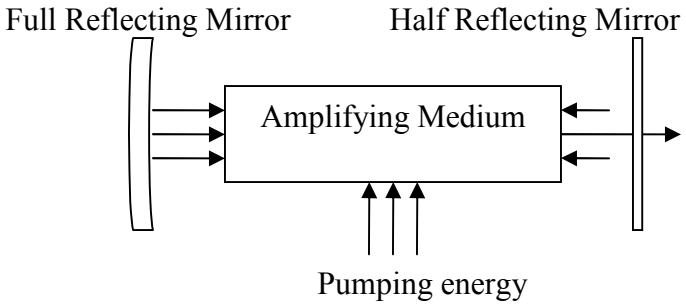

Fig 2.4: Principle of a laser oscillator

Ruby lasers were the first lasers used for SLR; they emit at 694.3 nm, a dark red light; but the minimum pulse width of 2-5 ns limits the achievable SLR accuracy to several centimeters, ruling out now the use of Ruby lasers for SLR.

The SLR site at Graz uses a 2 kHz DPSS (Diode Pumped Solid State) Nd: Vanadate laser system, which is very stable, almost maintenance free, and which produces short pulses (10 ps) with excellent stability. The pulse generation is started with a SESAM oscillator (SEmiconductor Saturable Absorber Mirror); this is followed by a Regenerative Amplifier, which is controlled by an external Pockels Cell to switch in/out the pulses; the amplified pulse is fed into a post amplifier, followed by a Second Harmonic Crystal to convert > 50% of the IR (1064 nm) energy into green (532 nm). This last amplifier is pumped by pulsed diodes (with about 90 A in 60 μs), while the first two modules are pumped with CW diodes. The pump diode modules are user replaceable, without having to realign the system; lifetime of the pump diodes is specified with > 5000 h; by minimizing the current, and by fully automatic software control (e.g. automatic switching off at longer periods of inactivity) having demonstrated already more than 7 years of continuous operation before exchanging the pump diodes. Due to the low energy per shot, we receive mainly single photons from higher orbiting satellites, like LAGEOS or higher; from Low Earth Orbiters (LEOs) we still get multiphoton returns, resulting in close to 100% return rates [5].

The short laser pulses generated by the laser oscillator are led to the transmitting telescope via a series of mirrors, and sent towards the satellite. The divergence of the laser beam is variable in order to optimize the returns from different targets. The transmitting and receiving telescopes are rigidly fixed on the mount, moving in azimuth (±270°) and elevation (-5° to +185°) which allows the pointing in all directions. Both these axis can be controlled with an accuracy of 5 arc seconds. For stations using telescopes with separated transmit/receive telescope, it is sometimes difficult to maintain correct laser beam pointing due to Coude path mirror drifts etc. Different stations use different techniques; the Graz station uses a CCD camera to check the outgoing laser direction, and to correct the beam pointing to the centre of display by slightly tilting the last mirror using tiny piezo-driven motors [6].

2.3.2 Receiver

The receiver includes the optical receiving telescope and the photon detector used to determine the event time of pulse return. The receiving telescope at the Graz-Lustbuhel SLR facility is a Cassegrain system with 50 cm diameter. In order to avoid wrong return signals a 0.3 nm bandwidth spectral filter is used which only allows light at the laser wavelength to pass through. There is also a spatial filter by means of a variable iris aperture to set the field of view between 150 to 1500 μrad. Beyond that a so called range gate is set which specifies a narrow time window (usually 200 to 400 ns) within which the return signal is expected to arrive. The setting of range gate depends on the coarse distance of the satellite a priori known from the ephemeris data. These spectral, spatial and timing filters ensure a noise reduction as much as possible.

The core part of the detection package is the photon detector which detects, amplifies and converts the received photons to current. The ratio of the generated electronic pulses to the rate of incident photon pulses defines the quantum efficiency of the detector; the larger this ratio, the better the ability to detect the faint signal. Basically there are three types of photon detectors (1) Photo-multipliers (PMT), (2) Micro-channel-plate (MCP) and (3) Single Photon Avalanche Diode (SPAD).

2.3.2.1 Photo-multiplier

Photo-multipliers are vacuum tubes with their cathodes treated with special photo-emissive material. The sensitivity of the detector highly depends on the type of the thin material. One disadvantage of PMTs is their rather slow impulse rise time of about 2-20 ns. The rise time is the time span between the moment the incident pulse hits the cathode and the instant the resultant current reaches its maximum.

2.3.2.2 Micro-Channel Plate

In the mid 80's the so called micro-channel plates were introduced for photon detection. Micro-channel plates consist of several millions of capillary tubes made of glass. These tubes have diameter 10-20 μm and length of about one centimeter. All these tubes together build a small plate and are inside coated with a special electron emissive material. These tubes are arranged parallel, but show a small angle of several degrees against the direction of incident electrons. An incident electron hits the inner side of a tube and initiates an emission of further electrons to generate an electric pulse. To some extent every individual tube is working similar to a PMT.

2.3.2.3 Single Photon Avalanche Diode (SPAD)

The state of the art photon detector is a semiconductor diode called Single Photon Avalanche Diode (SPAD). Avalanche diodes are special photo diodes, which are operated slightly below their break down voltage. When gated, the applied voltage is increased above the break voltage. An incident photon creates free electrons; the high charge field in the low current zone of the pn- junction is extremely accelerating these electrons.

Which consequently trigger the emission of secondary electrons and so initiates an avalanche effect. Avalanche diodes amplify the signal by a factor of 106 when operated above their break voltage; this is high enough to detect single photon events. Such breaks also occur after a few µs anyway: This is called dark current, and is about 400 kHz for the Graz SPAD: When gated, the SPAD, even in complete darkness, will produce a break pulse within 2.5 µs average; to reduce this effect the SPAD chip is cooled down to -60°. The main advantage of SPADs is their robustness, high sensitivity, and "digital" output. The main drawback is the relatively high dark noise (as compared to PMT and MCP); during daylight, the inherent single photon sensitivity produces some MHz of background noise which cannot be avoided, and has to be handled by the software (PMT and MCP produce "analog" output pulses, and thus can be switched to multi-photon detection, avoiding most of the daylight background noise, however loosing then the high single-photon sensitivity).

All three detector types show typical time walk effects; multi-photon inputs create output pulses which are higher (PMT, MCP) or appear earlier (SPAD) than those from single photons. A special detection circuitry developed in Graz efficiently compensates this time walk effect; the initial 240 ps time walk (when increasing from single photon to 1000 photons) is reduced to < 10 ps time walk. In addition, the Graz SPAD circuitry is also compensated for temperature drifts (all semiconductors are sensitive for temperature changes); the final product hence is called C-SPAD.

The return signal from HEO satellites is a single photon only, nevertheless the daylight background noise is in the order of 5 MHz; thus the software of the Real Time tracking system has to filter the measured values, to reject noise points, and to display and store only valid or possible identified returns.

2.3.3 Timing Unit measuring Time of Flight (TOF)

The detector output triggers a timing unit which actually measures the round trip time of laser pulse. There are two approaches used in timing devices, the time interval counter and the event timer approach. Time interval units measure the TOF of the optical pulse, while in event timer; the TOF is computed by differencing the laser fire and the satellite echo epoch.

These timing devices are not only used to measure the two-way time of flight, but also the epoch of the start pulse. Therefore the clocks are synchronized usually with GPS time, using a Time & Frequency GPS receiver (which also outputs the stabilized reference frequency of 10 MHz, supplied to the event timer system.

2.3.4 The process control computer

The process control computer calculates the satellite ephemeris data from satellite predictions in terms of Earth fixed X/Y/Z coordinates at specified time intervals.

Based on the ephemerides and knowledge of the SLR station position the process computer continuously determines azimuth and elevation angles which are transmitted to the mount controller. The coarse distance between the ground station and satellite is computed simultaneously for a proper range gate setting. The time of laser firing and the two-way time of flight are stored by process control computer. This computer also handles the acquisition of meteorological data as well as other system and data flow control tasks.

2.4 The Laser Satellite Effects

For achieving a duplex communication link the response of satellite with onboard retro reflectors is prerequisite. Dedicated SLR satellites are completely spherical, completely passive, and are fully covered with retro-reflectors, so that there is always at least one reflector with an adequate field of view visible from the SLR station, independent of the elevation and attitude of the satellite.

The principle of operation is that a light beam that hits the retro-reflector is always reflected back in the same direction, independent of the angle of incidence. A single retro-reflector has a specific field of view with in which it is able to reflect most of the received power back to the transmitter. However in order to increase the tracking capabilities to lower elevations, often numerous reflectors (reflector array) are mounted at slightly different angles.

The overall response of a retro-reflector array is called cross section; the cross-section/response of a laser satellite depends on the size and design of the arrays, and the specifications of the cube corners. It is a function of incidence angle, velocity aberration, wavelength, and polarization if the cube corners are uncoated. The cross section vs. incidence angle or the full cross section matrix can be used to obtain more accurate signal strength predictions for satellites where there are large variations in the cross section [7].

The retro-reflectors of non-geodetic satellites are not arranged concentrically with respect to the satellite's center of mass. Thus, a proper relation between the reflectors and the center of mass has to be found and adequately considered for each ranging measurement. The same reference has to be considered at the space segment and is called the center of mass (CoM) correction. The CoM correction describes the geometric relation between the individual reflectors and satellite's center of mass. Obviously this relation can be easily determined very precisely for spherical satellites. Measurements to satellite mock-ups are sometimes performed on ground to achieve sufficiently accurate CoM correction values.

2.5 Atmospheric Refraction

Each laser pulse emitted from the laser station travels twice through the Earth's atmosphere before being detected at the ground station. This produces a considerable delay and, as a consequence, considerably affects the measured range. Therefore, atmospheric refraction correction depending on the current state of atmosphere has to be applied.

The atmospheric models together with the local meteorological measurements i.e. pressure, temperature and humidity are used to compute proper refraction corrections in SLR measurements. This is an advantage for SLR: Pressure can be measured very accurately, has no local effects (like temperature or humidity), and can be easily and accurately modeled and extrapolated for the various altitudes.

2.6 Earth tracked satellite

The onboard Retro reflectors on the laser satellites are totally passive instruments having no intelligence or automatic processing. Depending on the various applications SLR satellites can be categorized to types i.e. geodetic satellites, earth sensing satellites and positioning satellites.

Geodetic satellites: Geodetic satellites are mostly passive spheres having the advantage that the centre of mass is correctly determined. Lageos1 & 2, Starlette, Stella, Ajisai, Etalon-II, BLITS and Westpac are examples of geodynamic satellites.

Earth sensing satellites: The category of Earth sensing satellite comprises space crafts that carry instruments designed to sense the Earth with the goal to acquire data on the environmental state of the Earth and its change on a global scale. ERS1 & 2, ENVISAT, Tandem-X, Grace-A, Grace-B are examples.

Positioning satellites: This class of satellites which are equipped with navigation systems and retro-reflectors include GPS-35/36, Glonass, GALILEO and COMPASS satellites. These satellites are racked by SLR for POD (Precise Orbit Determination) to improve the orbit accuracy provided by the international GPS service (IGS). There are also a number of SLR satellites which are used for experiments and research like GOCE, CRYOSAT, and REFLECTOR etc. Covering all the satellites and their launch objective is beyond the scope of this thesis, for details about satellite visit the ILRS International Laser Ranging Service website [8].

2.7 Special Features of Graz SLR Station

SLR station development has been a continuous process of research and technical modification during the last 4 decades. The SLR Graz station is one of the most productive, most accurate and most stable stations, and often plays a role of pathfinder for new innovations and experiments. In 2003, the Graz SLR station has been upgraded to higher repetition rate of 2 kHz; the first station in the world working with higher repetition rate which dramatically enhanced its overall performance. The Graz station has some unique features regarding laser ranging. The small team at Graz is developing and maintaining most of hardware/software tasks themselves i.e. maintaining ps laser system at 2 kHz, Coudé path adjustments and receive transmit path alignment themselves additionally setting up and aligning single photon detection system. Build a stable SPAD time walk compensation circuitry and setting up a fast response timing system for ultra-fast pulses.

Write convenient to use real time system for detection, filtering and storing real time returns and writing software for data handling/calibration and checking meteorological values.

2.7.1 Previous 10 Hz system vs. the new 2 kHz SLR at Graz

Initially the Graz station was using a 10 Hz, Nd: YAG laser with 100 ps pulse width; it was using a passive mode locking dye to reduce the pulse width to 35 ps, and an active mode locking system to reduce the amplitude variations to 10 %. It also for the first time introduced the Semi Train pulse technique. The idea behind the Semi Train is to emit a series of fixed spaced short pulses instead of one single pulse. About 10 pulses per shot with a well-defined time separation of 8759 ps were emitted with continuously decreasing energy level. In the case that the first return pulse could not be detected, there still was a chance to detect any of the remaining pulses. Since the Semi Train separation interval is known, the Semi Train return signals can be folded to the first pulse during post processing (and also during real time tracking).. This Semi Train technique drastically increases the detection probability, especially when using single photon detection with low quantum efficiency [9].

In 2003, this 10 Hz laser (35 mJ @ 532 nm, 35 ps pulse width) has been replaced by a 2 kHz, DPSS Nd:Van laser system, using a SESAM seed laser with a Regenerative amplifier and a post amplifier; this laser delivers 400 uJ @ 532 nm per shot, with a pulse width of 10ps FWHM; due to the low energy per shot, only single photons from higher orbiting satellites are received , like LAGEOS or higher; from Low Earth Orbiters (LEO), close to 100% return rates are achieved.

2.7.2 Time Walk Compensation

As already mentioned, SPADs when operated above break voltage are able to detect single photons with picosecond accuracy. However, when multi-photon events are detected the measured epoch time is shifted significantly towards earlier epochs and thus introduces a ranging error. This undesired effect is called time walk effect and has to be compensated. It has been verified by Graz SLR team that there is strong correlation between the incident signal strength and diode's impulse rise time. This effect can be compensated by means of ultra-fast comparators which measure the rise time differences and translate them to appropriate time shifts.

2.7.3 Automatic Range Gate Shifting

The range gate is a time window in which the return signal is expected to be detected by laser station. Obviously in order to avoid the detection of wrong echoes not originating from transmitted pulse the length of the range gate should be as short as possible. The C-SPAD has to be gated about 65 ns before expected arrival of the return photon(s), to establish a stable, uniform electrical field in the depletion zone.

On detection of a start pulse, the epoch time of this start pulse is determined, the epoch of the expected return photon calculated and stored in the Range Gate Generator (RGG) because in the 2 kHz system up to 300 pulses are traveling at the same time to or from a satellite, the RGG uses FIFO registers to store and handle the individual gate epochs.

The next expected RG epoch is compared to an actual time scale; if this time arrives, the RGG issues the Range Gate pulse. This system is implemented within an FPGA (Field Programmable Gate Array) device, but would achieve only resolutions of 100 ns (10 MHz); to improve the resolution, a programmable, analogue delay generator covers an additional resolution of 0 – 100 ns, thus increasing the resolution to < 0.5 ns.

2.7.4 Convenient to use Real time Control Software

The Real-Time Control of the SLR Station Graz is based on a 2.4 GHz PC; to get maximum speed and deterministic real-time response, the PC is running on MS-DOS; all RT programs are written in FORTRAN. The ranging programs are designed to allow untrained observers to range successfully to satellites after a minimum training period of a few hours only; many automatic routines make otherwise tricky things simple and straight forward. The noise is initially reduced using the automatic control of range gate width, range gate shift etc. and software filter is implemented in form of identification routines.

The software filtering is achieved through identification routines which identify the real returns from the false alarm based on the identification bandwidth. If a residual (observed minus calculated range) lies in a certain band (100 ps) and previously minimum number of residual also exist in this band then it is marked as the identified residual and is stored on the hard disk and displayed on the screen of the PC. This minimum number can be set by observers to adjust sensitivity versus amount of false alarms; the acceptance band width is adjusted by other routines automatically, according to satellite, range gate width and other parameters.

This simple procedure is fast, effective, and gives a very nice user interface for a variety of satellites: Low Earth Orbiters with close to 100% return rate result also in easy interpretable graphics as high orbiting satellites – like GPS - which can have return rates far below 1%. Other routines are filling all identified returns into histogram bins; the bin with maximum identified returns is plotted on the screen.

2.7.5 Laser Back Scatter avoidance

One of the problems of kHz laser systems arises from the backscatter of the laser pulse crossing the lower part (up to about 5 km altitude) of the atmosphere; this loads significant optical noise on the detector during the first 50 µs after laser firing; any single photon return during this time might get lost within this backscatter; for a 1 kHz system, this will be the case for 20% of all shots (40% for a 2 kHz system). The problem was avoided completely by appropriate shifting of laser firing times in case of an overlap situation; this method was introduced first by Graz station.

This method involves insertion of a 50 μs delay into Fire Time Counter, whenever a Return is predicted within the next 50 μs. This will be necessary again as soon as this shift becomes effective in the return times; and it will slightly reduce the repetition rate (about 1.9 kHz instead of 2 kHz).

2.7.6 Automatic Calibration

To keep the system at the highest possible accuracy, it is calibrated at least once per hour; during the calibration, the laser pulses are attenuated by de-phasing the pump diodes of the last amplifier. The laser diodes are still pumped with the same pulses to keep the thermal equilibrium, but about 300 μs too late, so that the last amplifier does not contribute anymore. These attenuated pulses are directed into our near calibration target, about 1 m in front of the telescope [4]; in each calibration run, 10000 returns are measured – which takes only about 10 seconds at 2 kHz and 50% return quote – and averaged to give the calibration value plus statistical information (skew, kurtosis, peak minus mean etc.). The calibration value is necessary to correct and refer all measured distances to the invariant reference point (the crossing point of azimuth and elevation axis within the telescope). The main emphasis is to watch closely any changes of the calibration values (usually stable within a few ps), to monitor the behavior of the system, and to record all drifts etc.

3. Event Timer

Accurate timing is crucial for modern SLR application. Timing devices capable of measuring time with a resolution and precision of a few picoseconds require intelligent techniques and sophisticated equipment. The SLR station has to measure the Time-of-Flight of a laser pulse from the station to the satellite and back. To get the highest possible accuracy for the distance, this time of flight (TOF) has to be measured as accurate as possible.

There are mainly 2 different methods for such high-accuracy TOF measurement Time interval counting and Event timing. Time Interval Counters: measures the time for the laser flight from the station to satellite and back. HP5370 and SR620 were used as interval timers in SLR community in the past with conventional 10 Hz SLR systems, but at present these are not any more in use because of their non-linearity, temperature instability and also they are not applicable for kHz SLR: Due to the high repetition rate (some kHz) there are always more than 1 pulse – up to 300 pulses for high orbit satellites for a 2 kHz SLR system – simultaneously traveling between SLR station and satellite.

Event timers determine laser firing epochs and epochs of the returns independently; The PC uses these epoch times, calculates the difference and thus the time-of-flight, giving the distance to the satellite. The event timers have extended functional possibilities and provide much better precision (up to units of picoseconds) as compared with conventional time interval counters. These features are important for many applications but especially for Satellite Laser Ranging SLR) where an extreme precision of measurement is vitally needed. Currently the event timers are considered as the most suitable devices for advanced SLR applications and are being developed by different SLR stations. Such a system has been built and installed 1999/2000 in Graz, and is used since that for all SLR measurements. This Graz Event Timer (ET) measures each event with an accuracy of ±2.5 ps, a non-linearity of max. ±2.5 ps, and is extremely stable for long periods of time and large temperature ranges. However, it needs about 400 μs to fix the event time, limiting the maximum repetition rate for this ET to 2.5 kHz [10].

The Event Timer A032-ET is an advanced version of the earlier model A031-ET of Riga event timers. As compared to this model, the A032-ET offers better single-shot resolution (<10 ps RMS), 60 ns dead time, and client-server interaction support. The A032-ET is a computer-based instrument that precisely measures epoch times when events (input pulse comings) occur. More than 10 SLR stations are using A032-ET in SLR operation. Another upgraded version of Riga event timer A032 is presented in 16th international conference of international Laser and Lunar ranging 2008 [11]. Compact event timer for One Way Laser Ranging offering timing resolution of 130ps is reported at 16th international conference of international Laser and Lunar ranging 2008 [12].Such devices are already built on individual stations and by commercial vendors.

3.1 Medium Resolution Digital Event Timer in Graz FPGA

We developed a much faster (20 ns response time), but medium resolution (250 ps) event timer within the GRAZ FPGA, dedicated – and accurate enough - for range gating purposes. After detecting a laser start pulse event time, the expected return event time is calculated, and loaded into the Range Gate Generator (RGG), which then activates the detector short before arrival of the return photon(s). While the present RGG uses a combination of a digital 100-ns-resolution FPGA counter PLUS a programmable analog delay chip, we implemented now a fully digital Range Gate Generator into the FPGA - using a 5-ns-course counter, and a 500 ps vernier to improve linearity and stability [13].

Most common methods to measure interval times employ a standard frequency (clock), which determines the basic resolution of these measurements. To achieve higher resolutions, a vernier is most commonly used to interpolate within one time period of the standard frequency.

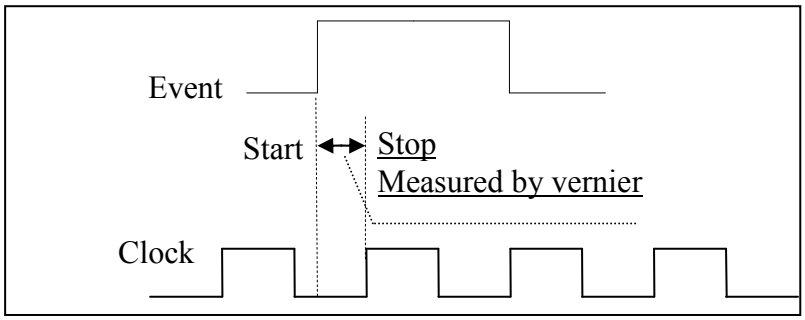

Fig. 3.1: A digital vernier interpolates between 5 ns clock pulses

To implement a series of identical, cascaded delay chains (consisting of standard logic gate e.g. AND) we had to disable the automatic optimization of the Quartus Compiler for the Altera FPGA device. These delay chains- consisting of varying number of AND gates- were built in Altera FPGA Apex 20k chip on the Graz FPGA card (fig.3.3) to test and compare the timing resolution and jitter (fig.3.2).

This FPGA contains the entire logistics for the range gate generator (RGG) with a resolution of 0.5 ns can store up to 300 range gates and managed automatically. The card automatically and asynchronously reads and stores all of the event timers measured events, which can be read quickly from the demo PC.

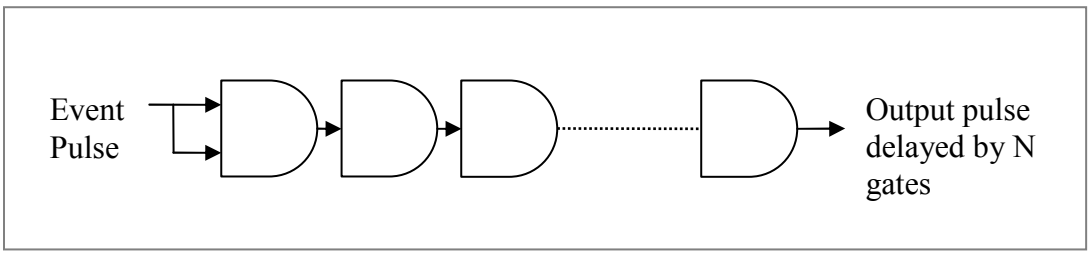

Fig. 3.2: Delay Chain of N-AND Gates

Several 64-bit serial I / O interfaces are also implemented, which are connected via BNC cable to the telescope, the observer cabin and the laser table, each of these interfaces allows easy control/adjustment of mirrors, switches, security bits, signals for the acoustic receiving indicator, etc. All of these functions are already implemented and used for SLR Graz for 2 kHz range gating and controls.

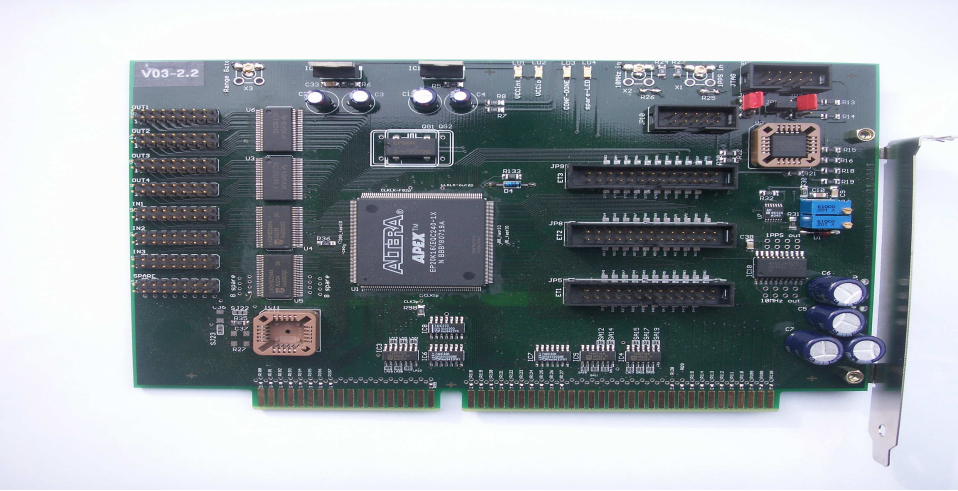

Fig. 3.3: Graz ISA PC Card; FPGA containing Event Timer

Table 3.1-Measuring delays and Jitter

No. Of Gates	Delay ns	Jitter ps	Difference in two delays ns	Delay Per Gate ns
10	26.7805	23		
20	30.2225	20	3.442	0.3442
30	33.949	21	3.7265	0.37265
60	45.472	22	11.523	0.3841
100	59.926	21	14.454	0.36135
200	94.0325	23	34.1065	0.341065
250	112.2425	24	18.21	0.3642

Table 2.1 shows that the delay caused by each AND gate is approx. 350 ps on average, which can be reduced by floor plan layout optimization (arranging the logic cells in order inside the FPGA chip) providing the standard vernier resolution of 250 ps with 20 ps jitter. Repeating the same experiments with different type of standard logic gate (AND, OR, NOT NOR and NAND) where one delay chain consists of one type of logic gates, produce the same result as the vernier uses standard gates with 250 ps transit time per gate.

We also tested the temperature drift of a 100-AND-gate delay chain; it drifted with about 10 ps/C° (fig. 3.4), which is quite acceptable considering the required resolution, and the location of the PC / ISA Card / FPGA in the air conditioned laser room.

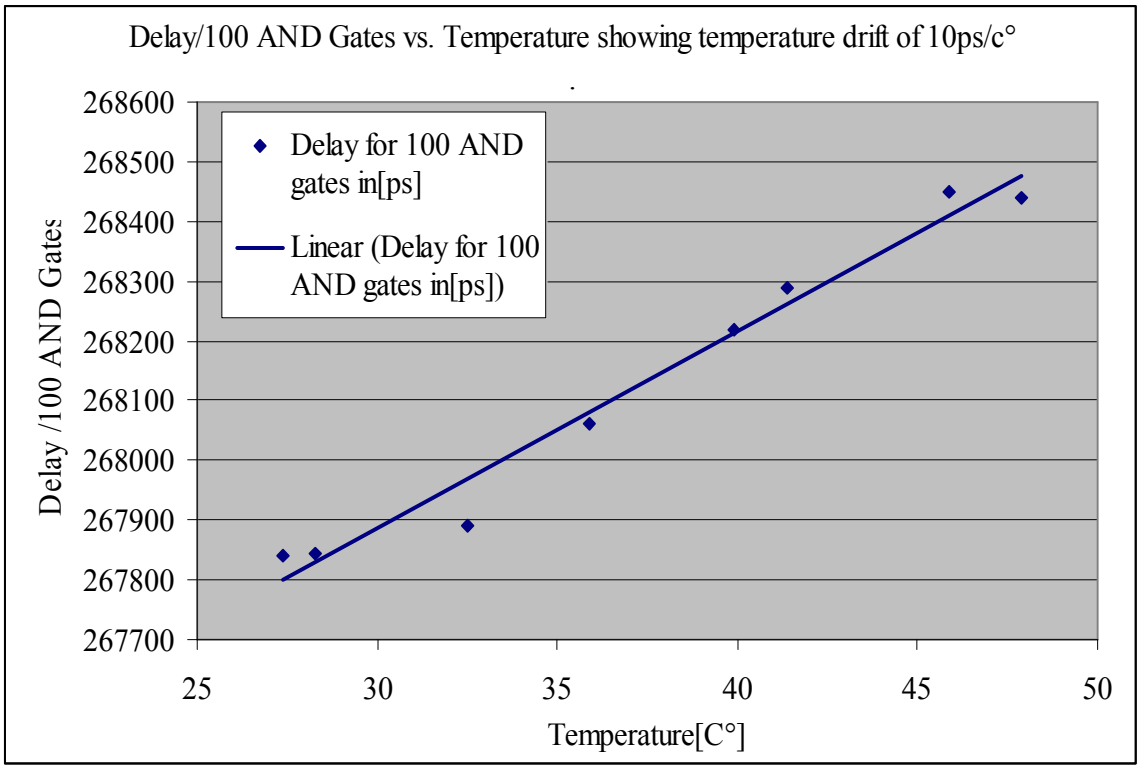

Fig. 3.4: Delay of a 100-AND-Gates Delay Chain vs. Temperature

3.2 Event Timer Implementation

The fast response digital event timer is implemented based on above mentioned vernier method. This method uses a 200 MHz counter and a vernier for the 5 ns intervals. The vernier uses standard AND gates with 250 ps transit time per gate (fig. 3.2). To implement a series of identical, cascaded delay gates we had to disable the automatic optimization of the Quartus Compiler for the Altera FPGA device. The event pulse (e.g. Laser Start Pulse) starts traveling through several parallel chains of AND Gates; each chain consists of an increasing number of AND gates; the next following 5 ns clock pulse is used as a STOP pulse for this simple vernier (fig. 3.6). If the start pulse reaches the end of a chain BEFORE the STOP pulse, a "1" is latched into an output register; if not: a "0"… (fig.3.5). The bits in this output register represent a measure for the 0-5 ns interpolation; together with the latched actual reading of the 200 MHz coarse clock this forms a 250 ps resolution event time.

The event timer is implemented into the ISA card FPGA and optimized its floor plan layout to achieve best linearity and uniform resolution. Simulation of such a circuitry gives promising results for the required speed and resolution of this Event Timer (fig. 3.6).

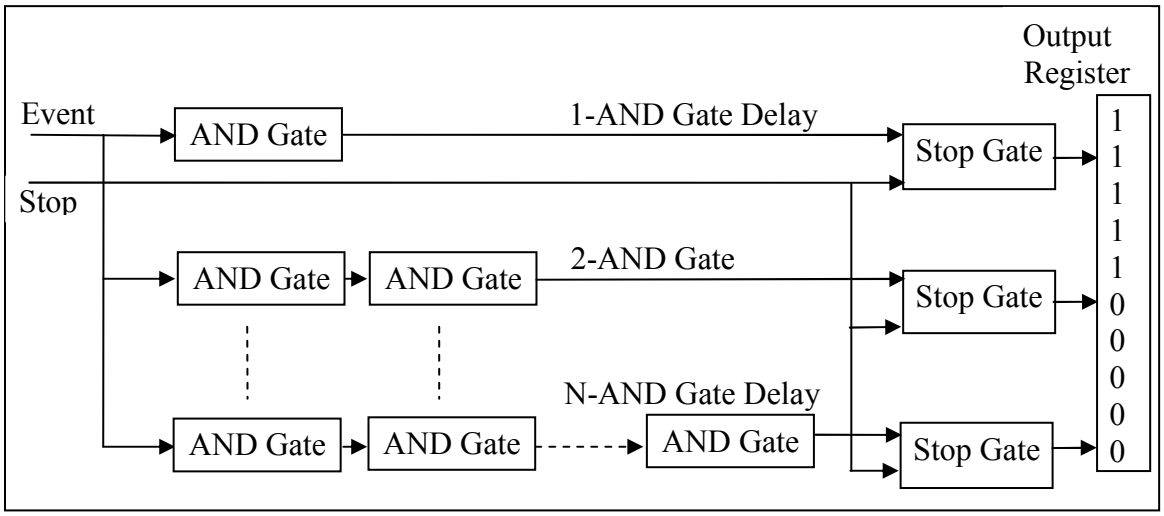

Fig. 3.5: Event timer unit, using chains of AND delay gates of increasing length

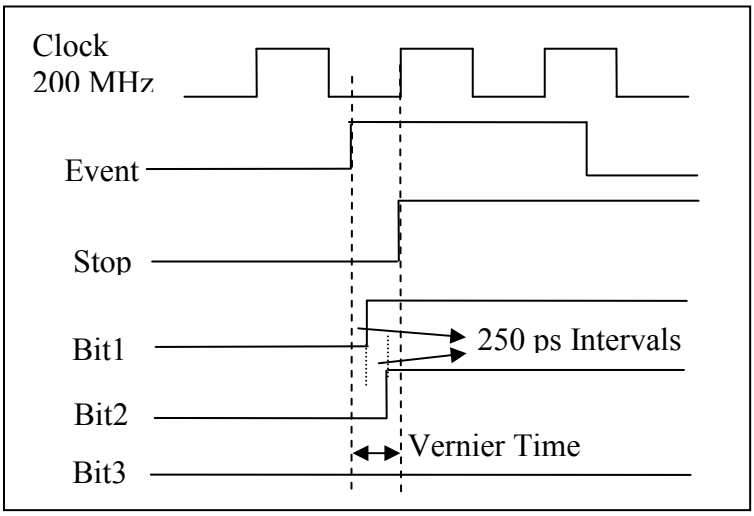

Fig. 3.6: Vernier measurement, interpolating 5 ns intervals

Although an event timing accuracy of < 300 ps is fully sufficient for the purpose of Range Gate Epoch determination, we tested possible improvements by implementing 4 such Event Timer Units in parallel (fig. 3.7) into the FPGA. All 4 event times are read by PC and averaged there; this average reduces the FPGA event timer jitter to 217 ps RMS. The Event timer is tested and at Graz SLR station for its performance and comparison with the existing Graz event timer. The newly developed event timer proved to be useful for range gate generation and setting purpose.

3.3 Event Timer Experiment and Results

We implemented a test setup using a DG535 Pulse Generator, a Stanford SR620 Time Interval Counter, and a GPS system (1 pps) to test the linearity of designed event timer.

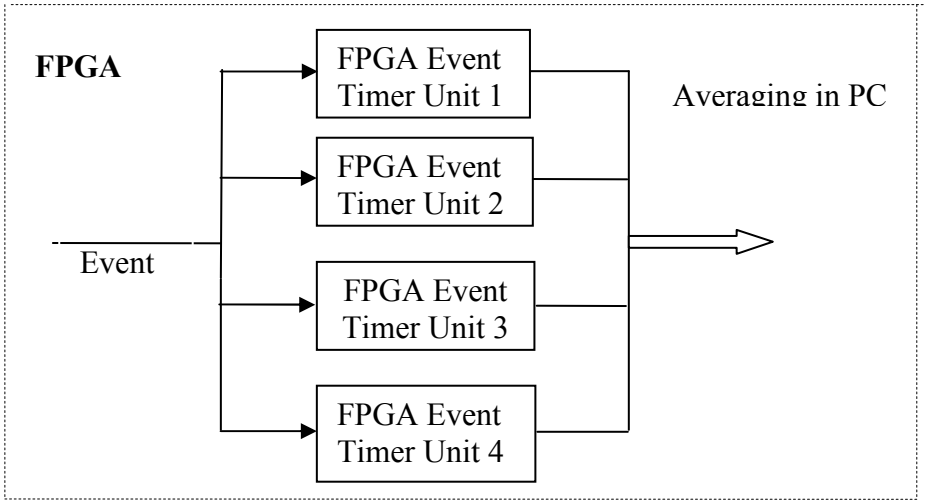

Fig. 3.7: Four parallel Event Timers

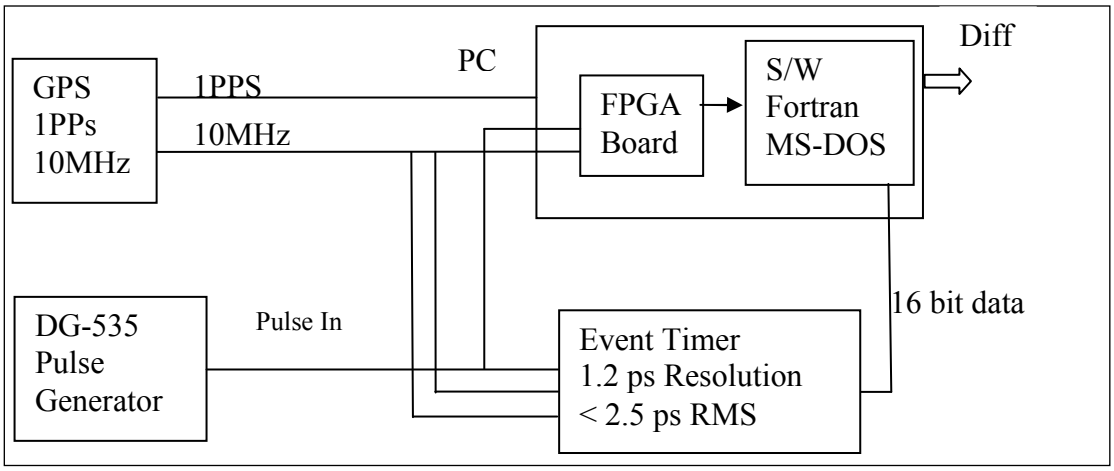

Fig. 3.8: Test setup to compare Graz ET and FPGA ET measurements

We compared its results with those of our ultra high precision (1.2 ps resolution, < 2.5 ps non-linearity) Graz ET [10].The differences between both showed an RMS of 260 - 290 ps (fig.3.9).

Resolution and non-linearity of a single FPGA Event Timer unit is more than adequate for our purpose of fast RGG setting; for even better resolution, a multi-channel Event Timer can be implemented. Due to its very high speed, it is well suited for the existing 2 kHz SLR system and also for systems with significantly higher repetition rates. The present event timer can be used further for some applications like SLR event timer for fast Range Gate setting (used in Graz SLR), Sub-ns event timing of arriving aircraft transponder signals, any other application which needs sub-ns event timing and time intervals jitter analysis of regular signals.

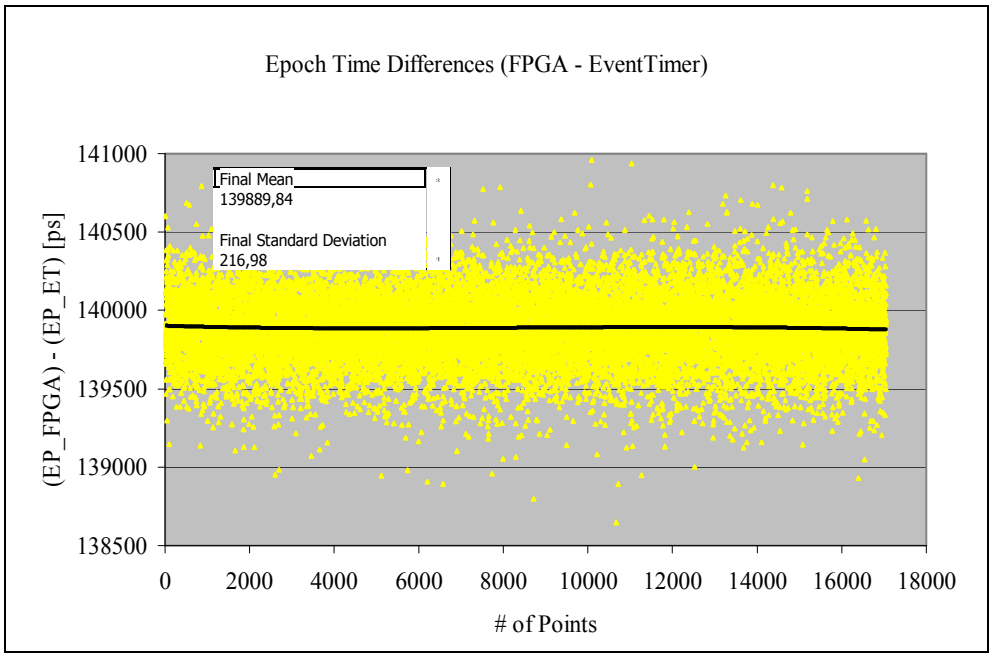

Fig. 3.9: Four parallel Event Timers: Standard deviation of 217 ps

3.4 Range Gate Generator

We used a 200 MHz clock and a chain of AND gates to implement a Range Gate Generator (programmed via PC) - which generates a range gate pulse short before the actual return of the laser photons - with a resolution of 500 ps and an accuracy of < 1 ns.

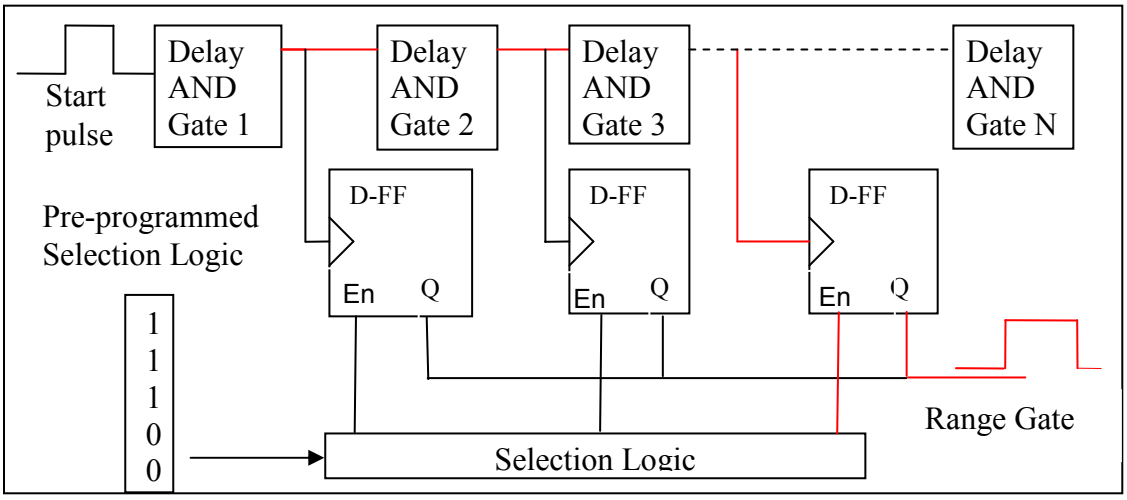

Fig. 3.10: Block Diagram of Digital Range Gate Generator

The start pulse (fig. 3.10) travels through the chain of AND gates. The output of each gate switches its associated D-Flip-Flop as soon as the start pulse has passed. Only ONE out of these D-Flip-Flops is activated by the pre-programmable selection logic, and generates the Range Gate pulse (fig. 3.10).

3.5 Experiments and Results

A test setup using a DG535 Pulse Generator, a Stanford SR620 Time Interval Counter, and a GPS system (1 pps) measured the linearity of the Range Gate Generator.

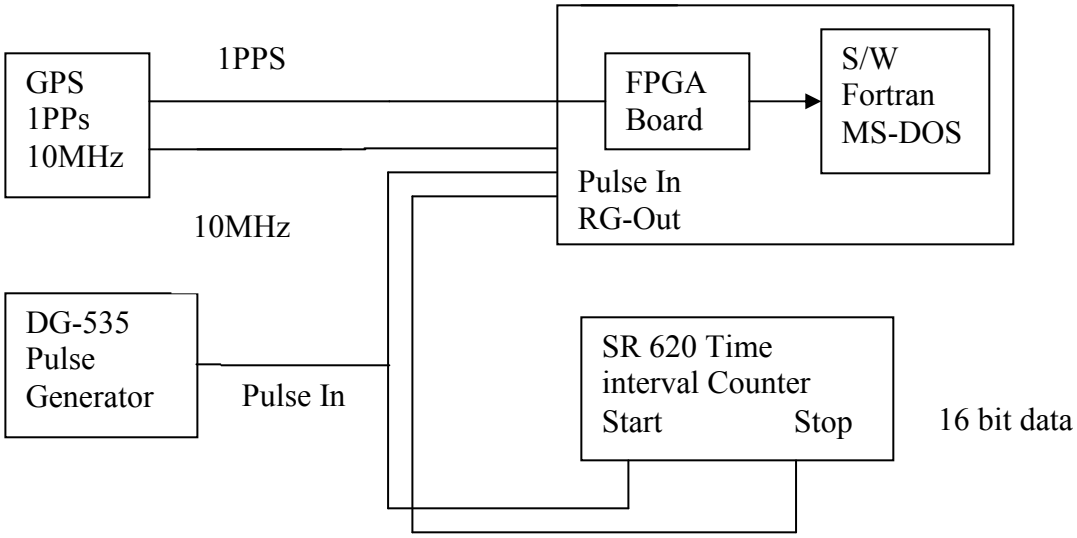

Fig. 3.11: Test setup to test the linearity of Range Gate Generator

We tried 3 different placements (floor plan layouts; both manual placements and/or automatic placements of the AND gates and D-Flip-Flops within the logical cells) of the Range Gate circuitry inside the FPGA to find the optimum linearity (fig. 3.11); the selected final placement has the best R-squared value ("R2" in fig. 3.12) and linearity.

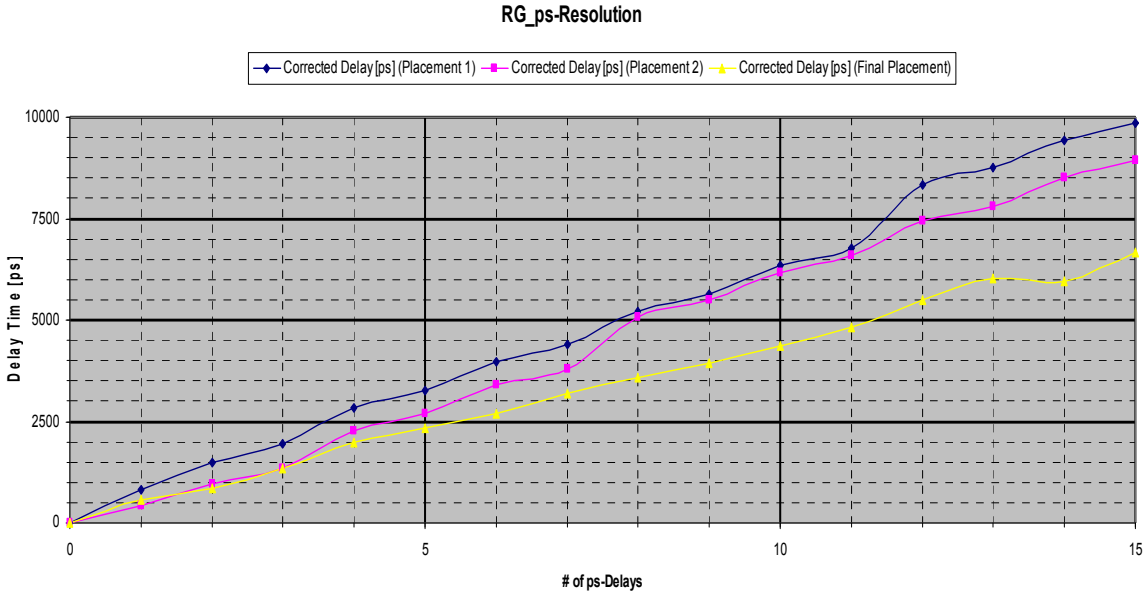

Fig. 3.12: Delay Time (ps) vs. Delay Chain Length

The ISA FPGA Card now contains a 250 ps resolution event timer and a fully digital Range Gate Generator. Both are used to speed up the Rang Gate setting for the present SLR system. Both circuits now allow significantly higher speed, improved linearity, and better stability.

4. The FPGA-Based Range Gate Generator

In Satellite Laser Ranging (SLR) systems, laser firing times are not known in advance to better than some 10 ns; therefore they have to be measured accurately to determine the return event time to within a few ns, and to program a Range Gate Generator (RGG) which activates the detector some 10 ns before return photon arrival. The available time for that depends mainly on the laser repetition rate; while this is not a problem for the usual 10 Hz or few kHz SLR stations, it needs fast calculations for higher repetition rates; e.g. for a 100 kHz SLR system, we have a maximum of 10 μs to measure the start epoch time, to calculate the expected return event time, and to load the RGG.

The start event time can be measured within some 10 ns, using FPGA circuitry [13]. To calculate the return time, we tested 3 different FPGA based methods; each of these methods had to interpolate for the given epoch within predefined time-of-flights or distances. (1) An embedded processor on the FPGA uses an 8-point Lagrange interpolation; however, this needs about 500 μs (only useful for a 2 kHz SLR system). (2) A low level design (VHDL based multiplication / division etc.) using also 8-point Lagrange interpolation is much faster (few μs only), but due to its 32-bit arithmetic it could not achieve the required <1 ns accuracy (at least one order was missing). (3) For the third low level design, we used linear interpolation – giving high speed (4 μs) - between closely spaced supporting points (reducing the interpolation errors to less than 1 ns)

Most SLR systems use detectors which have to be gated a short (some 10 ns) before the expected arrival of the return photon. This Range Gate Event Time is calculated – usually using some interpolation schemes - after measuring the laser firing time, and loaded into the RGG. For higher laser repetition rates, the available time for that is decreasing (10 μs for a 100 kHz SLR system). A commonly used algorithm is the 8-point Lagrange interpolation [15], because it is smooth (it does not introduce oscillations) and accurate. We implemented this Lagrange interpolation algorithm, using a) the NIOS processor on the FPGA, b) a VHDL design with hardware arithmetic. The 3rd solution used a linear interpolation, again with hardware arithmetic on the FPGA.

4.1 Lagrange Interpolation using Embedded Processor

To implement the 8-point Lagrange interpolation with the soft core NIOS II processor (implemented in the Altera FPGA), we used an Altera De2-70 board with Cyclone-II EP2C70 FPGA (fig. 4.1) [16]; this board also contains other hardware modules, e.g. memory chips (SSRAM, SDRAM, Flash), I/O devices (LED, LCD, switches, SD card slot, 7-segment display) and Connectors (JTAG, USB, VGA, RS-232, PS/2, IRDA).

We implemented a complete embedded processor system, with the Altera NIOS processor, and its operating system, within the FPGA [15].

The NIOS processor hardware system contains also the SOPC (system of programmable chips) and other hardware description files (fig.4.3).

Fig. 4.1: DE2-70 Altera Board

The SOPC is created using the SOPC builder (a part of Quartus compiler (Altera Corporation, [17])), which configures the system inside the FPGA. This FPGA/SOPC system then contains the user defined NIOS processor, memory and I/O controllers. We wrote several description files to interface between FPGA and the other on-board components, like clock, SDRAM, SSRAM, I/O lines and user defined hardware modules. This NIOS processor based hardware system is then loaded onto the FPGA after assigning proper pin configuration to interact with board I/O components.

The 8-point Lagrange interpolation program is written using the NIOS-IDE compiler, and then loaded into the target memory (SSRAM). The NIOS processor can load and execute the program from SSRAM automatically. A load-enable line (Fig. 4.2) interrupts the NIOS processor to load the data points from the SD card. The processor - running at 200 MHz - reads the pre-calculated data points and stores them on the SDRAM. A single record of data points defines a complete satellite state vector (time, X, Y, Z).

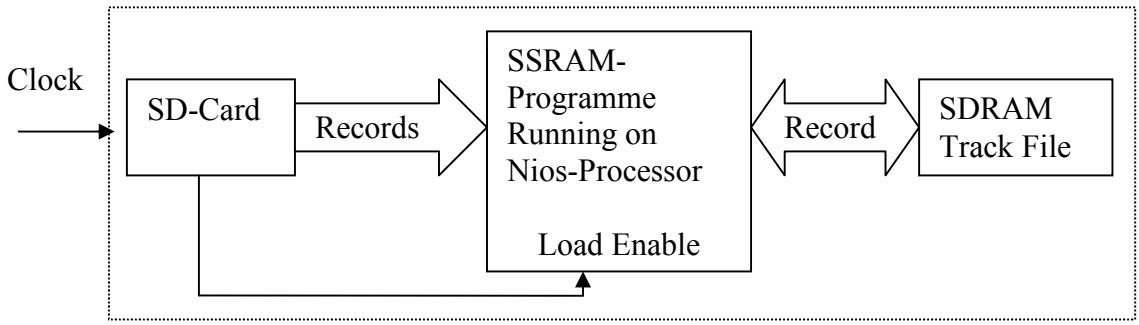

Fig. 4.2: NIOS Processor: Loading and storing data points

Once the data points are loaded, the processor waits for a start epoch time (in LPM register, user defined; fig. 4.4). When a start epoch arrives, the processor searches through the SDRAM, loads 8 records from the SDRAM (the last 4 records BEFORE the start epoch, and the first 4 AFTER the start epoch), interpolates within this data for the start pulse epoch, and stores the resulting range gate epoch into an output register (fig.4.4).

In a real SLR system, the Range Gate Generator then will produce a RG pulse at this epoch time, to activate the detector. We built the system using the on-board 50 MHz clock; it needed about 3 ms to calculate the range gate, which is too slow even for the Graz 2 kHz SLR system.

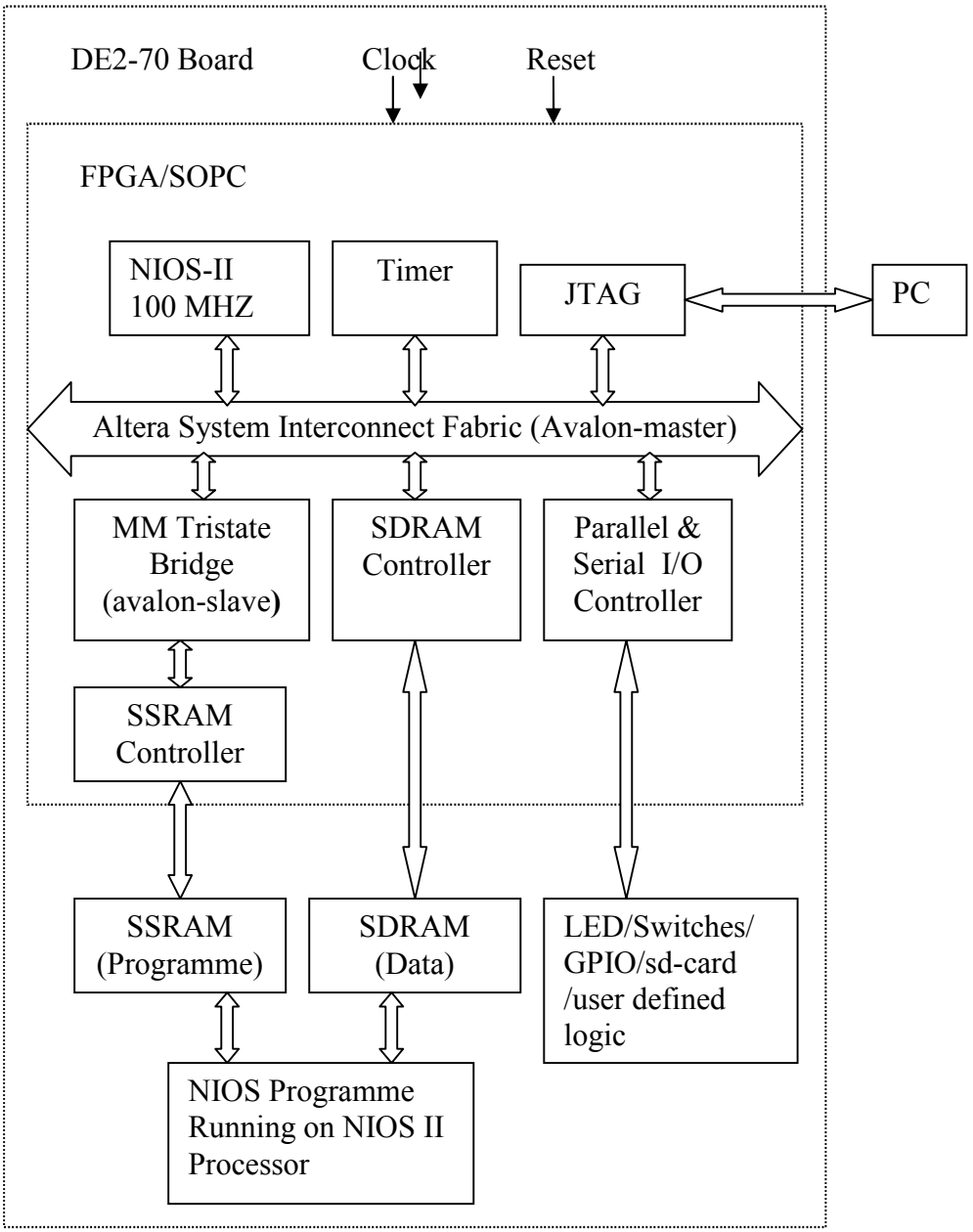

Fig. 4.3: Block diagram of NIOS System on the DE2-70 board

To improve speed, we changed the processor clock to the maximum possible 200 MHz, reducing the calculation time to 500 µs for a single range gate calculation. Supplying time-of-flight values only instead of X/Y/Z, we improved the speed by another factor of 3; however, this would limit the laser repetition rates at about 6 kHz. We conclude that such an embedded system is not suitable for high repetition rate SLR Systems, in spite of maximizing its calculation speed.

4. 2 Lagrange interpolation using VHDL modules

We then implemented the 8-point Lagrange interpolation, using low level VHDL arithmetic modules, and Altera LPM (library of parameterized modules) to minimize the calculation time. The data set for the interpolation consisted of epoch time / range value pairs.

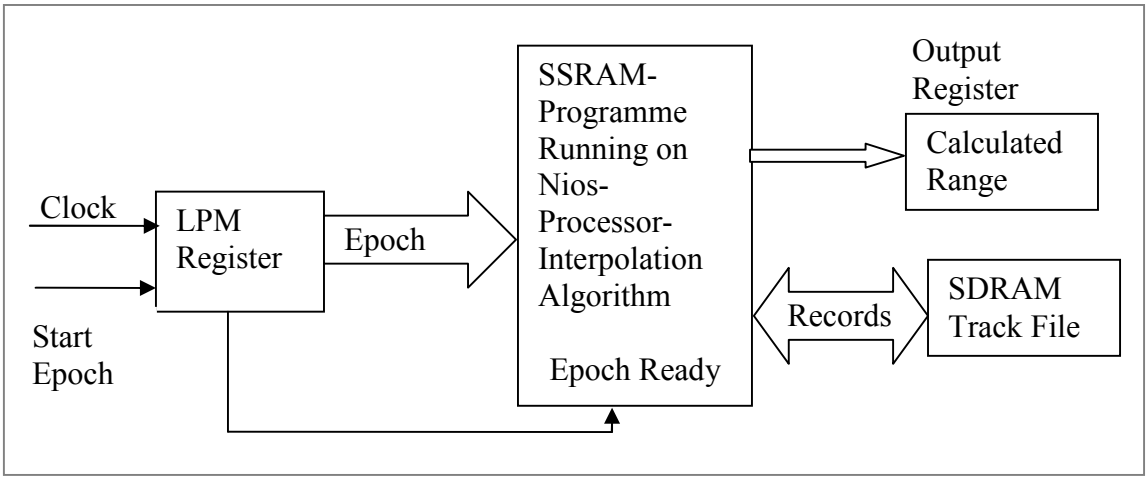

Fig. 4.4: Calculating Range Gate with NIOS processor

The interface unit (Fig. 4.5) reads the data points when the external load_en (load enable) signal occurs; and stores the records into the LPM-RAM (Random access memory). The interface unit activates the Write_En (write enable) signal and increments the address [7..0] to write the next record. We used selection control logic and LPM–Multiplex (multiplexer) to direct the appropriate address to LPM-RAM because three different units (interface unit, index finder, and interpolator) are accessing the RAM for writing and reading.

The Index-Finder (fig.4.5) unit waits for the start epoch; as soon as the start epoch time arrives, it compares this epoch time with the time values in the RAM, to determine the 2 closest time values (before and after). It stores and provides their indices to the interpolator unit. The interpolator unit loads the corresponding 8 records - as needed for the Lagrange interpolation - into its internal arrays, interpolates the data and stores the resulting RG event time into the output register.

We tested the calculation speed and the resulting accuracy of the calculated range gate. The implemented low level circuitry is capable of calculating the range gate within 6 µs which is more than adequate for the present 2 kHz system, and allows for future high repetition rate SLR systems (up to the 100 kHz range). However, the accuracy was limited (10 ns accuracy in the best case) because the used Altera Quartus Compiler only offers 32 bit arithmetic modules.

Even normalizing the data points for begin of each interpolation interval – thus reducing the size of the numbers significantly – was not enough; for the required 1-ns accuracy; 64-bit arithmetic modules – not available for that system – would be necessary.

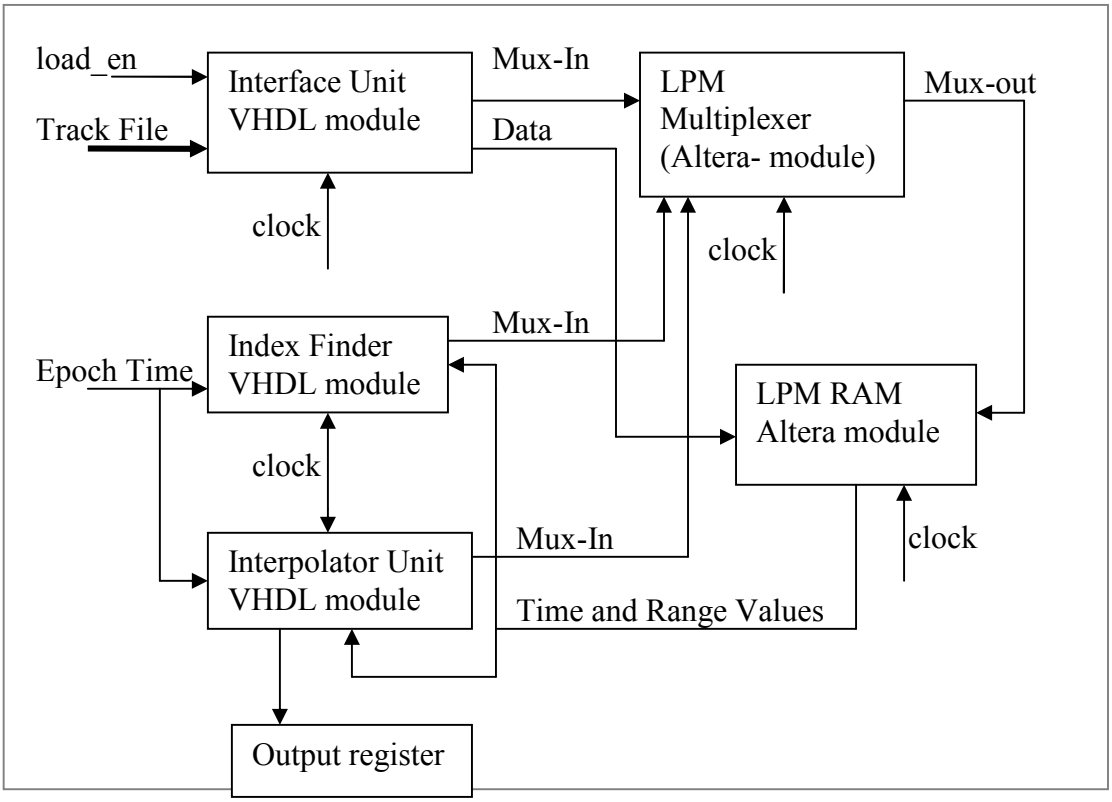

Fig. 4.5: Block diagram of low level implemented circuitry

4.3 Linear Interpolation using VHDL modules

To improve the accuracy – and to keep the high calculation speed – we shortened the interval between the data points, and implemented a linear interpolation scheme. The intervals were chosen to get a maximum of 2000 points per satellite pass (instead of about 100 for the Lagrange data points); the errors introduced by linear interpolation for the short intervals than remain below 1 ns, except for a few LEO (Low Earth Orbit) passes with elevations close to 90°. Instead of data pairs (epoch time and range) we use only start epoch, time interval value, and the list of up to 2000 ranges, which reduces memory requirements by 50%. The available memory on our FPGA board does not allow for more than these 2000 ranges. These ranges were pre-calculated in the attached PC, using Lagrange interpolation. The implemented linear interpolation circuitry has a 32- bit interface (Fig. 4.6). The records transferred here are divided into two parts: A 4 bit sub-address and a 28 bit data value (Table. 3.1). The 4 bit sub address is used by the Address Decoding and Routing Unit (ADRU), to route the 28 bit data to its respective memory place.

If the sub-address is 0000, the Address Decoding and Routing Unit would interpret that a new series of 28 bit data is downloaded now, and will route the following data to the RAM according the next sub-addresses. Similarly, the Address Decoding and Routing Unit detects and stores a few additional values, like start time, time bias, cable delay values etc.

Table. 4.1: Sub Address and Data Values

Sub ADD	28 bit –Data Values
0000	memory write
0001	Start Epoch
--	----------

Due to the limitations of the 32-bit arithmetic modules we also subdivide the epoch time into 2 parts: A 1-s-Integer values, and the fractional part. The Index Finder Unit (IFU) uses the Integer value to find the required index, while the fraction part is used for the linear range interpolation. Index Finder Unit (IFU) waits for the epoch time; as soon as the start epoch time arrives, it calculates the index of 2 time values (before and after) using the start epoch of track file interval and 1-s integer part of epoch time, then selects two range values from LPM RAM.

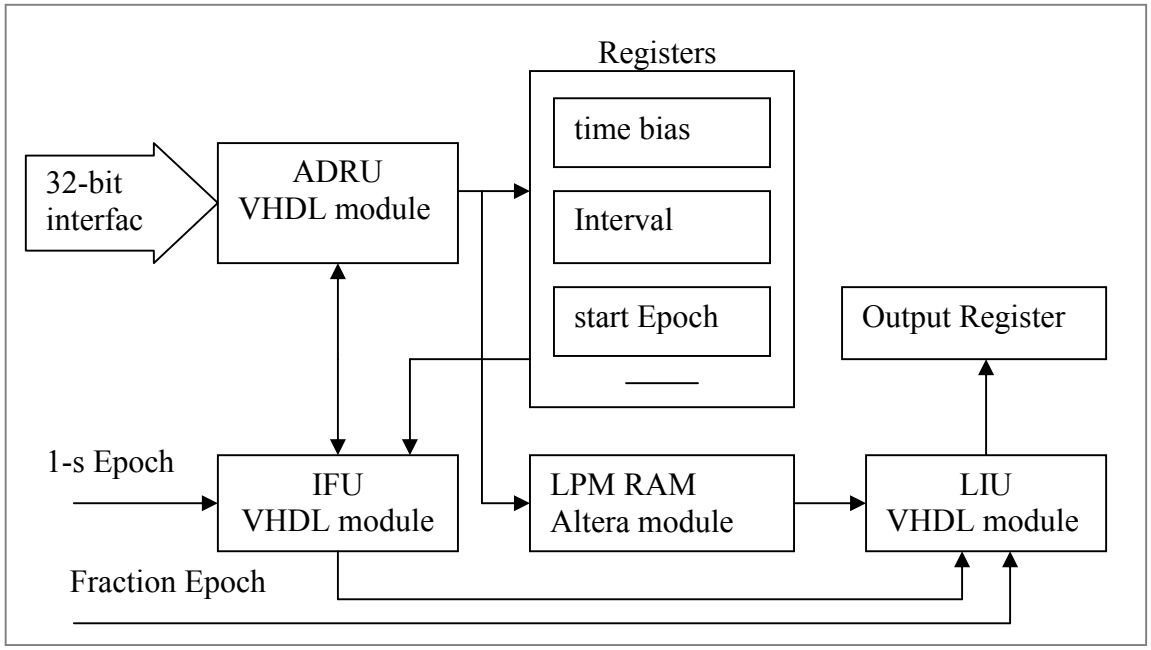

Fig.4.6: Block Diagram of Linear Interpolator Design

The Linear Interpolator Unit (ILU) contains all required arithmetic subunits. It fetches two range values according to the index as provided by the IFU and calculates the range gate value using the proper range values, interval and fractional part of epoch time value.

The calculated range gate epoch time is corrected with the previously stored parameters, like cable delays, calibration constants etc. and stored in the output register. This VHDL Linear Interpolator requires only a few more negligible pre-calculations in the PC, but more memory on the FPGA.

However, this can be solved by transferring only a small part of the required data into the FPGA (e.g. once per second) instead of transferring the full data set at pass begin. It is very fast (4 µs for a single interpolation), and sufficiently accurate (< 1 ns). Thus it is well suited for future high repetition rate SLR systems up to 100 kHz.

5. Laser Back Scatter

In the case of higher repetition rate SLR systems like Graz kHz SLR, multiple pulses are traveling through the atmosphere at any time. While within atmosphere, the transmitted laser pulse produces backscatter. If this backscatter coincides with a just returning photon reflected form a satellite, this photon most probably will be lost for detection, due to a detector blocking by backscatter (overlap situation).

Laser backscatter occurs within 5 to 10 km from the receiver; because the detector has to be gated at least 60 ns before the expected arrival of the satellite photon, this backscatter will most probably trigger the detector within these 60 ns, blocking the detection of the satellite photon; the detection probability of return photons is significantly decreased. This overlap effect can be observed easily in the Graz raw files of observed passes of any satellite (Fig.5.1) as repeated periods of dense return points. Laser back scatter phenomena increases the noise by a factor of 5. Such an increase will certainly affect the signal to noise ratio. Graz station working at 2 kHz is transmitting up to 300 pulses simultaneously traveling at the same time to or from a satellite. During the normal routine detection of SLR data in Graz such overlap situations are avoided automatically within the Range Gate Generator programmed in FPGA, which knows in advance the next fire times and return times. The FPGA automatically detects if the return photons are expected within 50 µs of laser firing time; in case, a delay of 50 µs is inserted before the next laser shot. This is called overlap avoidance. During the period of overlap, the repetition rate at Graz SLR is slightly decreased (from 2 kHz to about 1.9 kHz). Graz station can enable/ disable laser back scatter avoidance implemented in the Graz FPGA [18]. Some other techniques are also being developed and implemented to avoid laser back scatter [19]. One possibility is the inclusion of an optical gate, which can suppress backscatter impinging on the photocathode when the detector is gated “off”; however, these devices are usually too slow (few ms switching times), and inherently have < 100% transmission for the return photons.

Laser backscatter can be observed easily in the raw files of observed pass of any satellite when the back scatter avoidance circuitry in the Graz FPGA is disabled (Fig.5.1). While the “normal” background noise (caused by sun light and detector dark noise) is more or less constant throughout the pass, the additional noise caused by backscatter within overlap periods appears as repeated periods of higher noise. This increased noise decreases significantly the detection probability of return photons, and adds a significant amount of noise points in the collected data. Fig 5.2a shows the detected return density with out laser backscatter and fig 5.2b shows the part of the pass where a strong back scatter occurred on the receiver. The noise density increases multiple times during backscatter time in the fig. 5.1 as compared to the times without laser backscatter.

The study of laser backscatter is important while considering the higher repetition rate SLR. At Graz repetition rate of 2 kHz, such an overlap occurs at every 75 km satellite

distance change, and remains for about 7.5 km; for a 20 kHz system however, it will occur after every 7.5 km, resulting in constant backscatter overlap – leaving no chance to avoid it. However, with decreasing energy per shot at higher repetition rates at constant power the resulting backscatter will decrease.

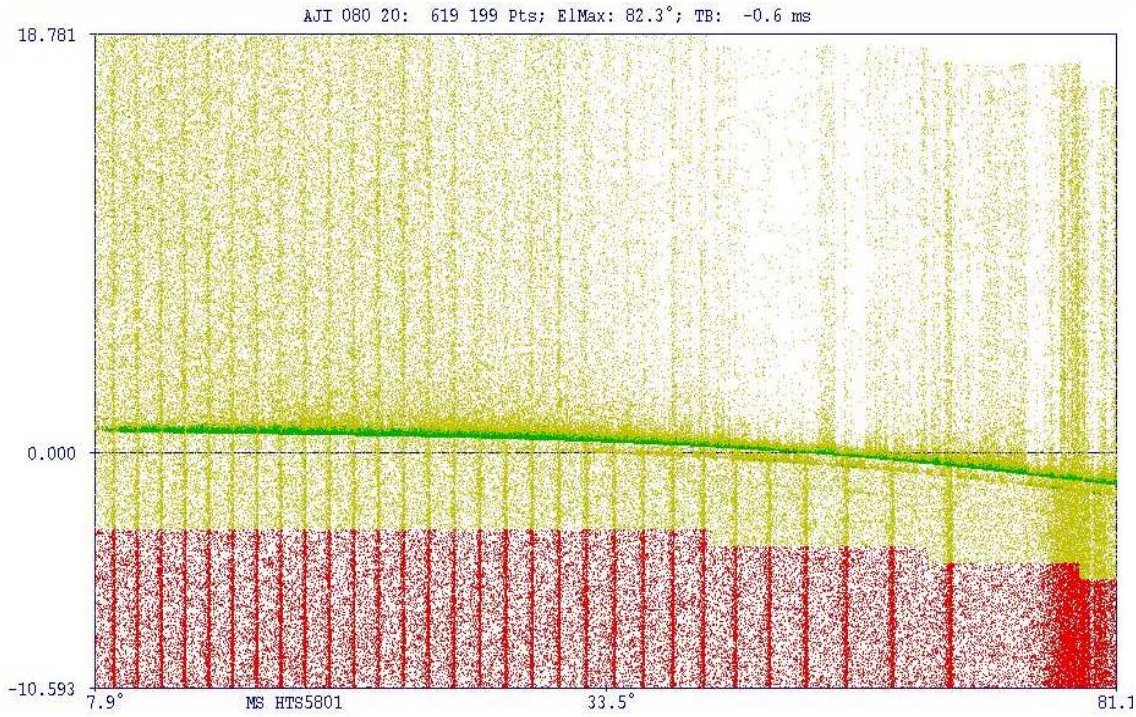

Fig. 5.1: Test pass of satellite Ajisai, showing the repeated periods of overlap

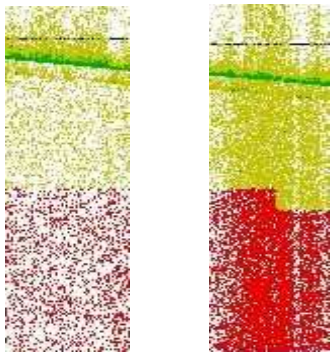

Fig. 5.2a Fig. 5.2b

Fig. 5.2a: A segment of the test Pass (a) no laser backscatter (b) laser backscatter

The analysis is done on the night passes of satellites on the year 2009. While ranging the satellite at lower elevation the laser backscatter is stronger (more noise points/second) and less in duration due to higher speed of approach and vice versa for satellite's closest approach. The duration of laser backscatter varies with ranging distance to the satellite-longer for higher satellites.

5.1 Laser Back Scatter Study

To accomplish a study of overlap phenomena we collected Graz real time data, disabling the automatic overlap avoidance FPGA circuitry. Thus the detector is collecting the sum of detector dark noise (about 400 kHz for C-SPAD in Graz), solar background noise (some MHz during day, close to ZERO during night), and backscatter noise during overlaps. These observations are collected during night times assuming that all additional noise points in the overlap regions are the result of laser backscatter in the atmosphere as solar noise is not present .Fig. 5.1 shows a pass from Ajisai satellite during night tracking on the day 80 of 2009. Repeated periods of overlap are clearly visible when the satellite returns were removed from the data set, and only the total amount of noise points per time was plotted; these tests were extended to a list of different satellites (Champ, Envisat, Ajisai, Lageos and GPS).

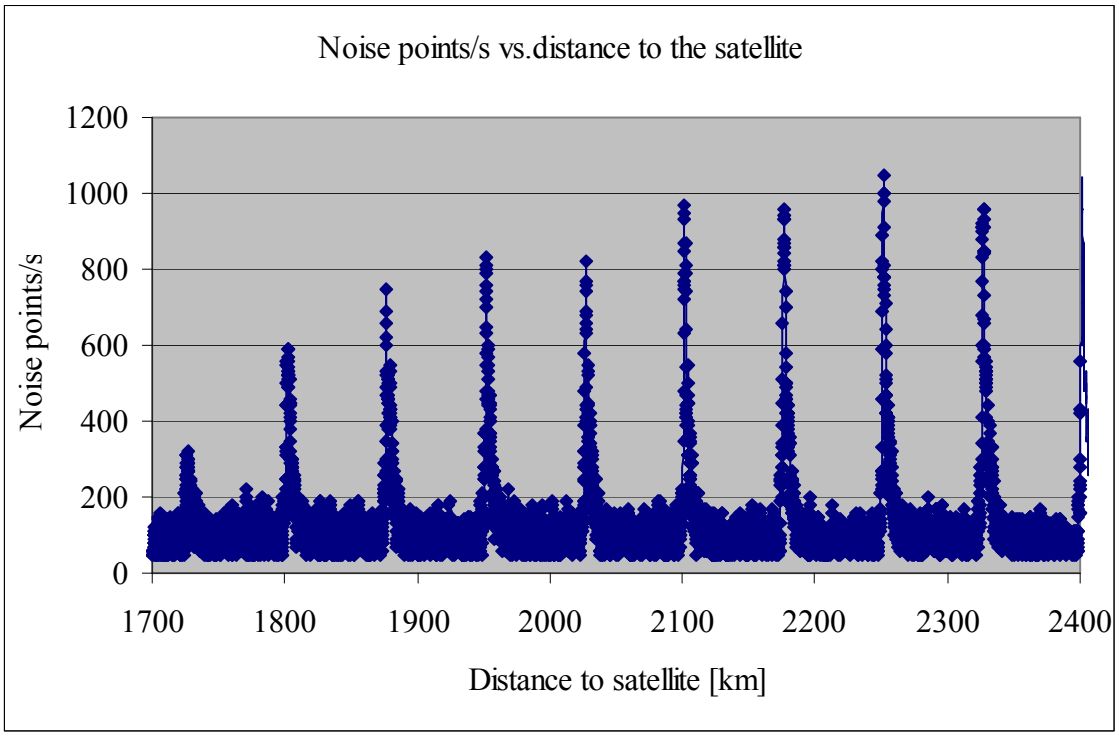

Fig. 5.3: Overlap data collected from Ajisai pass

An Ajisai test pass (fig. 5.3) shows that on the average there are 100-140 detected noise points/s; when the laser backscatter occurrence started, the number of noise points increases, reaches a peak (500-700 noise points per second) and then slowly comes down. On the average 650 noise points per second were recorded for all different satellites. This depends on the satellite pass if it is approaching toward the observing station or going away from the station.

5.1.1 Dependence of Laser Backscatter on Repetition Rate and Energy

In all collected passes of laser satellites mentioned above, with the Graz SLR system of 400 uJ @ 2 kHz it is observed that laser back scatter occurs whenever the distance to the satellite changes by 75 km. This value is a simple consequence of pulse repetition rate; at higher rates, the overlaps will appear at shorter distance changes; e.g. at 10 kHz repetition rate, overlaps will appear whenever the distance to the satellite changes by 15 km; however, the duration of the overlap depends only on the involved atmosphere, and will remain constant at any repetition rate. Intensity of backscatter will increase with higher laser power (e.g. when increasing the laser power from 0.8 W laser up to 5 W level which is possible see Appendix A), but it will decrease at higher repetition rates due to lower energy per shot.

5.1.2 Duration of Laser backscatter

Detectable backscatter occurs up to distances of about 8-9 km; plotting one overlap region for a standard Ajisai pass, we can observe that overlap starts at 2634 km / 160 noise points per second), builds up suddenly to a peak at 2626 km / 1060 noise points (Fig.5.4) and slowly drops down then.

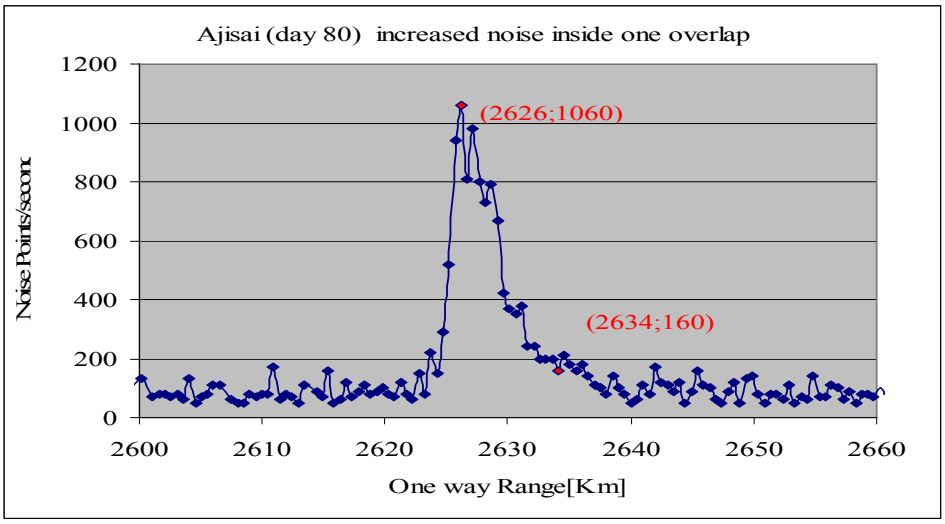

Fig. 5.4: AJISAI pass: A single overlap region

The Range Gate in Graz SLR is opened for a period of 200 ns, which implies that we are observing overlaps in segments of 60 m, which are sliding towards – or away from - the receiving telescope; the closer to the telescope the stronger the backscatter will be. A region with out overlap normally has 50 to 150 noise points per second (within the 200 ns range gate) but in the region of overlap we can observe 600 to 1100 noise points at the peak of overlap.

In the existing 2 kHz system at Graz the range gate is opened 2000 times per second approximately 60 ns before the expected return signal; in this way the system collects without laser backscatter 100 noise points at average which accounts for 540 kHz noise normally; but in the regions of overlap 650 noise points per second on the average corresponding to a noise of 5 MHz which is almost equal to solar noise. Thus the backscatter increases the noise observed during night up to daylight values, and will double daylight noise.

The duration of overlaps varies for different satellites, depending on speed of approach. Speed of approach for lower satellites is higher than that of higher satellites. Champ has least duration of 2-3 second of overlap because of highest speed of approach while in case of GPS 35 the overlap duration is 27-30 s having lowest speed of approach (Fig. 5.5).

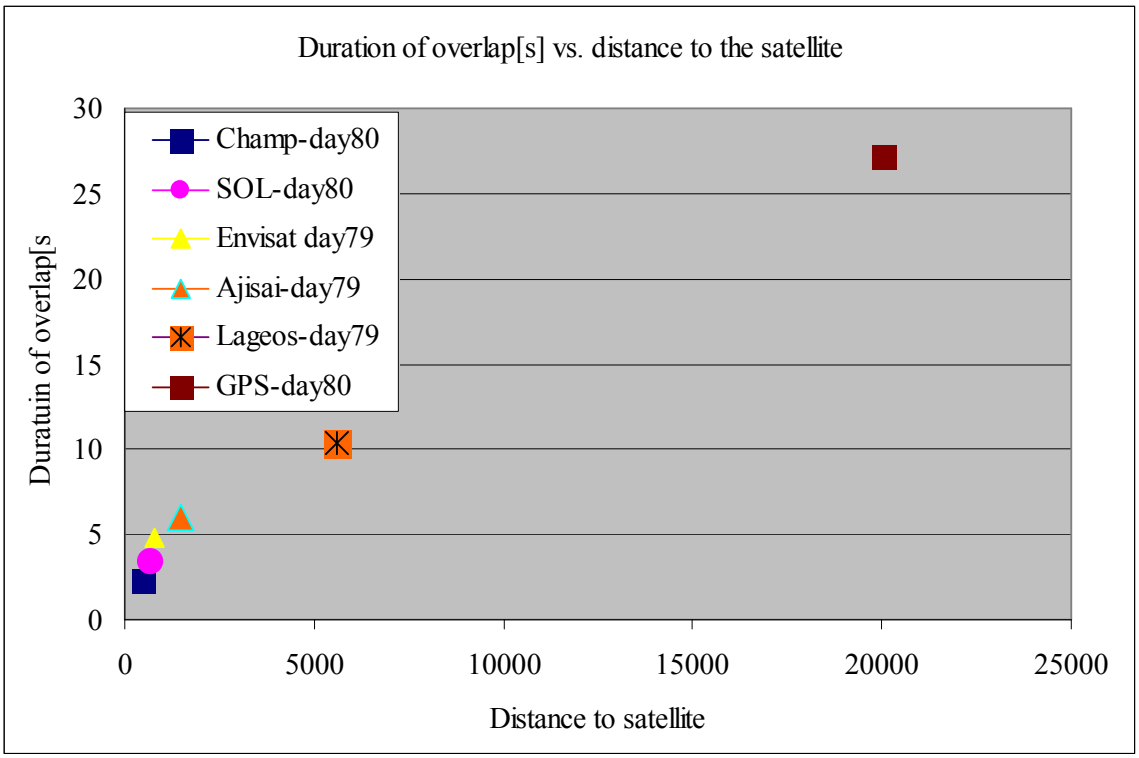

Fig. 5.5: Duration of overlap for different satellites

5.1.3 Density of Back Scatter Noise

Backscatter intensity also depends on elevation angle, which can be seen when observing full passes. Below are two passes showing very clear dependence on angle of elevation (fig. 5.6 & fig. 5.7). Overlap regions have longer duration at higher elevations because the rate of change of distance is on the point of closest approach. Backscatter intensity varies also with troposphere properties (transparency at 532 nm); we observed backscatter at different days, measuring different amounts of overlap noise ranging from 600 noise points per second to 1100 noise per second.

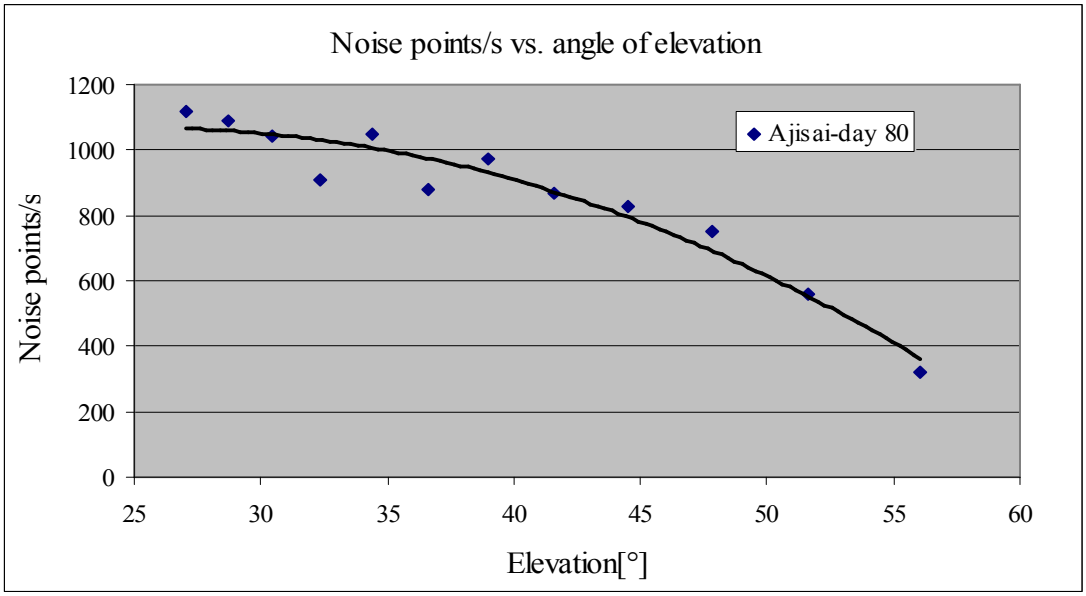

Fig. 5.6: Noise peaks vs. elevation in regions of overlap-Ajisai Pass

Relatively clear atmosphere would result in lower amount of additional overlap noise due to overlap. Because backscatter can be detected at distances of up to 5-10 km, depending on atmospheric transparency, pointing elevation of laser telescope etc.; thus at about 18 kHz repetition rate we would see constant overlaps, with increased noise. The overlap noise starts increasing and stays until 8 km and drops down suddenly or the other way round increases suddenly and drops down slowly depending on if the satellite is approaching or going away (fig. 5.4).

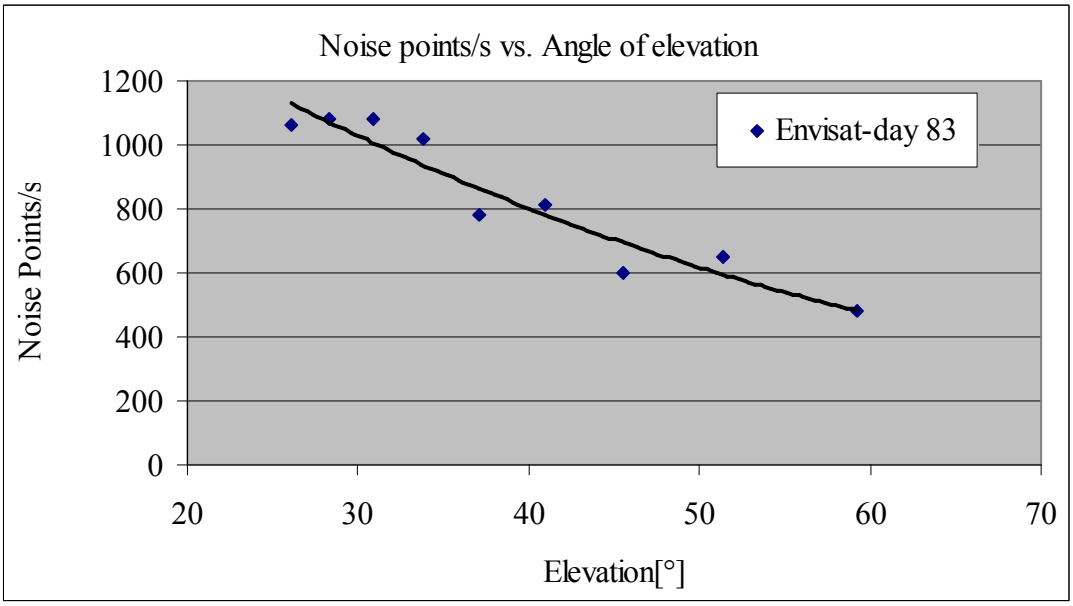

Fig. 5.7: Noise peaks vs. elevation in regions of overlap-Envisat Pass

The station fires 2000 pulses in a second and there are multiple pulses in the air traveling back and forth. The range gate is opened about 60 ns before the actual return and in this time the backscatter can be detected if it occurs with in the first few kilometers (5-6 km) in the low atmosphere.
The layer of backscatter occurrence moves closer and closer to the detector and then disappears as the approaching photons reach after the next laser firing.

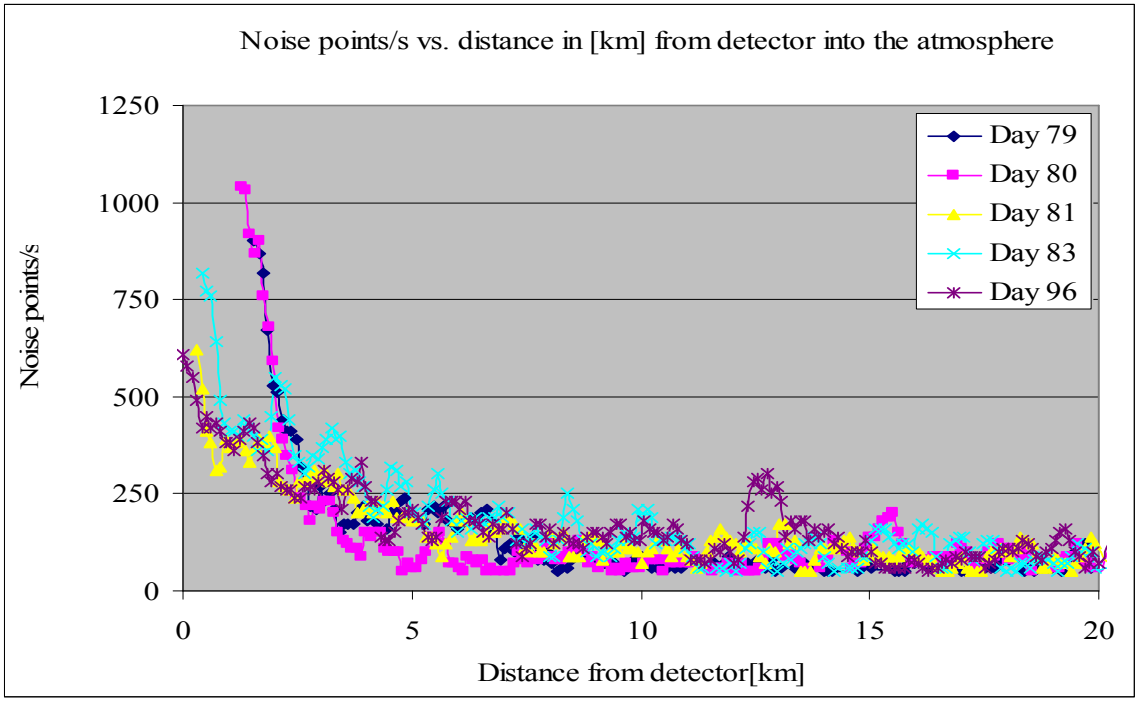

Fig.5.7: Back scatter noise recorded for Ajisai on different days

Fig 5.8 shows the increased backscatter noise with in first few kilometers of the atmosphere for different days of Ajisai pass during backscatter.

5.2 Final Consideration

At higher repletion rate up to 20 kHz system the laser backscatter will occur after every 7.5 km, resulting in constant backscatter overlap – leaving no chance to avoid it. However, with decreasing energy per shot at higher repetition rates – assuming again a constant power laser – the resulting backscatters decreases. One general possibility to avoid laser backscatter is to use separate transmit and receive telescope (some meters apart. Another possibility could be to use a suitable minimizing strategy i.e. on-off switching of overlap avoidance and try to send pulses always ahead of expected returns

Duration of overlap is longer for high satellites than for lower satellites. It is few seconds for GOCE, and 30 s for GPS satellite.

The laser backscatter is intense (more noise points per second) and the duration of backscatter (time interval) is less while ranging the satellite at lower elevation and vice versa for higher elevation and closest approach.

Noise is increased by a factor of 5 within overlap regions which decreases the signal to noise dominantly (cf. Chapter 6). The overlap noise can be eliminated up to 10 kHz of repetition rate. The increased noise due to overlap is a serious limitation to increasing the repetition rate more than 10 kHz.

6. Signal to Noise Ratio

The principle of SLR (Satellite Laser Ranging) system is to determine the orbit with very high accuracy after measuring round trip travel path from transmitter (ground station) to the detector (ground station). This chapter considers/evaluates the degradation of signal quality through the devices and very long atmospheric path. The signal quality at the output of the receiver is calculated using the radar link equation. The overall performance of the whole SLR system taking into account the attenuation of signal quality due to all types of noise(solar noise, laser backscatter noise and detector dark noise) is called signal to noise ratio .The ratio gives a measure of what we get out of what we have sent in terms of energy and number of photons. The received signal strength depends on many factors like the wavelength and energy of transmitted laser pulse, distance to the target, the target reflectance, the transmission of the atmosphere, receiver aperture area, throughput efficiency of the receiver, and sensitivity of the detector area etc and there are still other key factors influencing the performance of SLR related to the configuration/procuring of SLR electro-mechanical machinery.

Calculation of exact ranging accuracy in form of signal to noise ratio is difficult because of its dependence on many of highly unpredictable atmospheric parameters having range of values. Signal to noise ratio of higher repetition rate system is evaluated with higher energies and is compared to that of existing Graz SLR. Analysis is done over a range of values of different parameters in the radar link equation taking into account different sources of noise in the radar link channel of SLR.

6.1 The Radar Link Equation

Once a laser beam is transmitted it has to travel though the maelstrom of complex atmosphere to hit its target satellite being tracked and return to the firing station. The ratio between what is transmitted and what is received can not be calculated by a simple mathematical formulation as it is depending on very many factors discussed above. Though all factors vary greatly the laser ranging machinery share some common parameters on which the performance of one station compared to the other is possible. Mathematical combination of these parameters is called Radar Link Equation [21]. Radar link equation is expressed as below (Eq. 6.1).

$$N_{pe} = \eta_q E_T \frac{\lambda}{h_c} \eta_T G_T \sigma_{sat} [\frac{1}{4\pi R^2}]^2 A_T \eta_R T_A^2 T_c^2 \tag{6.1}$$

Detector Quantum Efficiency (η_q) allows the comparison of detectors which may use fundamentally different technology on an absolute basis. A high η_q means a high likelihood of a given incident photon producing a detectable signal.

This in turn influences the efficiency of the detector. Kilohertz photon-counting SLR and altimetry systems employ either Single Photon Avalanche Photodiodes (SPADs) or Micro Channel Plate Photomultiplier Tubes (MCP/PMTs) as detectors. Both detector types have high quantum efficiencies (40% to 55%) at the 532 nm SLR wavelength. Higher ηq will allow higher noise to be entered into the detector during the day time [22].

Efficiency and dark count rate of CSPADs are two limiting parameter is which evaluate over all through put of the SPAD detector. The dark count rate is the average rate of registered counts on the detector without any incident pulse. This determines the minimum count rate at which the signal is dominantly caused by real photons. The false detection alarms are mostly because of thermal increase and can therefore be strongly suppressed by using a cooled type of detector. It is important that every electronic pulse converted from a photon can be detected by the counting electronics so higher ηq is always recommended for SLR machine.

Laser pulse energy ET is the depending on available laser power and repetition rate of laser pulses. It is the most vital parameter in the radar link equation directly proportional to the signal strength. There is always a trade off for the given power increasing the repetition rate will decrease the energy. If average number of photoelectrons is less than noise or detection threshold level of counting electronics than it would not be possible to detect a return from the satellite. Decreased energy will decrease the strength of return signal. Graz kHz Laser Ranging System is operating at 300 μJ @ 2 kHz (0.6 watt).with the advancement of laser technology there are already available laser system with higher power e.g. 5 watt having the possibility to increase the repetition rate up to 100 kHz (see Appendix A).

Wavelength (λ) is of the laser pulse, most of SLR station are using laser at 532 nm wavelength. Two color laser ranging is used for better modeling the atmosphere [23].

Plank's constant (h) is a well known constant with a value of 6.626×10^{-34}.

Speed of light (c) is another well known parameter in radar link equation equals to $2.99 \times 10^{+8}$ m/s.

Transmit- and receive-path efficiency (η_T, η_R) are complex depending on the transparency of travel path and can not be exactly determined [24].

Transmitter gain (G_t) is expressed as

$$G_t = \frac{8}{\theta_k^2} \exp[-2(\frac{\theta_p}{\theta_k})^2] \qquad (6.2)$$

Where θ_k is far field divergence half-angle between the beam centre and $1/e^2$ intensity point and θ_p is the beam pointing error which is often much smaller than the beam wander induced by atmospheric turbulence [21].

Transmit Gain G_t in the radar link equation reflects obscuration/truncation of laser pulses.

Back Scattering Cross-Section (σ_{sat}) is characteristic parameter of on board retroreflectors depends on reflectivity, collecting area and solid angle of the retroreflectors; σ-sat provides the response strength of the satellite. Instead of single retroreflectors the laser satellite are equipped with retroreflectors arrays with different arrangements. A collective response of a laser satellite is defined and used in the radar link equation for return estimation [25].

Slant Range (R) is the line -of -sight distance between two points -station and the target satellite expressed as below (Eq. 6.3).

$$R = -(R_E + h_t)\cos\theta_{zen} + \sqrt{(R_E + h_t)\cos^2\theta_{zen} + 2R_E(h_s + h_t) + h_s^2 - h_t^2} \quad (6.3)$$

Where R_E is the earth radius (6378 km), ht is station height above sea level, θa zenith angle (complement of Elevation angle) of the observed satellite with respect to observing station at earth. h_s is the height of satellite, ht is the station height above sea level. Slant range has an inverse $1/R^4$ relation to the average number of received photoelectrons in radar link equation; provided all other parameters fixed High earth orbit (HEO) satellites will provide much less response as compared to low earth orbit satellites (LEO). The range parameter in the radar link equation is passive as it provides the number of photoelectrons at the provided but does not give any information about the maximum range at which a target can be detected. The minimum Signal strength is required for proper target detection as an input. The accuracy of range measurement depend on three parameters i.e. the accuracy in the measurement two way transit time of the pulse, accurate measurement of the atmosphere dependant variables and accuracy of mathematical values used for example speed of light. All the required station heights ht needed for slant range determination is provided on the ILR website.

Effective Area (A_T) is of area receiving telescope aperture, in bistatic SLR system, transmit and receive aperture areas will be different. In that case effective area should be calculated taking into account the obscuration at the secondary mirror and spatial filter at the detector.

Receive optic efficiency (η_R) almost every optical device has defined efficiency weighing its quality of functioning compared to other similar devices on the market.

One way atmospheric transmission (T_a^2) defines the atmospheric attenuation which is very complex phenomena depending on wavelength of the laser pulse, slant range path through the atmosphere and constituents (ozone, carbon dioxide, water vapors scattering and absorption of the laser beam) of the atmosphere itself.

One way transmissivity of cirrus cloud (T_c^2) is attenuation caused by cirrus clouds. Cirrus cloud cover is present in the sky even if it is barely visible. More detailed study of the individual parameters is beyond the scope of this thesis.

6.2 Communication Link at Higher Repetition Rate

Statistical analysis using radar link equation is carried out by varying different weather, altitude and frequency dependant parameters. Calculated results are compared with Graz real time return strength which proves that statistical model adequately explains the observed results. Graz average weather is derived from the comparison of mathematical and real received signal. This average Graz weather is used to further establish theoretical Communication link (signal to noise ratio) working lower to much higher repetition rate (10 Hz to 100 kHz) at Graz station. An analysis of total noise (solar, laser back scatter and dark) impacting the whole SLR data throughput is carried out too. Combining the received signal strength (returns per second@ varying repetition rate) with the total noise provides us a visible picture of signal to noise ratio at much higher repetition rate.

6.2.1 Establishing Link Budget Calculator

A study of radar link equation is carried out establishing a software link budget calculator. Graz coordinates and parameters are used being felicitous in availability and operating at higher repetition rate laser 400 μj @ 2 kHz. A list of satellite is chosen keeping in view the importance of altitude and different responses (σ-sat) due to different types and orientations of retroreflectors arrays on the particular satellite (table 6.1).As discussed already that in the radar link equation there is highly complex and varying atmospheric and weather effects on the overall signal quality depending on the clear/ cloudy atmosphere. There are some complicated atmospheric models which account gradients and meteorological parameters.

Table 6.1: List of satellite

Satellite Names	Perigee (Km)	σ-sat
Champ	475	1000000
Envisat	796	850000
Ajisai	1490	23000000
Lageos	5620	15000000
Etalon	19120	55000000
GPS	20030	19000000

While some simpler atmospheric models like the Marini-Murray and spherical models which only require the surface measurements of temperature, pressure and humidity.

The errors in the derivation of atmospheric parameters can cause sufficient errors in the range measurement. Using the average real time Graz data we calculated the average number of returns per second for the satellites listed in the table.

6.2.2 Average Graz Weather (AGW)

We derived a new term average Graz weather (AGW) to be used later for mathematical analysis of higher repetition and higher power SLR system. For establishing the term AGW the real time observations are collected from Graz SLR station. We used received real time returns from different satellites and by exploiting the quantum efficiency of Graz SPAD detector we calculated the number of returns per second from the satellites listed in table 1. Then using the same Graz parameters (300 μJ @ 2 kHz, Graz height above sea level, 20% quantum efficiency of Graz SPAD detector, Graz receiving aperture etc.) we derived the number of photoelectrons from radar link equation mathematically and exploiting the quantum efficiency achieved the returns per second vs. elevation angles. By varying weather/atmospheric dependant parameters (T_a^2, $T_c^2$and θ_k, θ_p used to measure Transmit Gain: G_t) in such a way that both measured and calculated data fit to each other (fig. 6.1).

We fixed the values of weather dependant parameters at the best fitting and called these fitted values collectively as average Graz weather. Average Graz weather can be seen best fitted to Lageos but we can see variations with fitting to other satellite real data.

This also explains the complex nature of weather and atmosphere and also the fact that we can not standardize these values for all satellite which best fit with their real returns as atmospheric affects also vary with varying the altitude of the satellite; the pulse speed up as it travels from ground station to lower density regions due to variation in group velocity and refractive index. Hence champ and GPS can not have exactly the same atmospheric degradation even if they are tracked on the same day/time and from the same SLR station. Single color SLR community is using unanimously Marini Murray atmospheric model to correct the atmospheric propagation delays in the real time SLR systems.

One can see very clearly the increase in the returns per second with increasing the angle of elevation for both calculated and measured curves. It is obvious by the fact that when a satellite approached the station the response will be highest at closed approach (at the elevation of 90°) and will decrease when satellite goes away and elevation angle is decreased.

6.2.3 Received Signal Quality at Higher Repetition Rate

The energy of the laser pulses decreases with increasing the repetition rate of laser pulses (section 6.1.2). Graz station is working at low power of 0.6 watt (300 μJ, 2 kHz).

If we want to increase theoretically the repetition rate the energy per pulse will decrease. Such a laser system @ 10 kHz will have pulses having 80 μJ per pulse and 8 μJ pulses at 100 kHz. Decrease in the pulse energy will directly degrade the number of received photoelectrons in radar link equation theoretically.

This can lead to a system having no return or non detectable returns in the real time system. There is need for new laser systems having relatively higher power at higher repetition rate so that a communication link with higher S/N can be established.

Such Laser systems are already developed and available to be used for SLR systems (see available laser system pages at the end of thesis).Assuming such a 5 watt system we developed a calculation to estimate signal strength (returns per second) at average Graz weather.

Using the radar link calculator a similar study is done to develop a curve between returns per second vs. angle of elevation [°]. Keeping all other parameters fixed we changed only the laser power to 5 Watt (2.5 mJ @ 2 kHz) instead of 0.6 watt (300 μJ @ 2 kHz) in the link calculator, number of returns per second increase with the ratio of increased power. One of such example is shown in the fig. 6.2 with Lageos 0.6 watt data and 5 watt data showing an increase in returns per second with a factor of 8.33 which is the same as the ratio of power (5 watt vs. 0.6 watt) at 2 kHz.

To see the effect on received signal strength due to variation in the repetition rate of Laser pulses we selected a range of repetition rates starting from traditional 10Hz to 100 kHz To see the effect on received signal strength due to variation in the repetition rate of laser pulses we selected a range of repetition rates starting from traditional 10Hz to 100 kHz at 5 watt laser power.

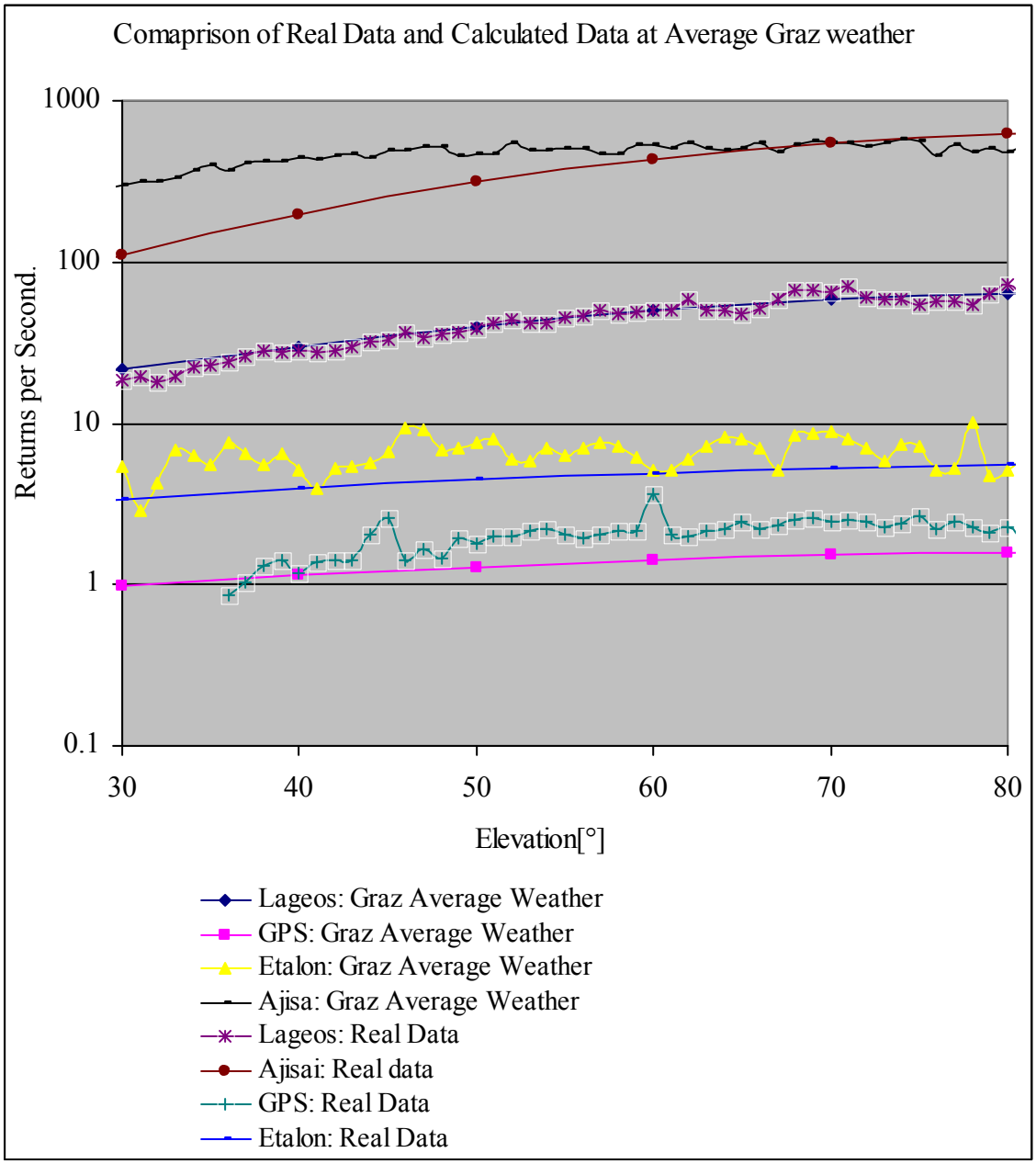

Fig. 6.1: Average Graz weather; Returns/ s vs. angle of elevation

Increasing the power will increase the returned signal strength is also the direct consequence of radar link equation. Using average Graz weather we derived the curves at different Elevation and different repetition rates. Fig. 6.3 shows the results of mathematical calculations for lower satellite with returns/sec vs. repetition rate at lower elevation (30°) and higher elevation (70°).

A significant increase in returns per second can be seen with the increasing the repetition rate in the start up to about 10 kHz and then the increase is not so significant because the pulse energy decreases with the increase in the repetition rate and number of returned photoelectrons also decrease, consequently to see the stronger returned signal we have to further increase the power at higher repetition rate system to keep the energy of the radar link equation constant.

Similar curves we achieved for higher satellites fig. 6.4 for higher satellites the increase in returns per second is not so significant even up to 10 kHz as the return energy in the radar link equation driving the mathematical model of SLR system is inversely proportional to 4th power of altitude of the satellite ($1/R^4$).

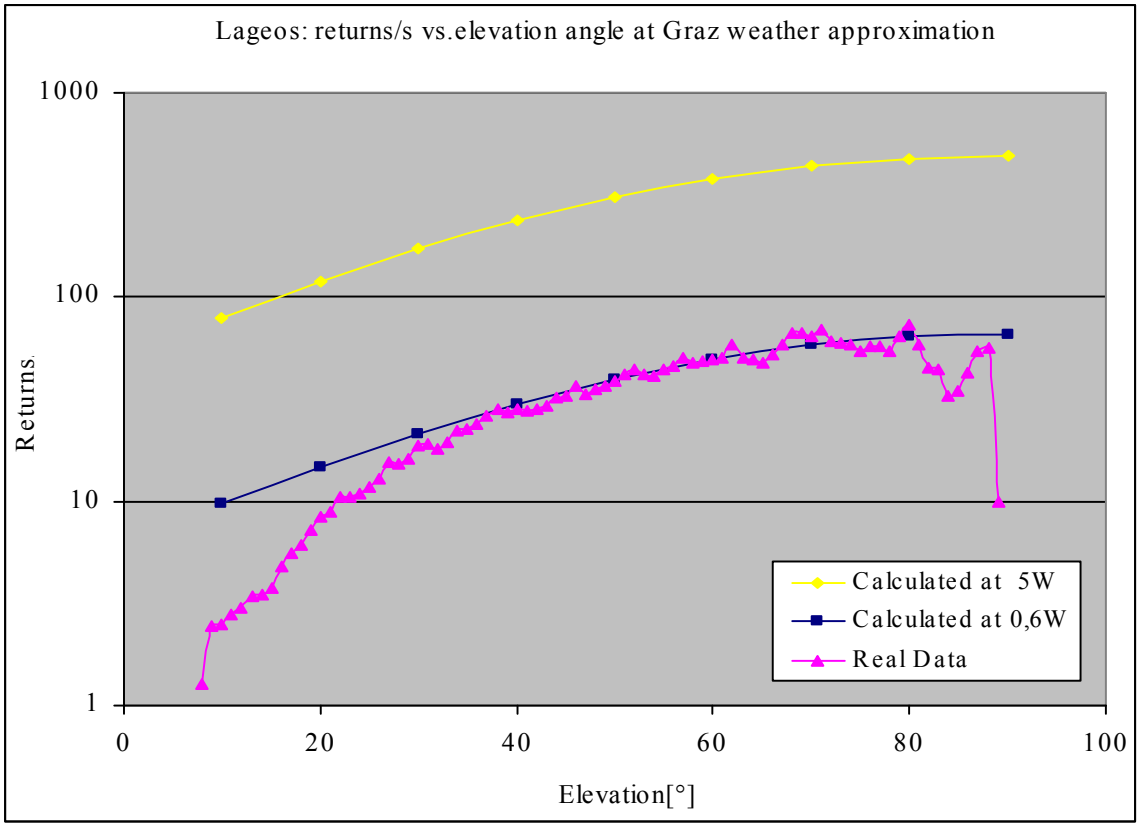

Fig. 6.2 Comparison of returns per second

For increasing the response of higher satellite with all other parameters constant we need relatively much higher energy/power laser to improve signal strength. Keeping the power constant and increasing the repletion rate will decrease energy per pulse and these pulses will have lower probability of round trip traveling and detection. Up to now we have been studying the signal strength of SLR system varying different parameters in its basic mathematical model. But we did not accounted the back ground noise which can reduce the returned signal badly.

6.3 Background Noise

The number of photoelectrons resulting from the background radiations can cause false alarms on the SLR sensitive detectors (Graz SPAD detector: 60 ns dead time) can reduce probability of detection of original returned signal.

There are mainly 3 sources of background noise, the solar noise, laser backscatter noise and detector dark noise. The total noise is sum of all three types of noise entering in the detector. Total noise is a phenomena depending heavily on the change in repetition rate mainly because of detector dark noise and laser back scatter noise.

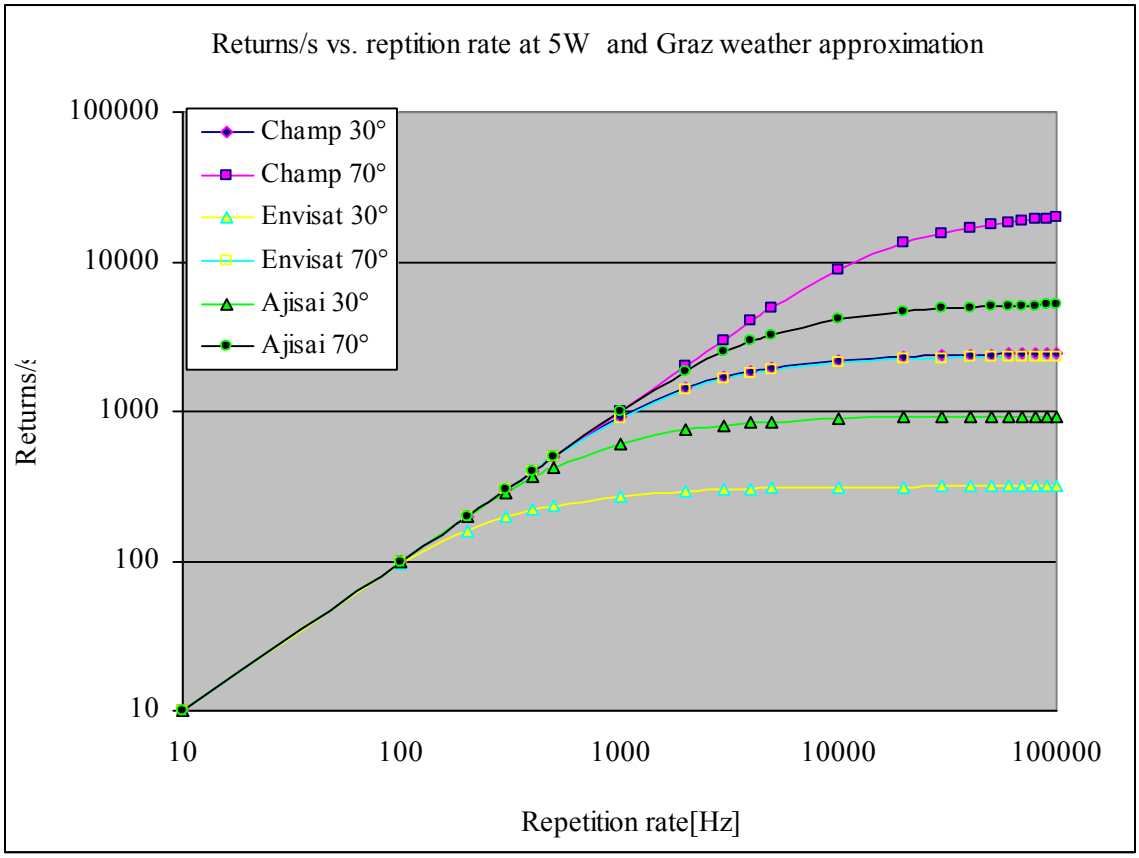

Fig. 6.3 Low satellites having returns/sec vs. repetition rate

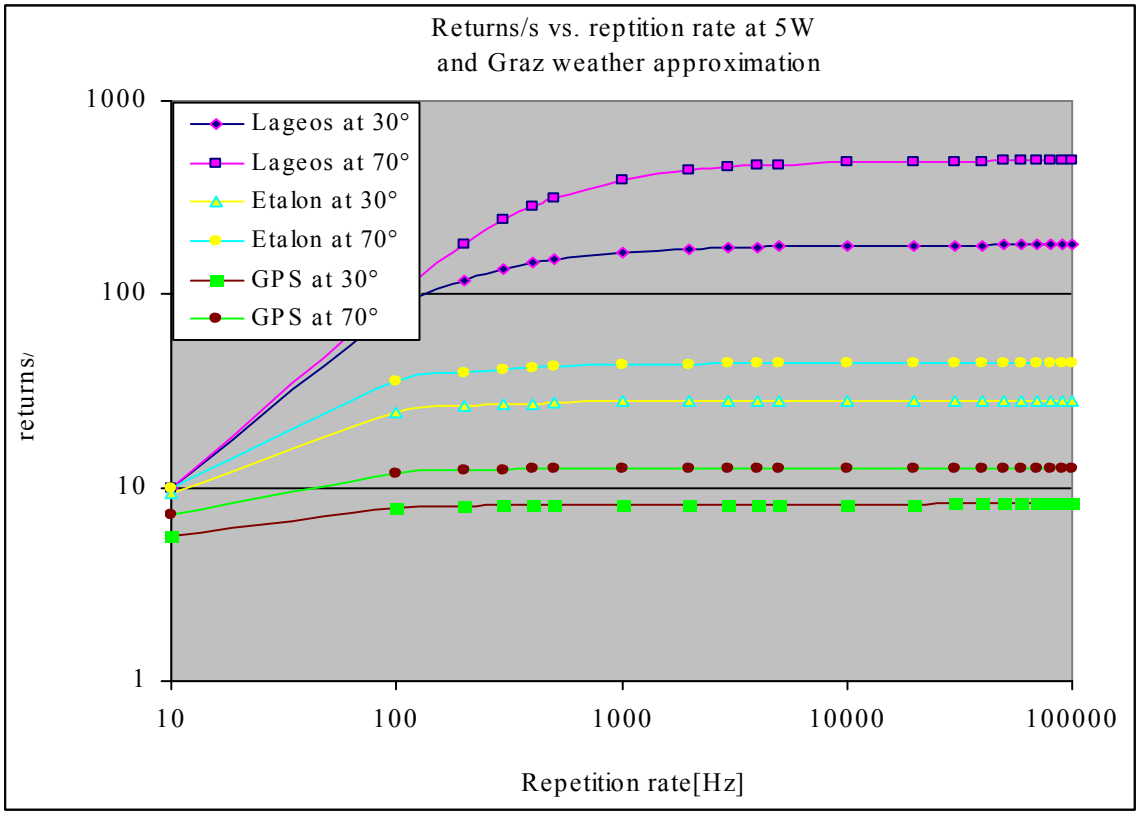

Fig. 6.4 Medium to higher satellites: returns per second vs. repetition rate [Hz]

6.3.1 Solar Noise

The most dominant source of noise during day time tracking operations is solar radiation. Solar photons enter the receiver by scattering off objects within the receiver Field-of-View (FOV) and are by far the dominant source of noise during daylight operations. Solar noise is a function of FOV (fig. 6.5). In SLR, these photons are scattered by atmospheric constituents, such as molecules, aerosols, fog, clouds, etc. Many stations in the world can take the daylight observations. There are some main technical problems for daylight tracking of the satellites i.e. pointing of the telescope; mount model problem for the telescope; generating control range gate narrower; the application of narrower Spectrum filter; the receiver filed of view want to be small and increasing the threshold amplitude (in case of MCP or PMT detectors).

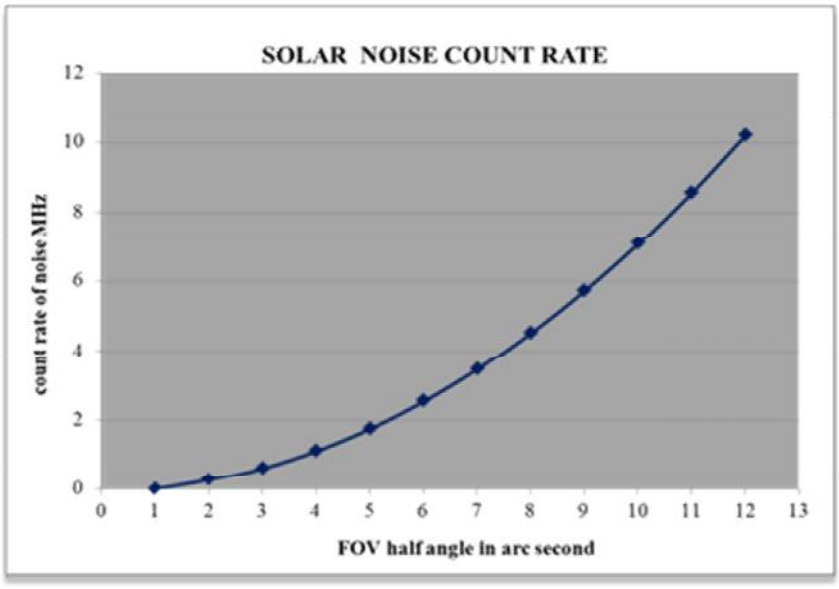

Fig. 6.5: Solar Noise vs. the FOV of the detector

Collectively all the above mentioned features collectively reduces amount of background light. The solar count rate seen by the detector is mostly reduced through the use of spectral and/or spatial filtering. According to my experience at the most successful station regarding kHz SLR, the Graz station is using many unique techniques to make the day time tracking successful and reduce the false detection probability i.e. Parallelism of transmitting and receiving paths is carefully maintained for correct beam pointing, Coude path fine adjustment and intensive light protective methods like reducing the width of range gate up to 60ns, decreasing the receiver FOV, use of spectral 0.3nm narrow band pass filter centered at 532 nm). The daylight tracking is necessary and the tendency of SLR in the future.

To calculate the solar noise mathematically at Graz station we used the following noise equation derived from spherical atmospheric model [26].

To calculate a numerical value for solar noise count on the day time for Graz station we used Graz parameters (Spectral filter FOV; receive aperture area; SPAD quantum efficiency; 532 nm band width etc.).

$$n = \frac{\eta_q \eta_r}{h\nu} \frac{N_\lambda(\Delta\lambda)\Omega_r A_r}{4\pi} \left\{ T_0^{\sec\theta_t} \ln\left(\frac{1}{T_0^{\sec\theta_t}} \right) \right\} \qquad (6.4)$$

Table 6.2 shows the values of parameters used in the noise count equation. The solar noise count concluded to be approximately 5 MHz which coincide with it value with the real data during day time tracking.

6.3.2 Detector Dark count

Detector dark counts are spontaneous and random photon events that occur in a darkened environment without any apparent external stimulus. Dark count rates are generally lower in the visible wavelength regime. While it increases as one move the operating wavelength deeper into the near infrared (NIR). Dark count rates can often be reduced by cooling the detector.

Table 6.2: Graz Parameter values used to calculate solar noise count rate

Symbol in Equation	Parameter description	Value
n	solar count rate result	≈ 5MHz
η_q	Quantum efficiency	0.2
η_r	Receive optics efficiency	0.3
$\Delta\lambda$	FWHM bandwidth of the spectral filter	0.3
$W_r = pw*w$	receiver solid angle using 150 urad FOV	7.85E-09
Ar	Receive Aperture Area	0.19625
$h\upsilon=hc/\lambda$	laser photon energy	3.72401E-19
$\{T_0^{sec\theta} \ldots\ldots\ldots\}$	Terms in Brackets {} =0,5 in worst case	0.5
N_λ	exo-atmospheric spectral irradiance	0.2

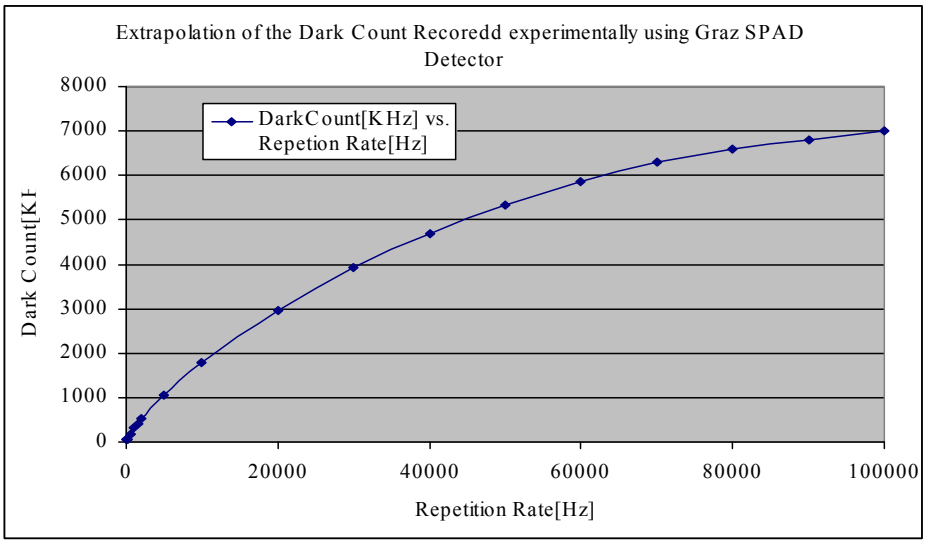

Fig. 6.6: SPAD detector dark count rate [kHz] vs. Repetition rate in Hz

By gating Graz SPAD detector with pulses, such that the pulse is start pulse for time interval counter and SPAD out pulse is the stop pulse for the time interval counter, repeating the measurement number of times depending on the repetition rate; we measured the hold time/ dark count of SPAD detector up to 50 kHz and the extrapolated the results to 100 kHz (fig.6.5, fig. 6.6).

6.3.3 Laser Back Scatter Noise

When ranging with kHz to satellites, there are repeated periods of overlaps between returning photons, and just fired laser shots. The backscatter of these shots from the first few km traveling through the troposphere – would cause significant noise on the single-photon-diode, reducing the detection probability for the return photon. This type of degradation of return signal is called Laser backscatter noise.

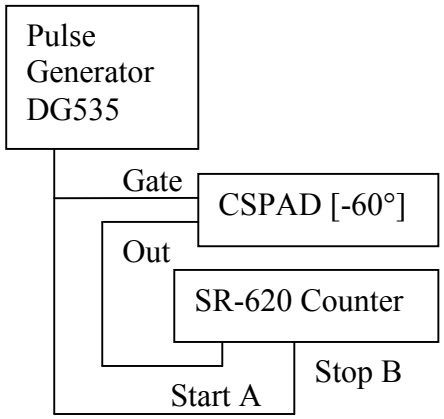

Fig. 6.7: SPAD detector dark count rate measurement setup

To avoid these situations completely at 2 kHz, Graz Station uses the same FPGA chip to produce all laser firing and laser control commands; if return photons are expected within 30 us after laser firings, an extra delay of 50 us is inserted before the following laser shot; because all necessary information – next expected Range Gates, and time of next fire pulse – are already known within the FPGA chip, this process can run fully automatically within the FPGA hardware, and without any further intervention from the control of PC.Reffering to section 5.1.2 about laser back scatter; at 2 kHz laser back scatter noise amounts to 5 MHz (5 mega noise points per second) by manipulating the fact that increasing the energy will increase the laser backscatter noise and increasing the repetition rate will decrease the energy per pulse concludes that at higher repetition rate backscatter will occur more frequently but due it will be less intense.

At 18 kHz Laser back scatter accrues after every 8 km and stays about 8 km so at 18 kHz there will be phenomena of unavoidable constant laser back scatter. Laser backscatter for the 5 watt system is calculated in 10 Hz to 100 kHz range and assumed by the virtue of already known system for overlap avoidance that the laser back scatter can be avoided up to 10 kHz.

6.4 Return strength of the signal under the noise(S/N)

The total noise (accumulating solar, backscatter and dark noise) is calculated and from the data return percentage is calculated under noise. Applying this percentage under noise to already calculated signal returns per second evaluates signal to noise ratio for variety of satellite and range of repetition rate.

The percentage return under total noise is calculated assuming that Back scatter can be avoided under until 10 kHz (see chapter 5, Laser Back Scatter) and noise is considered only in the first 65 ns window of range gate (Fig. 6.7). The percentage return decreases with the increase of dark count noise (dark count noise section 6.3.2) in the start and later a heavy decrease occurs because of larger amount of noise due to laser back scatter. The decrease is also summed up because of going to higher repetition rate energy of the laser pulse decrease causing the addition decay in the signal return strength.

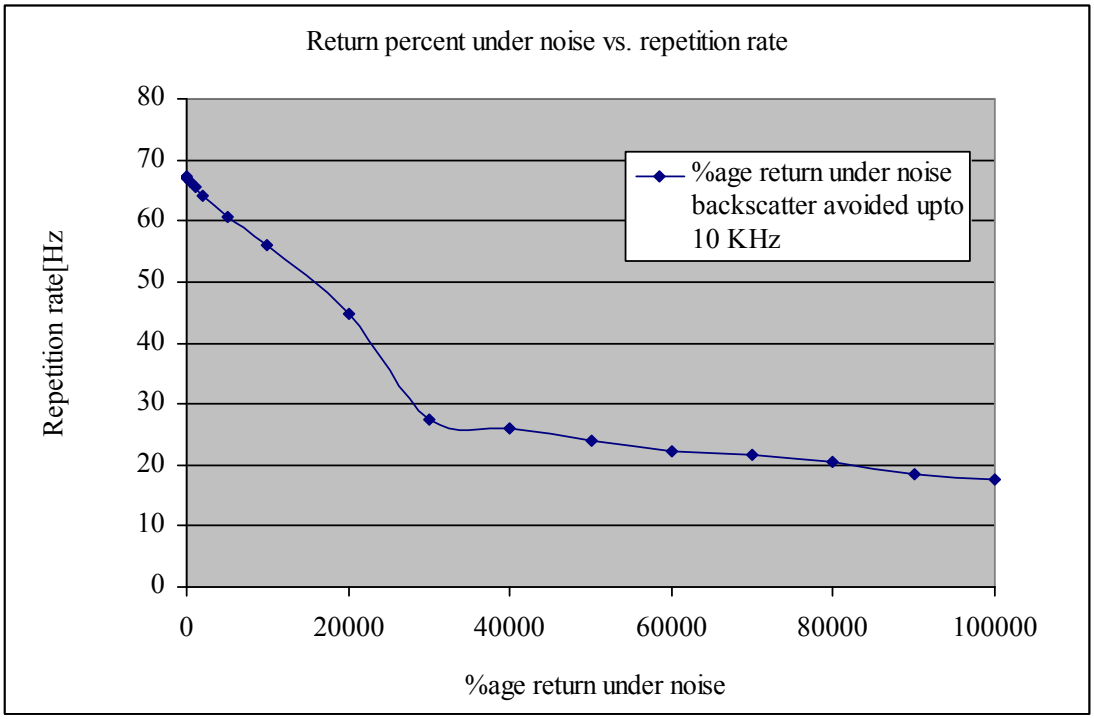

Fig. 6.8: Percentage return under noise

Signal to noise ratio of almost all the satellite follow the behavior of the curve shown in fig. 6.8.Tracking the low satellites with higher repetition rate has obvious advantages due to higher achieved signal to noise ratio while we get very low Signal to Noise ratio for high satellites because of very high altitude the signal drops by the power of 4.

Signal to noise ratio of low satellites is depicted in fig.6.8, there is significant increases in signal due increase of repetition rate i.e. 10-100Kpulses per second as compared to 2 k pulses; but the increase in signal to noise ratio is not so linearly increasing (2296.08 @ 10 kHz as compared 1189.43 @ 2 kHz) because of increase in the repetition rate decreases the pulse energy. Signal to noise ratio decreases because of increase in the dark noise with higher repetition rate and laser backscatter starts to contribute a significant amount of noise at 10 kHz and higher.

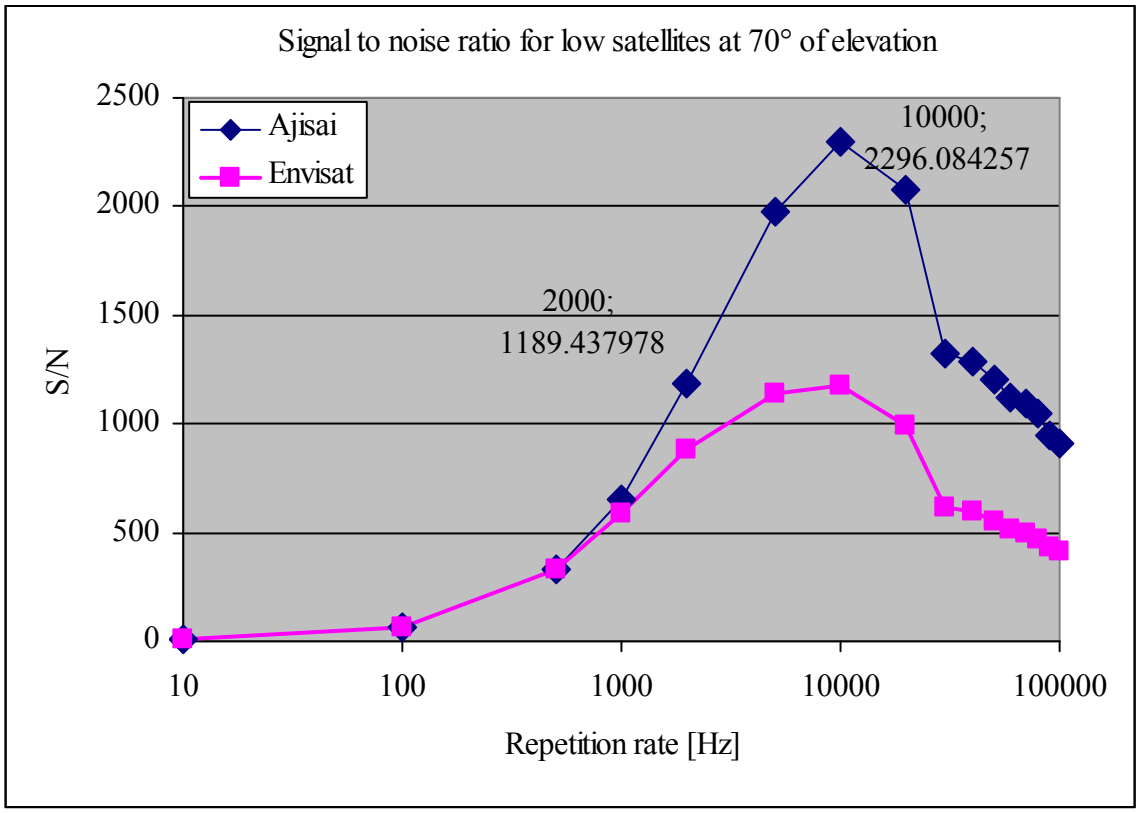

Fig. 6.9: Signal to noise ratio for low satellites at constant power of 5 watt

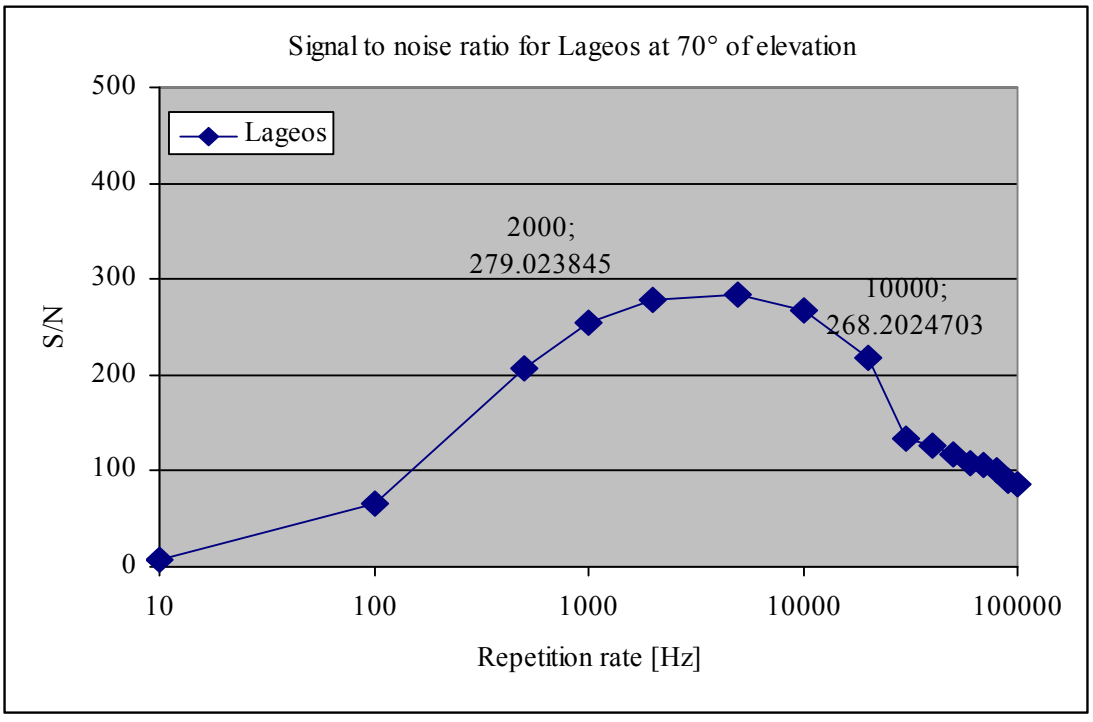

Fig. 6.10: signal to noise ratio for Lageos at constant power of 5 watt

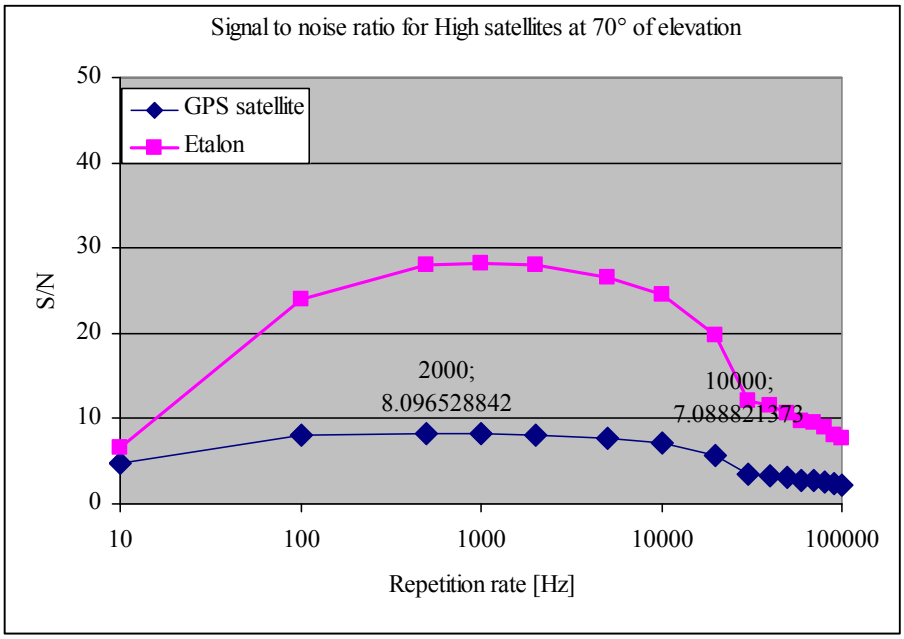

Fig. 6.9: signal to noise ratio for high satellites at constant power of 5 watt

For high satellites the signal to noise ratio further decreases due to its higher dependence on the slant range (raise to power 4) additional to decrease due to higher repetition rate and additional noise (fig. 6.9).

6.5 Final Consideration

The signal to noise ratio analysis concludes that the present Graz SLR system with 400 µJ @ 2 kHz can – and should - be upgraded with a constant power laser system with e.g. 5 W output; for LEO satellites, the system would produce e.g. 500 µJ @ 10 kHz, and provide all above mentioned advantages; for HEO satellites, the signal-to-noise ratio for the weak pulses of high repetition rates would drop below meaningful levels. Thus, the system should operate at lower repetition rate, but with higher energy per pulse (e.g. 50 mJ @ 100 Hz); such a system – although not yet available commercially - would be optimized for the upcoming difficult task of daylight measurements to HEO satellites like the 27 GALILEO satellites, to be launch within the next few years .

7. Simulation Application

This chapter presents concepts and implementation of identification routines for satellite returns with higher repetition rate SLR in the presence of very strong noise. The simulation program was aiming for an increased data yield of filtered SLR measurements in order to maximize the number of correctly identified returns. For this purpose the program is using multiple filtering algorithms. Some of them are already used for Graz kHz ranging, while the sliding bin algorithm is new for further screening of the data. At higher repetition rate (10 - 100 kHz), the received data will be loaded heavily with noise. The main purpose of the program is to simulate a 10 -100 kHz SLR system, create and plot the residuals, implementing / improving the identification routines, and optimizing various conditions for higher repetition rates. The purpose is neither to create an operational RT system for 100 kHz nor necessarily running with accurate RT timing. The program allows identification of GOOD returns at very low return rates (down to 0.02 %; i.e. 20 returns out of 100000 noise points. Automatic filtering of raw data in real time is used at Graz SLR since the upgrade to kHz SLR. Basically, every new residual is compared with the last 1000 residuals; if at least a few of them are within a small (e.g. 100 ps) band around the new residual, it is considered and marked as "identified return". In addition, the last 1000 residuals are filled into bins to form a histogram; the bin with maximum number of residuals is plotted, and acts as guidance for most automatic routines within the real time tracking system. Fig. 7.1 shows an unfiltered pass of satellite AJISAI; the signal here is strong, and returns are easily identified by the routines.

In case of high satellites where the signal to noise ratio is very week (like GPS, Etalon etc), the human observers are NOT able to identify good returns using the GUI interface; here the histogram and identification filters are essential to detect and identify the returns, and to adjust range gate width and position accordingly in real time. An example of such a week pass is shown in the Fig. 7.2.

One can clearly see time intervals where a reasonable or good signal to noise ratio exists for the measurement. However there are also times where only sparse data is recorded. In order to extract the valid returns out of all the recorded data points in near real-time the control software examines small portions of the pass of a few seconds length. The data is then converted to a histogram and if a suitable bin contains a sufficient number of echoes, these are extracted and stored away as satellite returns. By using more than one criterion at a time one can vastly improve the robustness of the filter procedure. At the same time the data yield improves substantially in particular for passes with a low signal to noise ratio

7.1 Generation of random signal for 10 - 100 kHz system

As mentioned above, the system is using arbitrary data to develop a GUI later to be used to detect real returns out of noise. The simulation program generates 100.000 random points (simulated residuals).

The program provides the facility to generate a selectable percentage of these 100.000 points as ”valid returns”: These are points on a straight line with a user specified jitter, as opposed to the randomly distributed noise points; any percentage above 0.001% can be selected.

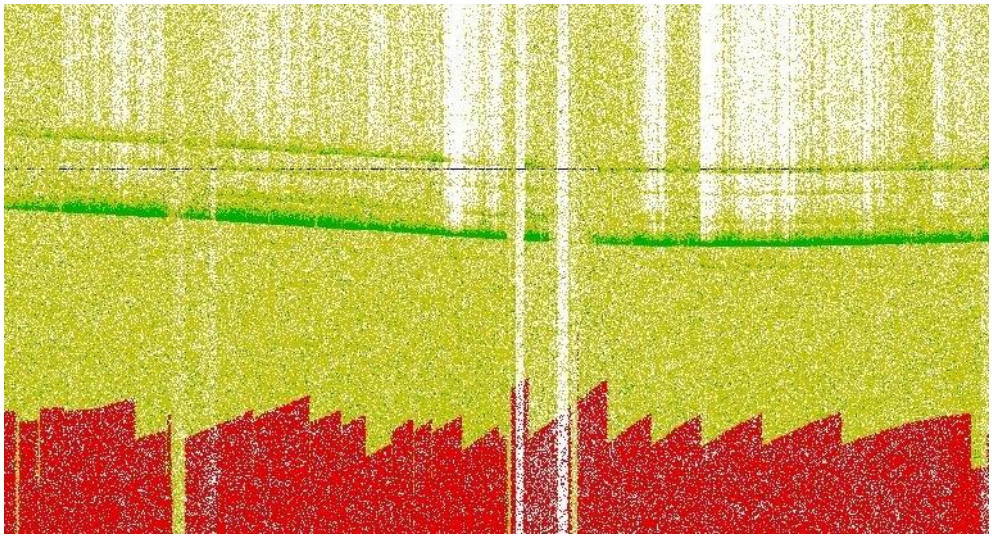

Fig. 7.1: Ajisai Pass tracked by Graz SLR

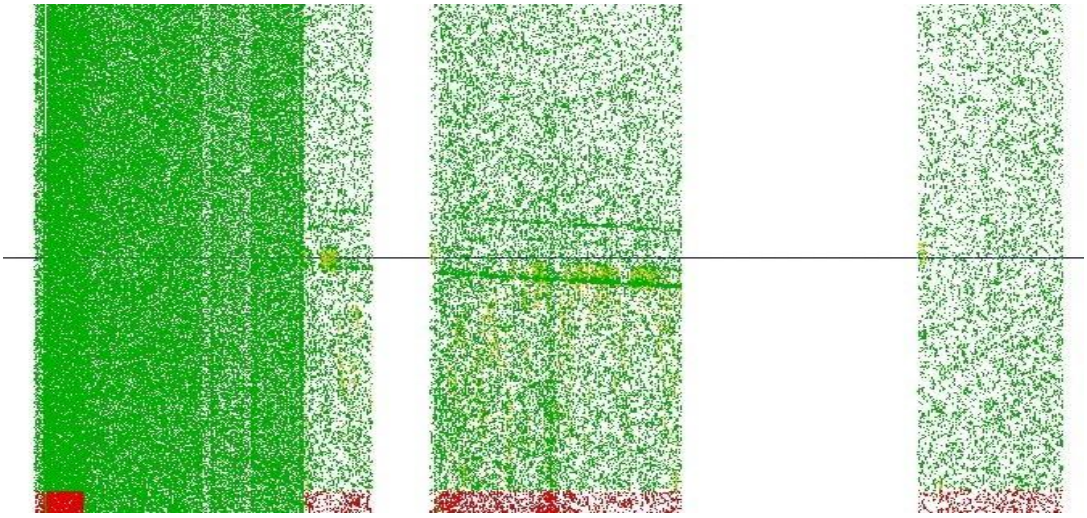

Fig. 7.2: Filtered pass from satellite GIOVE (GALILEO Test Satellite)

Once the user defined residuals are generated, they noise points are plotted as single black pixels, while the “valid returns” are emphasized as large red dots. A snapshot of the application display is shown on the fig. 7.3.

The simulation software consists of 3 parts: 1) The residual display window; 2) The histogram display window; 3) The user interface area consisting of options and variable controls edited by the user.

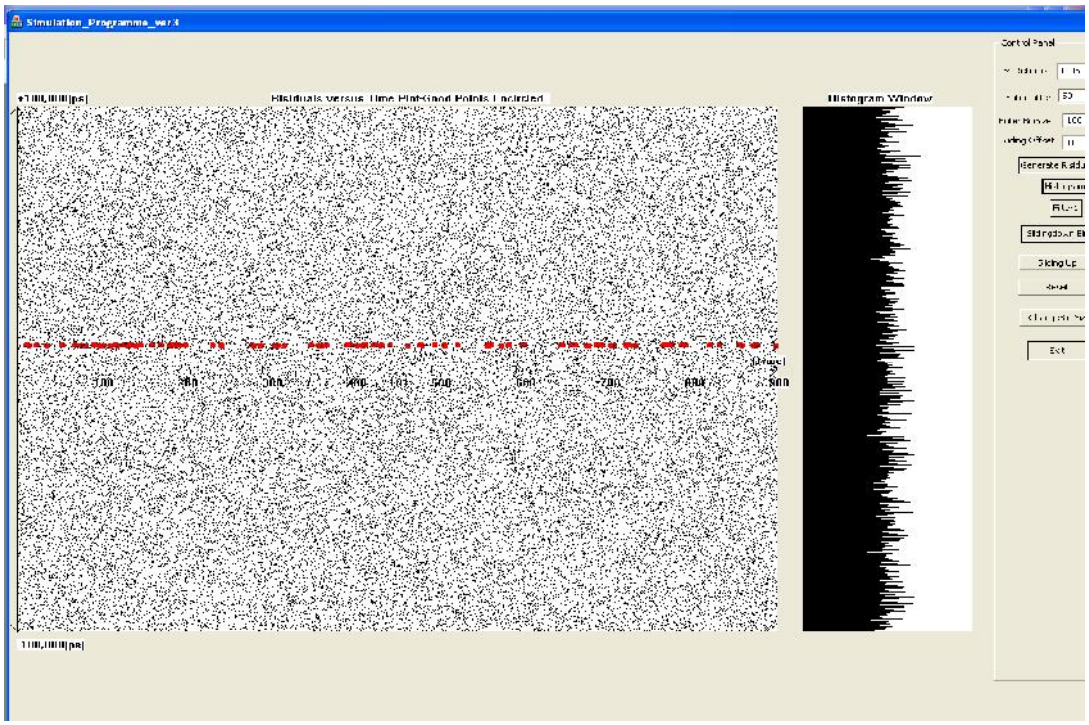

Fig. 7.3: GUI Display

7.2 Histogram Evaluation

The display window is divided into small bins (time slices of 100 ps width, adjustable for the user) for histogram calculations. The length of the time slice can be adjusted for 10 - 100 kHz repetition rates. Histogram analysis detects valid residuals out of noise in a reasonably short time slice (100 ps) named as hbins. Highest peak inside the histogram window indicates the maximum likelihood of this time slice having the maximum number of good returns. The width of the range gate can then be reduced automatically, which in turn enhances the data yield of the ranging operation. Fig. 7.3 show the histogram window of this application. When the S/N ratio is very low (e.g. 10 - 20 valid points within 100 k noise) and jitter is high compared to the hbin size in 100.000 noise points, the histogram fails to indicate the valid points out of noise. In such cases, a careful selection of hbin size can help to improve histogram analysis, or we need some other techniques to see the good residuals e.g. identification filtering and sliding bin algorithm. This analysis is slower using 100.000 points for histogram plotting and can only be used for post processing of higher repetition rate data but can not be used for real time SLR systems with higher repetition rate due to the required CPU time and power.

The histogram analysis used for the Graz real time SLR system is very efficient; whenever a new residual is identified as valid – via the bandwidth identification routines – it is placed in the relevant bin and increases the total number there. It is fully automatic and efficiently working.

If no further valid residuals are identified, it slowly reduces all bins of the histogram, thus keeping the highest peak still for some time - a simple way to continue tracking after short interrupts of e.g. clouds.

7.3 Identification Filter

The simulation is using an identification routine based on a band size of 100 or a few 100 ps as selected by the user. The selected bandwidth has to be within an appropriate range, and is optimized for each satellite, and for the actual tracking condition. If the jitter is high, a higher bandwidth is recommended for better detection.

The simulation program identification routine selects one by one each residual, finds the number of residuals inside the selected bandwidth, and provides a residual count tag with each residual. These are later compared to mark the band having maximum number of residuals. The routine allows a change of the bandwidth in steps of 1 ps, and to repeat the filter procedure. It clearly marks and shows the valid returns.

The identification routines used for filtering real time data in SLR Graz are slightly different: Graz uses two software identification filters requiring threshold values set by the observer and / or by routines for filter adjustment. During the real time tracking of the satellite every, new residual is compared to the last 1000 residuals kept in memory. If enough (e.g. threshold= 5) residuals are present within a band (e.g. 100 ps) around the new residual, the new residual gets an “identified” tag, is plotted as a green dot on the real time display and is stored on disk. This minimum number can be set by observers to adjust sensitivity versus amount of false alarms; the acceptance band width is adjusted by other routines automatically, according to satellite, range gate width and other parameters.

This simple procedure is fast, effective, and gives a very nice user interface for a variety of satellites: Low Earth Orbiters with close to 100% return rate result also in easy interpretable graphics as high orbiting satellites – like GPS -, which can have return rates far below 1%. Other routines are filling all identified returns into histogram bins; the bin with maximum identified returns is plotted on the screen – another useful and indicative feature for observers– and serves as a guide number for automatic control of range gate width, range gate shift etc. Thus, most noise points are eliminated, and usually neither displayed nor stored; this is advantageous not only for the user interface, but also minimizes storage sizes, amount of data to be handled etc [28]. The identification routine implemented in the simulation can only be used in post processing because it is very slow and needs much time for evaluation.

7.4 Sliding Bin Algorithm

The sliding bin algorithm is similar to the histogram analysis, but it can slide up or down the bins in steps smaller than the bin size. In this way, in any iteration a new set of data is filled into each bin; the bin with maximum number of residuals is kept for each shift. Finally, the 5 bins with the highest number of residuals are plotted in the histogram.

The algorithm was tested by sliding up and by sliding down the bins once each; it increases the probability of detecting the valid residuals better than the simple histogram or filter can do.

In many cases, it indicated the residuals even when the simple filter or histogram algorithms failed. Fig 7.4 shows such a case where filter identification (black dots) is wrong, but the sliding algorithm successfully finds the valid residuals.

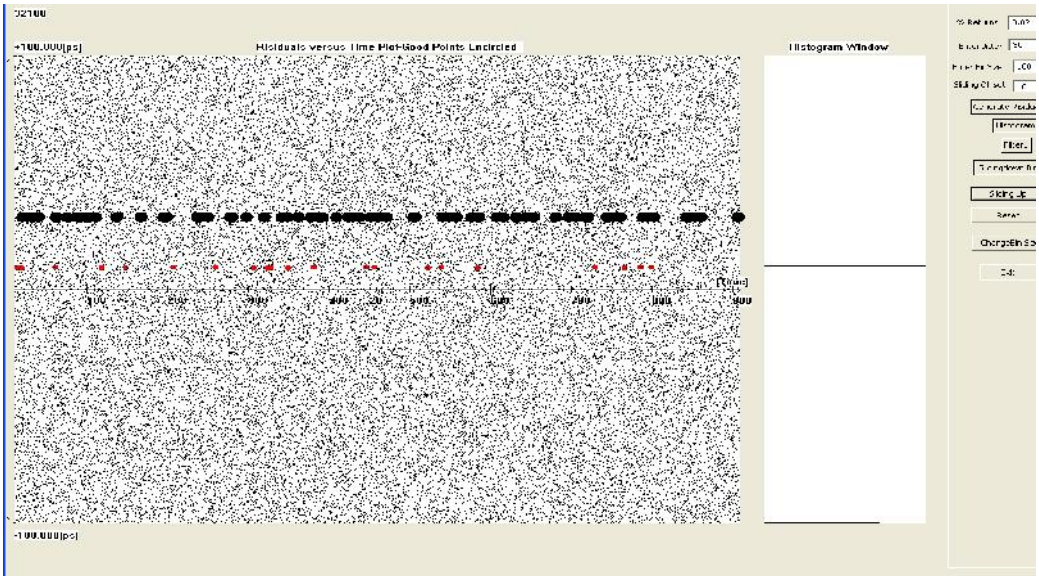

Fig. 7.4: Longest line in the histogram window marks the correct bin

7.5 Application Results

The simulation can perform 100% detection of 40 - 50 residuals out of 100000 noise points (i.e. a return quote of 0.04% to 0.05%) successfully. At 0.02% return quote, the sliding bin algorithm still detects the valid return, but with a probability of about 50% only – and at 0.01% valid returns, the detection probability decreases to a few percent. As stated before, the algorithm needs considerable CPU time, and is therefore intended only for post-processing the data, but not practicable for real time applications.

8. Real Time Demo Application

Accurate measurement of the time intervals of laser pulses going back and forth from ground stations to the laser satellites is basic principle of satellite laser ranging (SLR).The accuracy of SLR system is limited by different sources of errors i.e. errors in atmospheric corrections, orbit modeling, system (PC) computation limitation and TOF measurement device errors. Timing measurement serves for two purposes; to evaluate the TOF of the laser pulses with ps accuracy and time of emission of laser signal up to ns accuracy for range gate setting of the subsequent laser pulses. Timing system resolution, linearity and timing jitter, stability and temperature dependence are very important parameters of real time tracking accounting the overall performance of the SLR ground station. Graz station is using the Dassault modules along with on station built modules for event timing having < 2 ps RMS, and < 2.5 ps linearity error, maximum capable of measuring @ 2.5 kHz repetition rate [29]. We used for present real time demo program Riga ETA032 Timer which can measure continuously at mean rate of 10 kHz at the maximum and burst rate up to 16 MHz, better single-shot resolution (< 10 ps RMS) and 60 ns dead time [30].

The present demo program is a real time SLR program implemented for ranging the laser satellite with sufficient accuracy and much higher repetition rate (10-20 kHz).The demo program is an automatic program capable of calibration, ranging and range gate generation from low to very high repetition rate. The demo program consists of three parts i.e. a nano second [ns] part reading the fired start laser pulse from ISA FPGA card Graz, programming in real time the Range gate and loading it into the ISA FPGA card, performing the Calibration Task and storing it into Cal Record and the picosecond [ps] part reading in real time the fired and return epochs measuring the time of flight, calculate the residuals, display and store them into the Range Record.

Fig 8.1 shows the basic construction and interface with Demo PC (The PC having the control and processing software for higher repetition rate system). Demo PC is connected through various interfaces to the other PCs and Hardware modules. The interface to the other PCs demo software reads and performs different software on reading the information and commands from the external world while the hardware modules are reading, storing and synchronizing the timing information needed for calibration, tracking and range gating purposes.

To enable the system for automatic ranging we connect the demo pc with the main PC of Graz SLR station to download basic commands for operation such that start/stop tracking a pass, start/stop calibration, meteorology data, necessary flags and Range gate, range shift like information etc.-to be used for residual real time display, over RS232 link.

The whole demo system operation is initiated and processed over the arrival of these RS232 Commands. The prediction data is regularly downloaded from the Graz win PC using ftp download manger every four hours so that the demo pc has the necessary prediction data for the forth coming laser satellites to be tracked from Graz Station.

A fundamental feature of the Demo program is that it makes this equipment look, feel and act in a consistent manner during ranging or calibration and can perform these operations continuously upto 10 kHz repetition rate.

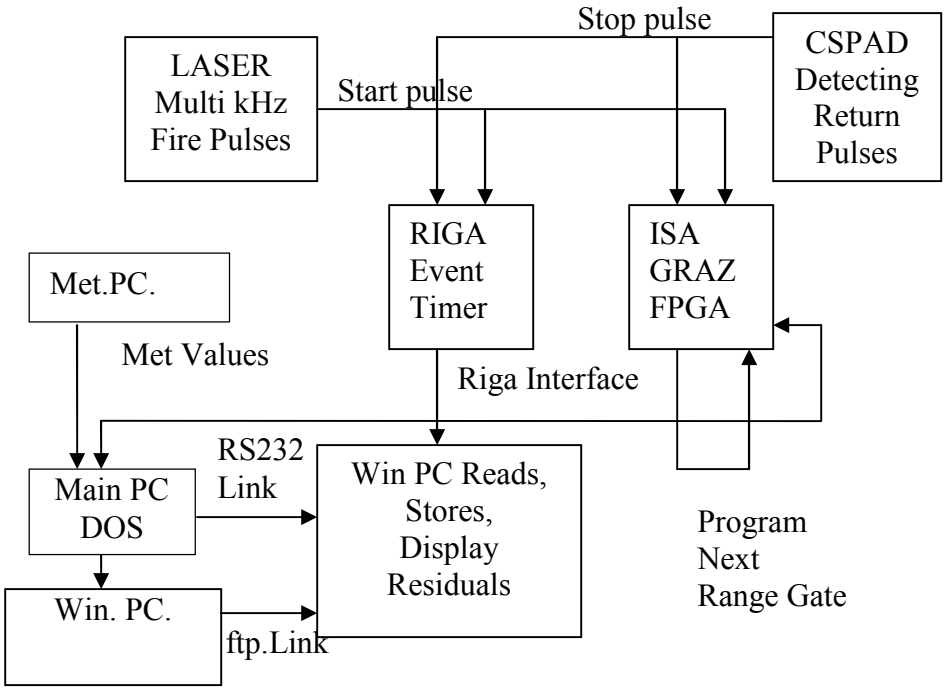

Fig 8.1 Demo Program Block Diagram of Hardware

8.1 Basic Parts of Demo Program

Hardware involves basically the whole machinery on SLR station Graz directly or indirectly. Such as telescopes, laser associated equipment and also linked to software system to download the prediction and important parameters from Graz PC. The demo system consists of following major H/W, S/W components

Platform: PC 3.00 GHz Dual Core Intel Processor, 2.9 GB RAM, referred to as Demo PC,
ISA FPGA Card: Programmed already programmed to perform the logistics of 2kHZ Graz SLR is used in demo program to setup the range gate @ 10 kHz,

Riga Event Timer: to measure the timing event, start and stop epochs up to ps accuracy,

CSPAD: triggered by the return epochs,

Necessary Cable connections: to make the hardware setup and interface the PC to the outer world,

Standard signals: of IPPs and 10 MHz,

Operating systems: Windows XP,

Application package: visual studio 2008,

Software language: visual c++ and fast NTport libraries to provide low level access to the ISA and parallel port of ISA FPGA Card and Event timer interface respectively.

Assembly language of Pentium Processor is used as a programming language for port read and writes functions,

Interfaces: serial RS 232 and

Protocols: ftp for transferring the prediction files from main PC to the demo pc.

8.2 RS232 Control

RS 232 control thread is implementing an algorithm which acts as the back bone of the demo program, controls and regulates all parts of demo program. It receives the command over RS-232 link automatically and it initiates the proper procedure after decoding the command. The command consists of start/stop a procedure or transmitting some values i.e. control flags, display information and meteorology data etc. RS232 thread functionality is explained via flow chart (fig. 8.2). Thread continuously iterates to read the next command sent by the main pc (fig. 8.1). It separates, decodes and displays the latest sequence of commands on the GUI.It further initiates one of three procedures i.e. 1) range gate setting; ns part 2) calibration 2) ranging; ps part.

8.3 Range Gating part with ns Resolution

Nano Second part of the Demo Program is built based on the interface of Demo PC with Graz ISA FPGA Card. The access to the ISA port is built using NT port Library.NT Port Library enables your Windows applications to real-time direct access to PC I/O ports without using the Windows Drivers Development Kit (DDK). The implementation of the I/O port access for ISA FPGA hardware modules is 16 bit I/O routines written in assembly language and Embedded into visual c++ environment to improve further the speed of access to the ISA port. Fig 8.3 shows the setup for this part of Demo Program.

ISA bus card for PC having a large FPGA (Field Programmable Array) and some glue logic, within the FPGA carries out numerous functions necessary for the kHz measurement. The card receives the 10 MHz standard frequency, plus the 1 pps signal (one pulse per second). This FPGA contains the entire logistics for the range gate generator (RGG) with a resolution of 0.5 ns can store up to 300 range gates and managed.

The card automatically and asynchronously reads and stores all of the event timers measured events, which can be read quickly from the demo PC. Several 64-bit serial I / O interfaces are also implemented, which are connected via BNC cable to the telescope, the observer cabin and the laser table, each of these interfaces allows easy control/adjustment of mirrors, switches, security bits, signals for the acoustic receiving indicator, etc.

All of these functions are already implemented and used for SLR Graz for 2 kHz range gating and controls. ISA FPGA using its internal hardware modules stores the laser fire and return epoch up to ns resolution. Nano Second [ns] Resolution thread continuously check the start epoch availability flag from ISA port and reads the start epoch as soon it is fired and stored on the ISA FPGA with ns accuracy.

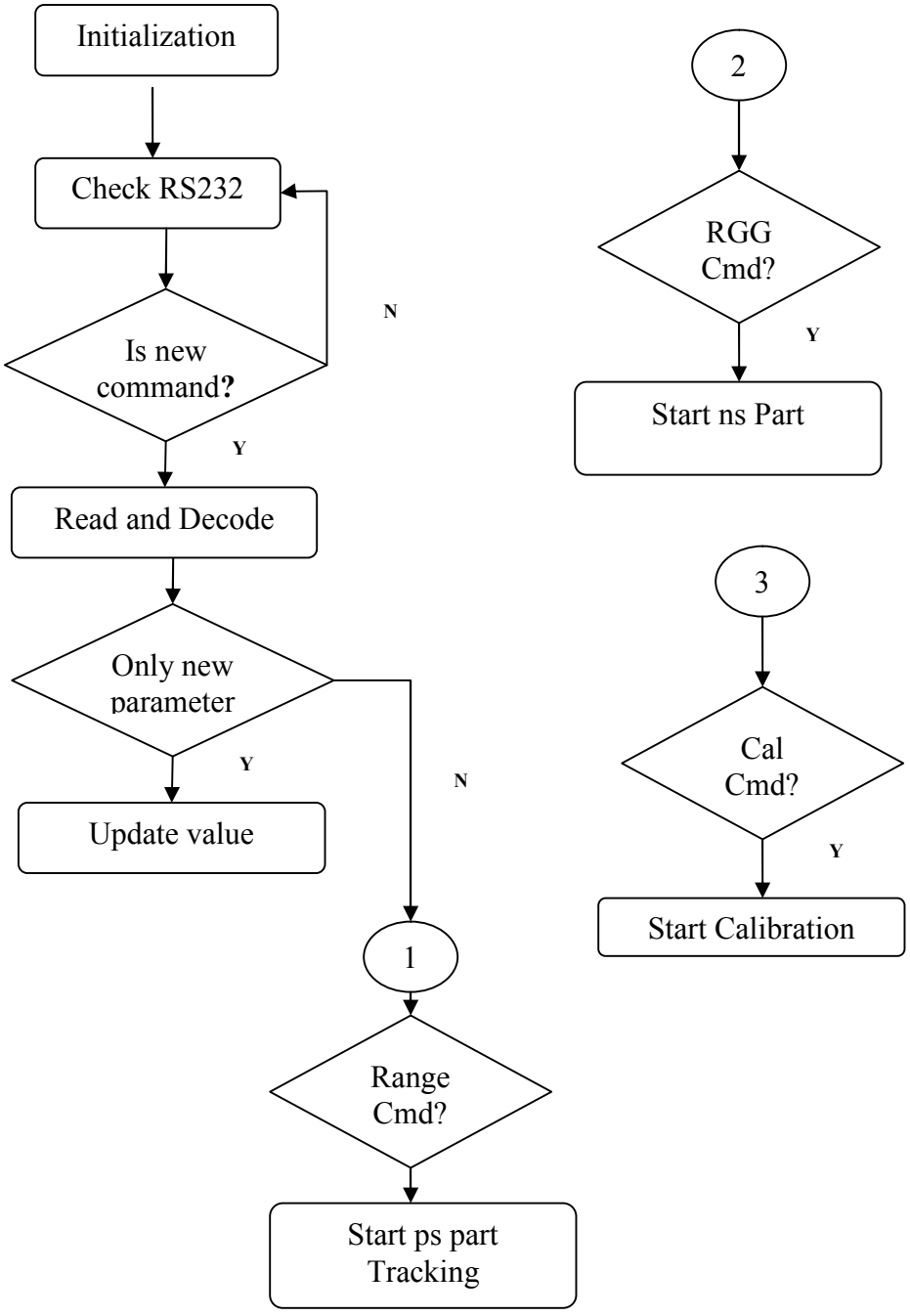

Fig. 8.2: Demo Application Flow Chart

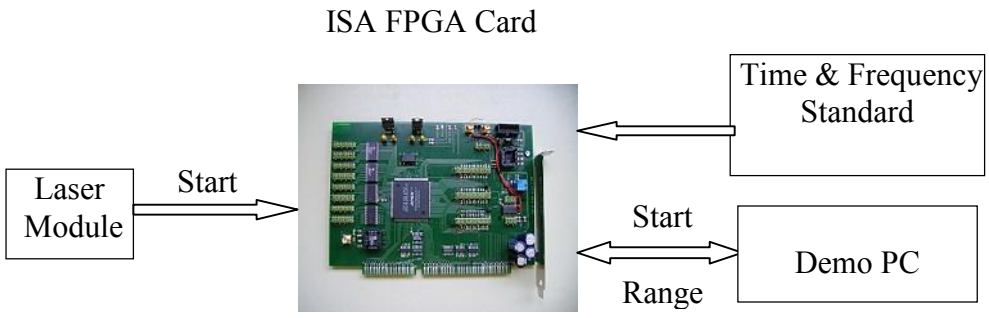

Fig. 8.3: ISA Graz FPGA interface with the demo PC

The demo PC then calculates the expected return time of return epoch using the prediction data available for the current tracked satellite. The expected return time is corrected and downloaded to the ISA FPGA to set the range gate before the arrival of return epoch and loaded into the Range Gate Generator; which then activates the detector short before arrival of the return photon(s). The C-SPAD has to be gated about 65 ns before expected arrival of the return photon(s).While this is done at present at Graz with a combination of a digital100-ns-resolution FPGA counter PLUS a programmable analog delay chip which is replaced now by a presently developed fully digital Range Gate Generator (RGG) into the FPGA - using a 5 ns course counter, and a 500 ps vernier – to improve linearity and stability, written in detail in Chapter 2 [31].

Average response time is about 40 us using low level interface and LPT thread (Low priority thread: A type of worker thread used in visual c++). Most of the response time was consumed for the data reading/writing and interpolation. These timing conditions correspond to the possibility of satellite ranging from at repetition rate up to 25 kHz. As derived already in chapter 4 that @ 20 kHz the phenomena of constant laser back scatter would occur which puts a limitation on going further to the higher repetition rate? With existing Graz SLR @ 2 kHz system up to 300 pulses are traveling at the same time to or from a satellite, the RGG uses FIFO registers to store and handle the individual gate epochs. The next expected RG epoch is compared to an actual time scale; if this time arrives, the RGG issues the Range Gate pulse. The same scheme can be implemented with the higher repetition rate system but in this case the number of one the was pulses will be higher for examples at 10 kHz we need 10 Range Gates per ms; for Lageos we need 700 Range Gates to be handled inside FIFO and for higher satellites with 180 ms time-of-Flight 1800 Range gates to be handled in the FIFO. The solution to the problem is to keep the FIFO size up to 2000 Registers then we can go to Lageos with out modifying the existing system and to buffer the Range Gates on the PC memory for higher satellites and next set of Range Gates is downloaded to the FPGA Range Gate FIFO according to the time scale. The next Range Gate has to be calculated and loaded into the FIFO with in 100 us for 10 kHz system.

Test of nano second part is made with real time tracking of the satellites upto Lageos concluding that it can successfully perform the range gate function.

It need on the average 38-40 us to complete range gate processing which proves it an effective range gate software and can be used easily upto 10 kHz repetition rate. We are quite in time as compared to the limit of 100 us for 10 kHz. The software is limited to 25 kHz but can be improved with better processor power or a dedicated process with in the FPGA.

8.4 The Calibration Task

Calibration of the ranging system is necessary for measuring the ranging error. It uses the same set up in fig 8.4 as is used for [ps].To keep the system at the highest possible accuracy, it is calibrated at least once per hour; during the calibration, the laser pulses are attenuated by de-phasing the pump diodes of the last amplifier (the laser diodes are still pumped with the same pulses to keep the thermal equilibrium, but about 300 ms too late, so that the last amplifier does not contribute anymore); these attenuated pulses are directed into our near calibration target, about 1 m in front of the telescope [32]; in each calibration run, 10000 residual are measured – which takes only about 10seconds at 2 kHz and 50% return quote and are then iteratively using 2.2 sigma elimination to keep any the valid residuals– and averaged to give the calibration value plus statistical information (skew, kurtosis, peak minus mean etc.). The main emphasis is on closely watching any changes of the calibration values (usually stable within a few ps), and symmetric distribution of the returns, i.e. peak minus mean should be about ZERO; The calibration residuals are displayed on the displaying window and the result is summed and added in one line into a cal file with time of calibration.

8.5 Real Time Traking with ps resolution

The [ps] thread reads start event (laser fire time) and stop event (return epoch) upto ps accuracy and measures the TOF of the individual pulse and store the result in the form of residual (observed minus calculated TOF: O-C). Most important component in this measurement is Riga A032 event timers which reads and stores start and stop event with a LSD resolution of 1 ps [33].

The Event Timer A032-ET is a computer-based instrument that precisely measures the times when events (input pulse comings) occur. The A032-ET can be used for various applications where picosecond-precision wide-range and high-speed timing measurements are especially needed. First and foremost the A032-ET is designed for applications related to Satellite Laser Ranging, and through the years of improvement is fully sufficient for kHz ranging up to 10 kHz.

The event measurement is performed in two stages. At first, the Event Timer Block transforms every input event into single 80-bit timing data block (subsequently referred to as TD-block) and sequentially accumulates them in a FIFO memory. Each TD-block contains the counting data (39 bits; 10 ns resolution) and interpolating data (40 bits), as well as one-bit mark specifying the kind of measured event (either Start or Stop).

The interpolating data are presented initially in an intermediate redundant form. At the next stage the PC takes out TD-blocks from the FIFO memory and processes them to obtain the corresponding epoch time-tags in a unified form. Further these time-tags are additionally processed to display the ranging results in real time.

To achieve the best precision, processing of TD-blocks takes into account the actual physical characteristics of time interpolation under actual operating conditions; these characteristics are defined through so called scaling (hardware calibration) before the measurement [34].

A032-ET Features: A032 has some very unique features which make it the most favorite choice for SLR community. It contains **-** two inputs A and B for the events being measured, time-tag marking specifying the input (either A or B) that provides the measured event, output data presentation as time-tags synchronized to real time clock**,** FIFO depth up to 12,000 time-tags, two software options supporting different order of event incoming**,** 16 MHz maximum measurement rate**,** up to 10 kHz mean rate of continuous (gapless) measurement (the A032.1 option)**,** Up to 500 Hz cycle repetition rate (the A032.2 option)**,** Internal online programmable gating with 10 ns LSD (the A032.2 option)**,** Fully remote control and timing data transfer via TCP/IP network and Self-calibration and precision testing.

The ET-device is flexibly controllable and, in particular, allows writing TD-blocks in the FIFO memory and reading of them by the PC software. The A032-ET allows two modes of operations. There are two currently available options of the A032-ET, which use the same specialized hardware but differ by the software. These options provide alternatively two basic kinds of measurement: A032.1 and A032.2 both have certain advantages and limitations.

The option A032.1 provides continuous (gapless) measurement of events at high (up to10 kHz) mean measurement rate, allowing bursts of the rate up to 16 MHz. This option is well suitable to measure the overlapped time intervals between Start and Stop events that come at the separate inputs (either A or B) of the Event Timer in any order. Specifically this is the case of advanced Satellite Laser Ranging at kHz repetition rate. In such applications the Event Timer is well competitive as compared with the highest-performance event timers currently available.

The option A032.2 provides cyclical measurement of events that come at the separate inputs of the ET-device in the strict order: in every cycle at first the Event Timer measures a single Start event coming at the input A, and then - a user-defined number of Stop events (up to 12,000) coming at the input B. The Stop events are measured within internal online programmable gate.

Specifically this is the case of conventional Satellite Laser Ranging where the measured Start-Stop time intervals do not exceed the repetition period of Start events.

In such applications the A032.2 considerably surpasses possibilities of the traditional time interval counters in both precision and functionality.

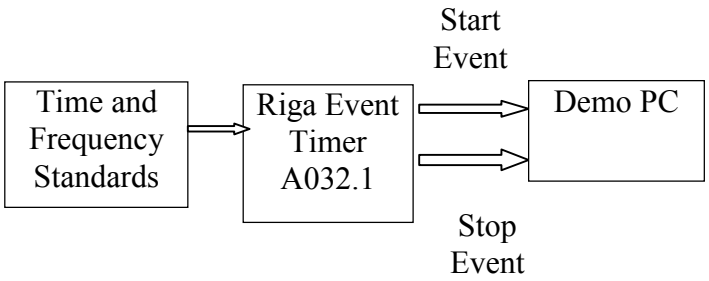

Fig. 8.4: Block diagram of the circuitry for Time-Of-Flight Measurement

The ps thread continuously checks the Riga event timer for the availability of a start/stop event and reads this event through 8 bit parallel interface using assembly language I/O routine written using NT Port Library. When a start-event occurs and the demo pc reads and stores the start event in a soft circular buffer and calculates the expected time of flight using Lagrange interpolation of the start event with the prediction data set. This is called calculated time of flight (TOF).

When a stop event occurs (for every return epoch) the [ps] thread compares in the real time stop event with circular buffer of start-events to find its matching pair of start-event and using these two event one start-event and corresponding stop the routine calculates the measured TOF. Difference of Calculated TOF and Observed TOF (O-C) are called residuals. The identification routine then classifies the residuals in to real returns and noise data.

Identified residuals are plotted on the display screen in real time. The results of ps part are quite promising and we can measure the TOF within 3mm accuracy. The system is limited to 10 kHz repetition rate due to limitation on the Riga function. This can be improved using a faster and wide-range interface instead of 8 bit interface. The system can successfully range to 10 kHz.

8. 6 Overall performances and testing

The performance of the system is checked at 4 kHz and it shows 50 % more returns in case of lower satellites and 45 % more in case of Lageos. The demo program includes all the problems and solutions mentioned above; it successfully demonstrates that a 10 kHz SLR system is already possible with presently available technology; it runs in parallel with the present Graz SLR system (operated in a simulated 10 kHz mode) on a dedicated Windows PC; it gets only basic information from the Graz SLR system (e.g. “which satellite is tracked now”); it reads the Riga event timer, calculates range gates, plots the resulting residuals, and stores all identified returns.

It also monitors all calibration actions, calculates and stores its own calibration values, and thus allows a completely independent 10 kHz parallel SLR measurement channel.

The demo program includes all the problems and solutions mentioned above; it successfully demonstrates that a 10 kHz SLR system is already possible with presently available technology; it runs in parallel with the present Graz SLR system (operated in a simulated 10 kHz mode) on a dedicated Windows PC; it gets only basic information from the Graz SLR system (e.g. “which satellite is tracked now”); it reads the Riga event timer, calculates range gates, plots the resulting residuals, and stores all identified returns; it also monitors all calibration actions, calculates and stores its own calibration values, and thus allows a completely independent 10 kHz parallel SLR measurement channel.

9. Conclusions

Satellite Laser Ranging (SLR) to artificial Earth orbiting satellites is one of the most accurate space geodetic techniques today. The precision of SLR has been improved by almost two orders of magnitude during the last three decades, reaching sub-mm for Normal Points. A global network of approximately 40 stations in 30 countries worldwide are presently doing range measurement to more than 30 satellites, delivering the data via well established communication links to global and regional data centers (cf. chapter 2), which - after final checks - provide this data to the scientific user community.

The majority of SLR stations are still working with 10 Hz systems; the SLR station Graz has successfully introduced 2 kHz SLR at the end of 2003, with several other SLR stations following. This thesis investigates problems of and possible solutions for higher repetition rate SLR systems (10 kHz or more); the resulting higher data rates of such systems promise increased accuracy, increased capability of automation, and additional advantages like significantly improved satellite spin determination. Higher repetition rates result in increasing amount of data for low Earth orbiting (LEO) satellites; due to averaging, the accuracy will also be increased significantly; the suggested configuration of a constant laser power system will also heavily boost the high Earth orbiting (HEO) satellite SLR results.

Investigation of signal to noise ratio for higher repetition rate systems concludes that the present Graz SLR system with 400 μJ @ 2 kHz can – and should - be upgraded with a constant power laser system with e.g. 5 W output; for LEO satellites, the system would produce e.g. 500 μJ @ 10 kHz, and provide all above mentioned advantages; for HEO satellites, the signal-to-noise ratio for the weak pulses of high repetition rates would drop below meaningful levels. Thus, the system should operate at lower repetition rate, but with higher energy per pulse (e.g. 50 mJ @ 100 Hz); such a system – although not yet available commercially - would be optimized for the upcoming difficult task of daylight measurements to HEO satellites like the 27 GALILEO satellites, to be launch within the next few years (cf. Chapter 6).

There is a constraint for repetition rates higher than 18 - 20 kHz, due to laser backscatter, overlapping with photons returning from a satellite. At the present Graz repetition rate of 2 kHz, such an overlap occurs at every 75 km satellite distance change, and remains for about 7.5 km; for a 20 kHz system however, it will occur after every 7.5 km, resulting in constant backscatter overlap – leaving no chance to avoid it. However, with decreasing energy per shot at higher repetition rates – assuming again a constant power laser – the resulting backscatter decreases, reaching similar values as experienced from background noise during daylight SLR anyway (cf. Chapter 5).

Another limitation for higher repetition rates is the achievable speed – measurement and read out - of available picosecond event timers; while the present Graz ET operates with 2.5 kHz maximum.

The Riga event timer – with the need to write assembly language routines for reading the results – was successfully operated with 10 kHz SLR repetition rate (i.e. 20 kHz for start/stop events). This can be improved possibly using a higher speed interface on the Riga Event Timer (instead of the presently used standard EPP / parallel interface).

With higher repetition rates, signal is decreasing due to lower energy per pulse, but noise will increase (cf Chapter 5: Signal to Noise Ratio); analysis of the resulting signal-to-noise ratio shows that it would be possible to identify less than 50 returns out of 100000 (noise) points (which means a return rate of < 0.05%), but it would require too much CPU power to be done in real time. While this is not a problem for LEO satellites (return signal is high enough), it again demonstrates that for HEO satellites a better S/N ratio is needed – with e.g. a 50 mJ @ 100 Hz laser system (cf. Chapter 7).

kHz SLR generally needs to upgrade its timing systems; higher repetition rates require faster epoch time tagging of fire pulses for fast range gate setting. Therefore, a fast Event Timer with sub-ns resolution was developed and implemented within the FPGA, which measures the start event time within some 10 ns. At 100 kHz, 100 range gates per ms are needed; e.g. for HEO satellites with a time-of-flight of up to 180 ms, the system has to handle 18000 Range Gates within the FPGA FIFO registers. This could be done by designing a new FPGA circuitry with higher capacity, or by calculating the range gates within the FPGA instead of downloading from outside, or by using software buffers in the control PC (cf. Chapter 8).

The demo program (cf. Chapter 8) includes all the problems and solutions mentioned above; it successfully demonstrates that a 10 kHz SLR system is already possible with presently available technology; it runs in parallel with the present Graz SLR system (operated in a simulated 10 kHz mode) on a dedicated Windows PC; it gets only basic information from the Graz SLR system (e.g. “which satellite is tracked now”); it reads the Riga event timer, calculates range gates, plots the resulting residuals, and stores all identified returns; it also monitors all calibration actions, calculates and stores its own calibration values, and thus allows a completely independent 10 kHz parallel SLR measurement channel.

A future upgraded Graz SLR system will use a 5 Watt @ 100 Hz to 10 kHz (or more) laser – when available – which is small enough to be mounted on the transmit telescope. The present investigation and design of high repetition rate SLR system will not only allow automatic and autonomous ranging operations, but significantly boost all SLR results and applications. In addition it will enhance - Graz SLR station add-on experiments and pave its way towards important scientific publications in future.

Bibliography

[1] **(ILRS) International Laser Ranging service (ILRS)** collects, merges, archives and distributes Satellite Laser Ranging (SLR) and Lunar Laser Ranging (LLR) observation data sets of sufficient accuracy to satisfy the objectives of a wide range of scientific, engineering, and operational applications and experimentation. Refer to List of Laser Satellites on the website: http://ilrs.gsfc.nasa.gov/satellite_missions/list_of_satellites/index.html.

[2] **Degnan, J.J.** Thirty years of Satellite Ranging, 9th International workshop on Satellite Laser ranging (1996).

[3] **ILRS** Several annual reports of ILRS on: http://ilrs.gsfc.nasa.gov/reports/ilrs_reports, (2010).

[4] **ILRS Board Meeting** Report of meeting by the governing board of ILRS at 3rd May (2010): http://ilrs.gsfc.nasa.gov/docs/ilrsgb_100503_presentations.pdf.

[5] **Kirchner, G., Koidl F.,** Graz kHz SLR System: Design, Experiences and Results, 14th International Laser Ranging Workshop (2004), San Fernando, Spain.

[6] **Kirchner, G., Koidl, F.** Low Cost Laser Beam Imaging for Daylight Tracking, 14th International Laser Ranging Workshop (2004), San Fernando, Spain.

[7] **David A. Arnold,** Retro reflector array transfer functions", Proceedings of the 13th International Workshop on Laser Ranging, October, 2002, Washington, DC.

[8] **(ILRS) List of SLR Satellites** http://ilrs.gsfc.nasa.gov/satellite_missions/list_of_satellites/index.html.

[9] **Kirchner, G., Hausleitner, W.** Satellite Laser ranging: Detecting single photons with ps accuracy. 2nd Conference on Academic and Industrial Cooperation in Space Research, Proceedings of a conference held 15-17 November, 2000 in Graz, Austria. Edited by R.A. Harris and David Raitt. European Space Agency ESASP-470, 2000. p.145

[10] **Kirchner, G., Koidl, F.,** Graz event timer system: E. T., Proceedings 12th International Workshop on Laser Ranging (2000), and Matera.

[11] **Bespal, k., Boole E., Vedin V.** The model A032-ET of Riga Event Timer, Institute of Electronics and Computer Science, Riga, LATVIA, 16th international Laser Ranging workshop (2008), Poland.

[12] **Kodet J., Prochazka I.,** Compact Event Timing and Laser Fire Control Device for One Way Laser Ranging. 16th International Laser Ranging workshop(2008), Poland.

[13] Iqbal F., Koidl F., Kirchner G. Medium Resolution Event Timer and Range Gate Generator in Graz FPGA Card, 16t*h* International Laser Ranging conference (2008)

[14] Luck J. Is your performance being ruined by interpolation errors? **,** EOS Space Systems Pty.Ltd. Queanbeyan NSW 2620 (2006), Australia.

[15] Altera Corporation. NiosII Software Development Handbook.

[16] Altera Corporation., Cyclone Device Handbook.

[17] Altera Corporation.,Quartus Handbook Volume 4, SOPC builder.

[18] Kirchner, G., Koidl F., Graz KHz SLR System: Design, Experiences and results, 14th International Laser Ranging Workshop (2004), San Fernando, Spain.

[19] Degnan, J., Caplan, D. Performance of a Liquid Crystal Optical Gate for Suppressing Laser Backscatter in Monostatic Kilohertz SLR Systems (2006).

[20] Sadovnikov M.A. Pulse repetition rate optimization in SLR stations to provide minimum systematic error of ranging,16th International Workshop on Laser Ranging (2008).

[21] Degnan J.J. Millimeter Accuracy Satellite Laser Ranging: a Review, in Contributions of Space Geodesy to Geodynamics: Technology, *Geodynamics Series*, Vol. 25, American Geophysical Union, pp 133-162, 1993.

[22] Degnan J.J. Impact of Receiver Dead time on Photon-Counting SLR and Altimetry during Daylight Operations, 16th International Laser Ranging Conference (2008), Poznan Poland.

[23] Mueller H. Analysis of Multi-Wavelength SLR Tracking Data Using Precise Orbits Deutsches Geodaetisches Forschungsinstitut, Muenchen. 15th International Laser Conference (2006), Canberra Australia.

[24] Stefan R. Link Budget Evaluation available at the website of International Laser Ranging Service. http://ilrs.gsfc.nasa.gov/.

[25] David A. A. Cross Section of ILRS satellites, Proceedings of the 13th International Workshop on Laser Ranging, October, 2002, Washington, DC.

[26] Degnan J.J, Impact of Receiver Dead time on Photon-Counting SLR and Altimetry during Daylight Operations, 16th International Conference (2008).

[27] Huber H., Schmidt M., Zoppel S. Advances of multi kHz repetition rate picosecond laser system for satellite laser ranging, 16th International Laser Ranging Conference (2008), Poznan Poland.

[28] Kirchner, G., Koidl F., Graz KHz SLR System: Design, Experiences and Results, 14th International Laser Ranging Workshop (2004), San Fernando, Spain.

[29] Kirchner, G.; Koidl, F., Graz Event Timing System: E.T. Matera, Proceedings (2000).

[30] Bespalko V., Boole E., Vedin V. The Model A032-ET of Riga Event Timers.15th International Laser Ranging Workshop (2006), Canberra, Australia.

[31] Iqbal F., Kirchner G., Koidl F. Fast response, medium resolution digital event timer and range gate generator for satellite laser ranging. Artificial Satellites, vol. 43, no. 4 – 2008, doi: 10.2478/v10018-009-0013-8.

[32] Kirchner G.and Koidl F. Automatic Ranging Software in Graz, Proceedings of 10th International Workshop on Laser Ranging Instrumentation (1996).

[33] Institute of Electronics and Computer Science Riga, Latvia, Manual : Event Timer A032 A032-ET.

[34] Selke C., Koidl F., Kirchner G., Grunwaldt L. Tests of the Stability and Linearity of the A031-ET Event Timer at Graz Station, Proceedings of the 14th International Laser Ranging Workshop(2004), San Fernando, Spain.

[35] Vedin V. Bespal K., Boole E. Precision testing methods of Event Timer A032 A032-ET (2006).

[36] Kirchner, G., Koidl, F., Prochazka, I., and Hamal, K., "SPAD on GaAsP for SLR: Calibration Ranging Results", Presentation to 12th International Workshop on Laser Ranging (2000), Matera, Italy.

[37] Kirchner, G.; **Koidl, F**.; **Dusleag, A**.; **Iqbal, F.**; **Leitgeb, E.** Observing variable stars and transiting exo-planets with single photon counting Proc. SPIE, Vol. 7355, 73550T (2009); doi:10.1117/12.822245.

Appendix A: Proposed Pico-Second Laser

On the next pages (Appendix A) the proposed pico-second Laser for High Repetition Rate SLR System is shown. The laser is manufactured by Photonics Industries. This type of a RG Series diode pumped pico-second laser produce over 3mJ per pulse at 1 kHz and more than 10Watts at 10 kHz. It is the most compact laser with the highest pulse energy in kHz range, available at the market. It can be used as 5W system @ 10 kHz assumed through out in analysis and design of this PhD-thesis. More details are visible on the next pages.

Higher power versions (25W and 40W @ 10 kHz) or pulse energy (5mJ/pulse and 8 mJ/pulse @ 1 kHz) are also available with added amplifier stages. Harmonic output such as 532 nm, 355 nm, 266 nm, and 213 nm can be ordered as needed.

RG Lasers

High Pulse Energy Picosecond Laser

RG Series

Photonics Industries' RG Series diode pumped pico-second lasers produce over 3mJ per pulse at 1kHz and more than 10Watts at 10kHz at 1064nm with ~ 15ps nominal pulse widths all while still maintaining TEM_{00} mode quality in a compact, industrial reliable package. It is the most compact laser with the highest pulse energy in kHz range in the market. Higher power versions (25W and 40W @ 10kHz) or pulse energy (5mJ/pulse and 8mJ/pulse @1kHz) are also available with added amplifier stages. Harmonic output such as 532nm, 355nm, 266nm, and 213nm can be ordered as needed.

Features

- Variable rep rate with two versions:
  - RG-L: Single Shot to 25kHz
  - RG-H: 20kHz to 1MHz
- Excellent beam quality (M^2 typically <1.3)
- Closed loop chilled
- Small form factor, compact laser head
- Industrial grade
- Diode pumped technology
- Wide range of powers and harmonic options available

Applications

- Process difficult materials
  - Quartz. other glasses
  - Ceramics
  - CIGS
- Metal welding. Cutting, and Deburring
- Improved micro and meso machining quality with less dross
- Cold ablation of materials with less “heat affected zone” than conventional nanosecond DPSS
- Improve cut quality and throughput for medical applications (e.g., heart stents)
- Stereo lithography
- LIDAR
- Satellite Laser Ranging

Photonics Industries
International, Inc.

The Pioneer of Intra-Cavity Solid-State Harmonic Lasers

Optical Specifications

Wavelength (nm)	**1064nm**	
Model Number	RG-L 1064	RG-H 1064
Average Power*	10W @ 10kHz	10W @ 100kHz
Pulse Energy	3mJ/pulse @ 1kHz	200µJ/pulse @ 50kHz
Long term stability (8 hour)	1% rms	
Polarization	Vertical	
Wavelength (nm)	**532nm**	
Model Number	RG-L 532	RG-H 532
Average Power*	5W @ 10kHz	5W @ 100kHz
Pulse Energy	1.5mJ/pulse @ 1kHz	100µJ/pulse @ 50kHz
Long term stability (8 hour)	2% rms	
Polarization	Horizontal	
Wavelength (nm)	**355nm**	
Model Number	RG-L 355	RG-H 355
Average Power*	3W @ 10kHz	3W @ 100kHz
Pulse Energy	1mJ/pulse @ 1kHz	50µJ/pulse @ 50kHz
Long term stability (8 hour)	3% rms	
Polarization	Vertical	
Wavelength (nm)	**266nm**	
Model Number	RG-L 266	RG-H 266
Average Power*	1.5W @ 10kHz	1.5W @ 100kHz
Pulse Energy	400µJ/pulse @ 1kHz	25µJ/pulse @ 50kHz
Long term stability (8 hour)	3% rms	
Polarization	Vertical	

Repetition rate	Single Shot to 20kHz	20 to 500kHz
Pulse width	<25 ps	
Spatial mode profile	TEM_{00}	
M^2	<1.3 (typical <1.2)	
Output Beam Diameter	0.9mm (Nominal)	
Beam divergence	5 mrad	
Beam Ellipticity	<10%	
Beam Point Instability	<50 urad (typical 5urad)	
Ambient Temperature	15 to 30 ^{o}C (59 to 86 ^{o}F) Operating Range	
Relative Humidity	Non condensing, 90% Max	

* For power at 1064nm>10W, 532nm>5W, 355nm>3W, or 266nm>1.5W please contact Photonics Industries' factory

Mechanical Specifications (Preliminary)

Cooling	**Closed Loop Chiller**
Laser head dimensions	191mm (W) x 127mm (H) x 600mm (L)**
Power supply dimensions	484mm (W) x 133mm (H) x 476mm (D)
Power requirement	400 Watts Maximum (100V or 220V)(excluding chiller)

** For 532, 255 and 266nm, L = 800mm

Due to Photonics Industries' commitment to continuous product improvement, specifications are subject to change without notice.

Photonics Industries
International, Inc.

390 Central Ave, Bohemia, NY, 11716
Phone: 631-218-2240
Fax: 631-218-2275
E-Mail: info@photonix.com
Website: www.Photonix.com